

Design and Evaluation of Jointed Plain Concrete Pavement with Fiber Reinforced Polymer Dowels

PUBLICATION NO. FHWA-HRT-06-106

SEPTEMBER 2009



U.S. Department of Transportation
Federal Highway Administration

Research, Development, and Technology
Turner-Fairbank Highway Research Center
6300 Georgetown Pike
McLean, VA 22101-2296

FOREWORD

This study evaluates fiber reinforced polymer (FRP) dowel bars as load transferring devices in jointed plain concrete pavement (JPCP) under HS25 static and fatigue loads and compares their response with JPCP consisting of steel dowels. Along with laboratory and field evaluations of JPCP with FRP and steel dowels, analytical modeling of dowel response has been carried out in terms of maximum bending deflection, relative deflection, and bearing stress of dowels.

Response of concrete pavement with FRP dowels is investigated through laboratory experiments and field implementation. This research showed that JPCP with FRP dowels provided very good load transfer efficiency (LTE). JPCP with FRP dowels provided sufficient LTE after 5 million cycles of fatigue tests under HS25 loading conducted in the Major Units Laboratory of West Virginia University.

Cheryl Allen Richter
Acting Director, Office of Infrastructure
Research and Development

Notice

This document is disseminated under the sponsorship of the U.S. Department of Transportation in the interest of information exchange. The U.S. Government assumes no liability for the use of the information contained in this document. This report does not constitute a standard, specification, or regulation.

The U.S. Government does not endorse products or manufacturers. Trademarks or manufacturers' names appear in this report only because they are considered essential to the objective of the document.

Quality Assurance Statement

The Federal Highway Administration (FHWA) provides high-quality information to serve Government, industry, and the public in a manner that promotes public understanding. Standards and policies are used to ensure and maximize the quality, objectivity, utility, and integrity of its information. FHWA periodically reviews quality issues and adjusts its programs and processes to ensure continuous quality improvement.

TECHNICAL DOCUMENTATION PAGE

1. Report No. FHWA-HRT-06-106	2. Government Accession No.	3. Recipient's Catalog No.	
4. Title and Subtitle Design and Evaluation of Jointed Plain Concrete Pavement with Fiber Reinforced Polymer Dowels		5. Report Date September 2009	
		6. Performing Organization Code:	
7. Author(s) Vijay, P.V., Hota V.S. GangaRao, and Li, H.		8. Performing Organization Report No.	
9. Performing Organization Name and Address Constructed Facilities Center Department of Civil and Environmental Engineering West Virginia University Morgantown, WV 26506		10. Work Unit No.	
		11. Contract or Grant No. DTFH61-99-X-00078	
12. Sponsoring Agency Name and Address Office of Research and Technology Services Federal Highway Administration 6300 Georgetown Pike McLean, VA 22101-2296		13. Type of Report and Period Covered Final Report, November 1999 to July 2003	
		14. Sponsoring Agency Code Insert FHWA sponsoring agency office code (i.e., HRTS-01)	
15. Supplementary Notes FHWA Contracting Officer's Technical Representative (COTR): Peter Kopac, Pavement Materials and Construction Team			
16. Abstract This study evaluates fiber reinforced polymer (FRP) dowel bars as load transferring devices in jointed plain concrete pavement (JPCP) under HS25 static and fatigue loads and compares their response with JPCP consisting of steel dowels. Along with laboratory and field evaluations of JPCP with FRP and steel dowels, analytical modeling of dowel response was carried out in terms of maximum bending deflection, relative deflection (RD), and bearing stress of dowels. In addition, field rehabilitation of JPCP was carried out using FRP dowels to evaluate its long-term performance. Laboratory tests included static and fatigue load application corresponding to HS25 load and 1.5 times HS25 load on concrete slabs (27.94- and 30.48-cm (11- and 12-inch) depth) with 3.81- and 2.54-cm (1.5- and 1.0-inch) steel and FRP dowels at different spacings (30.48 and 15.24 cm (12 and 6 inches)). Both 3.81- and 2.54-cm (1.5- and 1.0-inch)-diameter FRP dowels were installed in the field with 15.24-, 20.32-, 22.86-, and 30.48-cm (6-, 8-, 9-, and 12-inch) spacings. Load calibrated field tests were conducted on these pavements using a West Virginia Department of Transportation truck in 2002 and 2003. FRP dowel bars that were 1.5 inches in diameter were also used for pavement rehabilitation. Field data collected through an automatic data acquisition system included strain and joint deflections, which were used for assessing joint load transfer efficiency (LTE), joint RD, and pavement performance. Theoretical calculations are provided through different examples for JPCP with FRP and steel dowels by varying dowel diameters, spacing, dowel material properties, joint width, and base material properties. This research showed that JPCP with FRP dowels provided very good LTE up to and beyond 90 percent, which exceeds the American Association of State Highway and Transportation Officials and American Concrete Pavement Association criteria. JPCP with FRP dowels also provided sufficient LTE after 5 million cycles of fatigue tests under HS25 loading.			
17. Key Words GFRP, Glass fiber reinforced polymer, FRP dowel, JPCP, Jointed plain concrete pavement, Relative deflection, Joint efficiency, Dowel		18. Distribution Statement No restrictions. This document is available through the National Technical Information Service, Springfield, VA 22161.	
19. Security Classif. (of this report) Unclassified	20. Security Classif. (of this page) Unclassified	21. No. of Pages 160	22. Price N/A

SI* (MODERN METRIC) CONVERSION FACTORS

APPROXIMATE CONVERSIONS TO SI UNITS

Symbol	When You Know	Multiply By	To Find	Symbol
LENGTH				
in	inches	25.4	millimeters	mm
ft	feet	0.305	meters	m
yd	yards	0.914	meters	m
mi	miles	1.61	kilometers	km
AREA				
in ²	square inches	645.2	square millimeters	mm ²
ft ²	square feet	0.093	square meters	m ²
yd ²	square yard	0.836	square meters	m ²
ac	acres	0.405	hectares	ha
mi ²	square miles	2.59	square kilometers	km ²
VOLUME				
fl oz	fluid ounces	29.57	milliliters	mL
gal	gallons	3.785	liters	L
ft ³	cubic feet	0.028	cubic meters	m ³
yd ³	cubic yards	0.765	cubic meters	m ³
NOTE: volumes greater than 1000 L shall be shown in m ³				
MASS				
oz	ounces	28.35	grams	g
lb	pounds	0.454	kilograms	kg
T	short tons (2000 lb)	0.907	megagrams (or "metric ton")	Mg (or "t")
TEMPERATURE (exact degrees)				
°F	Fahrenheit	5 (F-32)/9 or (F-32)/1.8	Celsius	°C
ILLUMINATION				
fc	foot-candles	10.76	lux	lx
fl	foot-Lamberts	3.426	candela/m ²	cd/m ²
FORCE and PRESSURE or STRESS				
lbf	poundforce	4.45	newtons	N
lbf/in ²	poundforce per square inch	6.89	kilopascals	kPa

APPROXIMATE CONVERSIONS FROM SI UNITS

Symbol	When You Know	Multiply By	To Find	Symbol
LENGTH				
mm	millimeters	0.039	inches	in
m	meters	3.28	feet	ft
m	meters	1.09	yards	yd
km	kilometers	0.621	miles	mi
AREA				
mm ²	square millimeters	0.0016	square inches	in ²
m ²	square meters	10.764	square feet	ft ²
m ²	square meters	1.195	square yards	yd ²
ha	hectares	2.47	acres	ac
km ²	square kilometers	0.386	square miles	mi ²
VOLUME				
mL	milliliters	0.034	fluid ounces	fl oz
L	liters	0.264	gallons	gal
m ³	cubic meters	35.314	cubic feet	ft ³
m ³	cubic meters	1.307	cubic yards	yd ³
MASS				
g	grams	0.035	ounces	oz
kg	kilograms	2.202	pounds	lb
Mg (or "t")	megagrams (or "metric ton")	1.103	short tons (2000 lb)	T
TEMPERATURE (exact degrees)				
°C	Celsius	1.8C+32	Fahrenheit	°F
ILLUMINATION				
lx	lux	0.0929	foot-candles	fc
cd/m ²	candela/m ²	0.2919	foot-Lamberts	fl
FORCE and PRESSURE or STRESS				
N	newtons	0.225	poundforce	lbf
kPa	kilopascals	0.145	poundforce per square inch	lbf/in ²

*SI is the symbol for the International System of Units. Appropriate rounding should be made to comply with Section 4 of ASTM E380.
(Revised March 2003)

TABLE OF CONTENTS

CHAPTER 1. INTRODUCTION	1
GENERAL REMARKS	1
OBJECTIVES	2
SCOPE	2
CHAPTER 2. LITERATURE REVIEW	5
INTRODUCTION	5
LITERATURE REVIEW FINDINGS	5
CHAPTER 3. MATERIALS, EQUIPMENT, AND LABORATORY TESTING PROCEDURES	7
INTRODUCTION	7
MATERIAL PROPERTIES	7
GFRP Dowels	7
Steel Dowels	9
Concrete	9
Base.....	9
FORMWORK	9
TEST SETUP	9
Specimen Fabrication.....	9
<i>Material Preparations</i>	11
<i>Pavement Slab Casting</i>	11
<i>Test Specimens</i>	14
Test Setup and Instrumentation	16
<i>Static Testing</i>	17
<i>Fatigue Testing</i>	18
CHAPTER 4. EXPERIMENTAL RESULTS AND DISCUSSION	19
INTRODUCTION	19
JOINT CRACK PATTERNS OBSERVED IN LABORATORY TESTS	19
PRELIMINARY TESTS	22
JOINT DEFLECTIONS AND JOINT LTE	22
Joint RD	22
<i>Joint RD of Group 1</i>	22
<i>Joint RD of Group 2</i>	28
<i>Analysis of RD</i>	30
Joint LTE	32
<i>LTE of Group 1</i>	33
<i>Joint LTE of Group 2</i>	37
<i>Analysis and Discussion for Joint LTE</i>	40
Investigations on Pavement Pumping Problem	42
Strains on Dowels	47
CHAPTER 5. FIELD APPLICATIONS AND TEST RESULTS	49
INTRODUCTION	49
FRP DOWELS FOR NEW HIGHWAY PAVEMENT CONSTRUCTION	49

Field Locations.....	49
Field Installation	51
FIELD TESTS.....	54
Field Test Before Opening Highway to Traffic in July 2002	54
<i>Test Setup</i>	55
<i>Test Results and Analysis</i>	57
Field Test after Highway Opened to Traffic, June 2003	64
<i>Test Results from Field Test</i>	67
<i>Summary and Analysis of Test Results</i>	70
FRP DOWELS USED FOR HIGHWAY PAVEMENT REHABILITATION.....	74
Field Location	74
Field Installation	75
FIELD TESTS.....	77
Test Setup.....	77
Results and Analysis	78
<i>FRP Dowel Group</i>	78
<i>Steel Dowel Group</i>	79
CONCLUSION	80
Effect of Dowel Spacing.....	80
Effect of Dowel Diameter.....	81
CHAPTER 6. ANALYTICAL EVALUATION.....	83
INTRODUCTION.....	83
ANALYTICAL MODEL.....	83
Load Transfer Across a Joint	86
Dowel Bending Moment and Shear.....	89
Dowel Bar Deflection and Bearing Stress	89
Bearing Stress Between Dowel/Concrete Interfaces	90
Pavement Joint Efficiency	91
THEORETICAL CALCULATION SAMPLES FOR FRP AND STEEL DOWEL GROUP	92
Theoretical Calculation for Dowel Group with 3.81-cm (1.5-inch)-Diameter Dowels....	92
<i>Example 1</i>	92
Discussion for Contraction Joint Model	97
<i>Example 2</i>	98
Theoretical Calculation for Dowel Group with 2.54-cm (1.0-inch)-Diameter Dowels	101
<i>Example 3</i>	101
Discussion for Contraction Joint Model	105
<i>Example 4</i>	106
DISCUSSIONS ON 3.81-CM (1.5-INCH) AND 2.54-CM (1.0-INCH)-DIAMETER DOWELS.....	108
Comparisons for 2.54-cm (1.5-inch)-Diameter Dowel Bars	108
<i>Effect of Dowel Material</i>	110
<i>Effect of Dowel Spacing</i>	111
<i>Effect of Joint Width</i>	111
<i>Effect of Dowel Length</i>	112
<i>Effect on Bearing Stress</i>	112

Comparisons for 2.54-cm (1.0-inch)-Diameter Dowel Bars	112
<i>Effect of Dowel Material</i>	115
<i>Effect of Dowel Spacing</i>	115
<i>Effect of Joint Width</i>	115
<i>Effect of Dowel Length</i>	116
<i>Effect on Bearing Stress</i>	116
COMPARISON OF EXPERIMENTAL VERSUS THEORETICAL DATA.....	116
ANALYTICAL INVESTIGATION WITH RESPECT TO FRP DOWEL- CONCRETE BEARING STRESS	117
CHAPTER 7. CONCLUSIONS AND RECOMMENDATIONS	121
INTRODUCTION.....	121
CONCLUSIONS FOR LABORATORY TESTS.....	121
Joint RD	122
<i>For Specimens (Numbers 1, 4, and 5) Having Proper Crack Formation at Joint Locations (Table 6)</i>	122
<i>For Specimens Having Crack Formation away from Joint Location (Table 7)</i>	122
<i>For Base Material Properties (Table 6)</i>	122
Joint LTE	122
<i>For Specimens (Numbers 1, 4, and 5) Having Proper Crack Formation at Joint Location</i>	123
<i>For Specimens Having Crack Formation away from Joint Location (Table 7)</i>	123
Investigation of Pavement Pumping Problem.....	124
Strains on Dowels	124
CONCLUSIONS FOR FIELD APPLICATIONS AND TEST RESULTS	124
Conclusions for FRP Dowels Used for New Highway Pavement Construction	124
<i>Effect of Dowel Spacing</i>	124
<i>Effect of Dowel Diameter</i>	125
<i>Relative Deflection</i>	125
Conclusions for FRP Dowels Used for Highway Pavement Rehabilitation.....	126
CONCLUSIONS FOR ANALYTICAL EVALUATION.....	126
Conclusions for 3.81-cm (1.5-inch)-Diameter Dowels with 30.48-cm (12-inch)-c/c Spacing.....	126
<i>Effect of Dowel Material</i>	126
<i>Effect of Dowel Spacing</i>	126
<i>Effect of Joint Width</i>	127
<i>Effect of Dowel Length</i>	127
<i>Effect on Bearing Stress</i>	128
Conclusions for 2.54-cm (1.0-inch)-Diameter Dowels with 15.24-cm (6-inch)-c/c Spacing.....	128
<i>Effect of Dowel Material</i>	128
<i>Effect of Dowel Spacing</i>	128
<i>Effect of Joint Width</i>	129
<i>Effect of Dowel Length</i>	129
<i>Effect on Bearing Stress</i>	129
GENERAL CONCLUSIONS FROM THIS RESEARCH	129
RECOMMENDATIONS.....	131

APPENDIX A. TEST OF TIMBER TIE WITH FRP DOWELS	133
APPENDIX B. ANALYTICAL EVALUATION OF EFFECT OF FRP DOWEL SHEAR MODULUS ON PAVEMENT RD.....	141
APPENDIX C. FIBER BURNOUT TESTS FOR DETERMINING FIBER WEIGHT FRACTION AND FIBER VOLUME FRACTION FOR FRP DOWELS	145
REFERENCES.....	147

LIST OF FIGURES

Figure 1. Photo. Exposed failures with rusted dowel bars (Washington State Department of Transportation Pavement Guide)	2
Figure 2. Typical pavement problems—faulting and pumping	5
Figure 3. Photo. FRP dowels (2.54 and 3.81 cm (1.0 and 1.5 inches) in diameter)	8
Figure 4. Photo. Steel dowels 3.81 and 2.54 cm (1.5 and 1.0 inches) in diameter	9
Figure 5. Photo. Wood formwork	10
Figure 6. Diagram. Dimensions of formwork	10
Figure 7. Diagram. Trimmed dowel bar	11
Figure 8. Photo. Instrumented dowels and steel plate positioned in the wood formwork	12
Figure 9. Photo. Placing concrete into the formwork	12
Figure 10. Photo. Dowel being covered by concrete	13
Figure 11. Photo. Casting concrete cylinders	13
Figure 12. Photo. Surface finished specimens	14
Figure 13. Diagram. Concrete slabs for preliminary tests	14
Figure 14. Diagram. Concrete slabs containing two dowels	15
Figure 15. Diagram. Concrete slabs containing only one dowel	16
Figure 16. Photo. Experimental setup	17
Figure 17. Photo. LVDTs positioned on both sides of the joint	17
Figure 18. Photo. Typical crack observed in slabs number 1, 4, and 5 (table 7)	20
Figure 19. Photo. Crack observed in slab number 2 (table 7)	20
Figure 20. Photo. Typical crack observed in slab number 3 (table 7)	21
Figure 21. Chart. Joint RD for slab number 1 under static test	23
Figure 22. Graph. RDs under HS25 loading for slab number 1 at joint width of 0.635 mm (0.25 inch) (static and 1 million cycles)	23
Figure 23. Graph. RDs for slab number 1 under fatigue tests (joint width increased from 0.635 cm (0.25 inch) to 1.016 mm (0.4 inch) from 2 to 5 million cycles)	24
Figure 24. Chart. Joint RD for slab number 2 under static test	25
Figure 25. Graph. RDs for specimen 2 (0 to 2 million cycles)	26
Figure 26. Chart. Joint RD for specimen 3 under static test	27
Figure 27. Graph. RDs for specimen 3 (0 to 1.25 million cycles)	27
Figure 28. Chart. Joint RD for specimen 4 under static test	28
Figure 29. Graph. Pavement deflections under fatigue test for slab number 4 (0 to 5 million cycles, FRP dowel at 30.48 cm (12 inches) c/c)	29
Figure 30. Graph. RDs under fatigue test for specimen 4 (0 to 5 million cycles)	29
Figure 31. Chart. Joint RD for specimen 5 under static test	30
Figure 32. Graph. RDs under fatigue test for specimen 5 (0 to 5 million cycles)	30
Figure 33. Chart. Joint LTE for slab number 1	33
Figure 34. Graph. LTE corresponding to HS25 loading for slab number 1 (2.54-cm (1.0-inch) diameter at 15.24 cm (6 inches) c/c), static and 1 million cycles	34
Figure 35. Graph. LTE for slab number 1 under fatigue tests (> 1 million cycles and joint width increased from 0.635 to 1.016 cm (0.25 to 0.4 inch))	34
Figure 36. Photo. Dowel-concrete interface condition in slab number 1 after 5 million load cycles	35
Figure 37. Chart. Joint LTE for slab number 2	35

Figure 38. Graph. LTE under fatigue tests (HS25 loading) for slab number 2 (0 to 1 million cycles)	36
Figure 39. Graph. LTE under fatigue test for slab number 2 (1 to 2 million cycles)	36
Figure 40. Chart. Joint LTE for slab number 3	37
Figure 41. Graph. LTE under fatigue test for slab number 3 (0 to 1.25 million cycles)	37
Figure 42. Chart. Joint LTE for slab number 4	38
Figure 43. Graph. LTE under fatigue test for slab number 4 (0 to 5 million cycles)	38
Figure 44. Photo. Dowel-concrete interface condition in slab number 4 after 5 million load cycles	39
Figure 45. Chart. Joint LTE for slab number 5	40
Figure 46. Graph. LTE under fatigue test for slab number 5 (0 to 5 million cycles)	40
Figure 47. Diagram. Case one—60.96-cm (2-ft) base material removal under loaded side of slabs	43
Figure 48. Diagram. Case two—30.48-cm (1-ft) base material removal under both sides of slabs	43
Figure 49. Chart. RD for pumping tests (case one—60.96-cm (2-ft) base removal)	44
Figure 50. Chart. LTE for pumping tests (case one—60.96-cm (2-ft) base removal)	44
Figure 51. Graph. RD for pumping tests under 13.345 kN (3 kips) loading (case two—30.48-cm (1-ft) base removal under both slabs)	46
Figure 52. Graph. LTE for pumping tests under 13.345 kN (3 kips) loading (case two—30.48-cm (1-ft) base removal under both slabs)	46
Figure 53. Graph. Strain gauge reading in slab 1 (2.54-cm (1.0-inch) diameter at 15.24-cm (6-inch) spacing c/c) from static test to 1 million cycles under HS25 loading)	47
Figure 54. Chart. Strain gauge reading in slab number 4 (3.81-cm (1.5-inch) diameter at 30.48-cm (12-inch) spacing c/c) from static test under HS25 loading	48
Figure 55. Photo. Dowel installation at location 1 of corridor H, Route 250, Elkins, WV	49
Figure 56. Diagram. FRP dowel positions at location 1 of corridor H, Route 250, Elkins, WV	50
Figure 57. Photo. FRP dowel bars at location 2 of corridor H, Route 219, Elkins, WV	50
Figure 58. Diagram. FRP dowel positions at location 2 of corridor H, Route 219, Elkins, WV	51
Figure 59. Photo. FRP dowel bars bonded with strain gauges at loaded and unloaded sides	52
Figure 60. Photo. Embeddable concrete strain gauge with dowels	52
Figure 61. Photo. FRP dowels in dowel basket	53
Figure 62. Photo. Paving operation in progress	53
Figure 63. Photo. FRP dowel bars being covered by concrete	54
Figure 64. Photo. Dial gauges for measuring pavement deflection under truck loading	56
Figure 65. Photo. Data acquisition system used for field tests	56
Figure 66. Diagram. Dowel A1 (3.81-cm (1.5-inch) diameter, 22.86-cm (9-inch) spacing); refer to figure 58	58
Figure 67. Chart. Strains in dowel during loading and unloading cases for gauge A1-LT (3.81-cm (1.5-inch) diameter, 22.86-cm (9-inch) spacing)	58
Figure 68. Diagram. Dowel A2 (3.81-cm (1.5 inch) diameter, 30.48-cm (12-inch) spacing); refer to figure 58	59
Figure 69. Chart. Strains in dowel during loading and unloading cases for gauge A2-LT (3.81-cm (1.5-inch) diameter, 30.48-cm (12-inch) spacing); refer to figure 58	59
Figure 70. Diagram. Dowel C5 (2.54-cm (1.0-inch) diameter, 15.24-cm (6-inch) spacing); refer to figure 58	60

Figure 71. Chart. Strains in dowel during loading case for gauge C5-U1 (2.54-cm (1.0-inch) diameter, 15.24-cm (6-inch) spacing); refer to figure 58.....	60
Figure 72. Diagram. Dowel C6 (2.54-cm (1.0-inch) diameter, 20.32-cm (8-inch) spacing); refer to figure 58	61
Figure 73. Chart. Strains on dowel during loading case for gauge C6-U1 (2.54-cm (1.0-inch) diameter, 20.32-cm (8-inch) spacing); refer to figure 58.....	61
Figure 74. Chart. Strain from gauge A1-LT (3.81-cm (1.5-inch)-diameter FRP dowel at 22.86-cm (9-inch) spacing) from dynamic tests	62
Figure 75. Chart. Strain from gauge A2-LT (3.81-cm (1.5-inch)-diameter FRP dowel at 30.48-cm (12-inch) spacing) from dynamic tests	63
Figure 76. Photo. WVDOT truck used for field tests	65
Figure 77. Photo. WVDOT truck positioned near a joint for the test.....	66
Figure 78. Photo. Two LVDTs measuring pavement deflections across a joint	66
Figure 79. Photo. Measuring distance from tire to LVDTs (when loading is away from the selected dowel).....	67
Figure 80. Chart. Deflection on pavement joint 3 (with 3.81-cm (1.5-inch)-diameter and 30.48-cm (12-inch)-spacing FRP dowels) under loading.....	68
Figure 81. Chart. Deflection on pavement joint 2 (with 3.81-cm (1.5-inch)-diameter and 22.86-cm (9-inch)-spacing FRP dowels) under unloading.....	68
Figure 82. Chart. Deflection on pavement joint 2 (with 3.81-cm (1.5-inch)-diameter and 22.86-cm (9-inch)-spacing FRP dowels) under loading.....	69
Figure 83. Chart. Deflection on pavement joint 5 (with 2.54-cm (1.0-inch)-diameter and 20.32-cm (8-inch)-spacing FRP dowels) under loading.....	69
Figure 84. Chart. Deflection on pavement joint 6 (with 2.54-cm (1.0-inch)-diameter and 15.24-cm (6-inch)-spacing FRP dowels) under loading.....	70
Figure 85. Graph. Comparison of LTE from field test (average value was used for joint 2).....	72
Figure 86. Graph. Comparison of RD from field test (average value was used for joint 2).....	73
Figure 87. Photo. Locations of FRP and steel-doweled pavement joints	75
Figure 88. Photo. Drilling holes for inserting dowels.....	76
Figure 89. Photo. FRP dowels in position	76
Figure 90. Photo. Steel dowels in position	77
Figure 91. Photo. Concrete placement and vibration.....	77
Figure 92. Photo. Data acquisition recording strain readings.....	78
Figure 93. Chart. Strain from FRP dowels in rehabilitated pavement.....	79
Figure 94. Chart. Strain from steel dowel in rehabilitated pavement	80
Figure 95. Diagram. Semi-infinite beam on an elastic foundation.....	84
Figure 96. Diagram. Slope and deflection of dowel at joint face	85
Figure 97. Diagram. Load transfer distribution proposed by Friberg.....	87
Figure 98. Diagram. Load transfer distribution proposed by Tabatabaie et al	88
Figure 99. Diagram. Most critical dowel at the edge of a slab	88
Figure 100. Diagram. RD between concrete slabs (Porter and Guinn)	89
Figure 101. Diagram. Expansion joint model used for theoretical calculation	92
Figure 102. Diagram. Steps for calculating critical dowel load, joint RD, and bearing stress in JPCP	94
Figure 103. Diagram. Generalized effective dowels for load distribution	95
Figure 104. Diagram. Most critical load distribution on effective dowels	95

Figure 105. Diagram. Pavement contraction joint model	98
Figure 106. Diagram. Expansion joint model used for theoretical calculation	101
Figure 107. Diagram. Most critical load distribution on effective dowels	103
Figure 108. Chart. Dowel deflected shape (2.54-cm (1.5-inch) diameter)	110
Figure 109. Chart. Dowel deflected shape.....	114
Figure 110. Photo. Lab test of timber tie with FRP dowel bar as the load transfer device	133
Figure 111. Diagram. Four timber test cases	134
Figure 112. Diagram. Rosette strain gauges	134
Figure 113. Chart. Plot for longitudinal strain gauges (case I-A and case I-B).....	136
Figure 114. Chart. Load versus deflection (inches) of timber tie for case I-A	140
Figure 115. Chart. Load deflection (arm with regular gauge) for case I-B	140
Figure 116. Graph. Components of RD for dowel types A (2.54-cm (1.0-inch) diameter) and B (3.81-cm (1.5-inch) diameter), with $k = 11.072 \text{ kg/cm}^3$ (400 pci), $f'_c = 31.026 \text{ MPa}$ (4,500 psi), joint width = 0.635 cm (0.25 inch), and $G_d = 2.8 \times 10^3 \text{ MPa}$ ($0.4 \times 10^6 \text{ psi}$).....	143
Figure 117. Graph. Components of RD for dowel types A (2.54-cm (1.0-inch) diameter) and B (3.81-cm (1.5-inch) diameter), with $k = 11.072 \text{ kg/cm}^3$ (400 pci), $f'_c = 31.026 \text{ MPa}$ (4,500 psi), joint width = 0.635 cm (0.25 inches), and $G_d = 5.17 \times 10^3 \text{ MPa}$ ($0.75 \times 10^6 \text{ psi}$) ..	143

LIST OF TABLES

Table 1. Modulus of elasticity (MOE) test results of FRP rod specimens—ASTM D3916	8
Table 2. Shear test results of FRP rod specimens—single-shear fixture	8
Table 3. Dowel details in specimens	15
Table 4. Details of static testing	18
Table 5. Details of fatigue testing	18
Table 6. Parameters of dowel groups	19
Table 7. Cracks in the tested slabs	21
Table 8. Static load applied for specimen 1	22
Table 9. Load applied for fatigue tests on slab number 1	22
Table 10. Load applied for fatigue tests on specimen 2	25
Table 11. Load applied for fatigue tests on slab number 3	27
Table 12. Load applied for fatigue tests on slab number 4	28
Table 13. Load applied for fatigue tests on slab number 5	30
Table 14. RD of group 1 from static tests	31
Table 15. RD of group 1 from fatigue tests	31
Table 16. RD of group 2 from static tests	32
Table 17. RD of group 2 from fatigue tests	32
Table 18. LTE of group 1 from static tests	41
Table 19. LTE of group 1 during fatigue tests	41
Table 20. LTE of group 2 from static tests under corresponding HS25 load	42
Table 21. LTE of group 2 from fatigue tests	42
Table 22. Evaluation of pumping issue under 44.482 kN (10 kips) loading	45
Table 23. Evaluation of pumping issue under 13.345 kN (3 kips) loading	45
Table 24. Parameters of the field test at location 2, July 2002	55
Table 25. Joint details used for analysis	57
Table 26. Summary of FRP dowel strain during loading and unloading	63
Table 27. Parameters of the field test, June 2003	65
Table 28. Pavement joint for deflection analysis	67
Table 29. Summary of joint deflection under maximum loading force	71
Table 30. Values for LTE comparison from field test	72
Table 31. Comparison of RD values from field test	73
Table 32. Comparing joint 2 and joint 3	73
Table 33. Calculation summaries for 3.81-cm (1.5-inch)-diameter dowel ($k = 11.072 \text{ kg/cm}^3$ (400 pci), $f'_c = 31.026 \text{ MPa}$ (4,500 psi))	109
Table 34. Peak bearing stress and average bearing stress in dowel (3.81-cm (1.5-inch) diameter at 30.48 cm (12 inches) c/c) downward area	109
Table 35. Peak bearing stress and average bearing stress within 2.54-cm (1-inch) dowel (3.81-cm (1.5-inch) diameter at 30.48 cm (12 inches) c/c) length from joint face	110
Table 36. Calculation summaries for 2.54-cm (1.0-inch)-diameter dowel ($k = 11.0719 \text{ kg/cm}^3$ (400 pci), $f'_c = 31.026 \text{ MPa}$ (4,500 psi))	113
Table 37. Peak bearing stress and average bearing stress in dowel ((2.54-cm (1.0-inch) diameter at 15.24 cm (6 inches) c/c) downward area	113
Table 38. Peak bearing stress and average bearing stress within 2.54-cm (1-inch) dowel (2.54-cm (1.0-inch) diameter at 15.24 cm (6 inches) c/c) length from joint face	114

Table 39. Comparison of experiments versus theory for slab RD in static testing under HS25 loading	117
Table 40. Strains during loading and unloading on case I-A.....	135
Table 41. Strains during loading and unloading on case I-B.....	136
Table 42. Strains during loading and unloading on case II-A	137
Table 43. Deflections of timber tie on case I-A.....	138
Table 44. Deflections of timber tie on case I-B.....	139
Table 45. RD with low dowel shear modulus ($G_d = 2.758 \times 10^3$ MPa (0.4×10^6 psi))	142
Table 46. RD with high dowel shear modulus ($G_d = 5.17 \times 10^3$ MPa (0.75×10^6 psi))	142
Table 47. FWF and FVF for FRP dowel with 2.54-cm (1.0-inch) diameter	145
Table 48. FWF and FVF for FRP dowel with 3.81-cm (1.5-inch) diameter	145

CHAPTER 1. INTRODUCTION

GENERAL REMARKS

U.S. highways and roads made of jointed plain concrete pavement (JPCP) use load transfer devices, called dowels, across joints of a series of contiguous concrete slabs. Joints allow the movement and deformation of pavement to occur under mechanical loading and thermal variations. Joints may either be parallel to traffic (longitudinal joints) or perpendicular to traffic (transverse joints). Typical problems of jointed concrete pavement without an effective load-transfer device include faulting, pumping, and corner breaks.

As the American Association of State Highway and Transportation Officials (AASHTO) reported, pavement joints supported with dowels have a longer service life than joints without dowels.⁽¹⁾ Over time, traffic traveling over a joint may crush the concrete surrounding the dowel bar and cause voids due to excessive bearing stresses between the dowel and surrounding concrete. Concrete crushing may take place due to stress concentration where the dowel contacts concrete at the joint face directly above and below the dowel. Looseness of dowel support can decrease the load transfer efficiency (LTE) across the joint and accelerate pavement damage.⁽²⁾

Corrosion of the dowel bar can potentially bind or lock the joint. When locking of the joint occurs, no thermal expansion is allowed, and new cracks parallel to the joint are formed directly behind the dowel bars in the concrete. As temperature decreases, contraction of the concrete widens the new cracks, leading to reduction of load transfer. Once there is no load transferred across the joint, the load is then transferred to the subgrade, and differential settlement occurs in the adjacent slabs. Differential settlement of the adjacent slabs creates uneven surface and discontinuity at the joints, making vehicle travel uncomfortable and leading to slab repair or replacement.

Currently, steel dowels, typically epoxy coated with a diameter of 2.54 or 3.81 cm (1.0 or 1.5 inches) and length of 45.72 cm (18 inches), are widely used in JPCP. However, this coating is usually nicked or scraped before installation, leading to dowel corrosion and deterioration (figure 1). Fiber reinforced polymer (FRP) dowel bars, which are resistant to corrosive environments, can be used as effective load transfer mechanisms in JPCP. Currently, polymer matrix composites such as FRP are being used in a broad range of structural applications within the aerospace, automotive, marine, and construction industries due to their superior strength-to-weight ratio and high corrosion resistance.⁽³⁾

For this research, response of concrete pavement with FRP dowels was investigated through laboratory experiments and field implementation.



Figure 1. Photo. Exposed failures with rusted dowel bars (Washington State Department of Transportation Pavement Guide).⁽⁴⁾

OBJECTIVES

The main objectives of this study were as follows:

- To evaluate 3.81-cm (1.5-inch)- and 2.54-cm (1.0-inch)-diameter FRP dowel bars spaced at different intervals as load transferring devices in JPCP under HS25 static and fatigue loads and to compare their response (relative deflection (RD) and LTE) with JPCP consisting of steel dowels under laboratory and field conditions.
- To evaluate the performance (strain and deflection) of JPCP rehabilitated with FRP and steel dowels.
- To model FRP and steel dowel response and that of the pavement in terms of dowel maximum bending deflection, RD, and bearing stress.

SCOPE

Details of laboratory tests conducted at West Virginia University (WVU) structural laboratory were as follows:

- Two jointed concrete slabs with 3.81-cm (1.5-inch)-diameter FRP dowels and 30.48-cm (12-inch)-slab depth were tested under static loads during preliminary static load investigation.
- Five jointed concrete slabs with 3.81- and 2.54-cm (1.5- and 1.0-inch) steel and FRP dowels with spacings of 30.48 and 15.24 cm (12 and 6 inches) were tested under static and fatigue loads corresponding to HS25 load and 1.5 times HS25 load. The slab depth was 27.94 cm (11 inches) for all five slabs, similar to field installation depth.

- Using identical slab thickness, f'_c , joint depth, and joint width, the pavement performance (LTE, RD, and dowel strain) with FRP and steel dowels was evaluated with respect to the following:
 - Dowel diameter.
 - Dowel spacing.

FRP dowel bars were field installed in new highway JPCP construction on Route 219, Elkins, WV. Both 3.81- and 2.54-cm (1.5- and 1.0-inch)-diameter FRP dowels were installed in the field, and the dowel spacings that were used were 15.24, 20.32, 22.86, and 30.48 cm (6, 8, 9, and 12 inches). Two field tests were conducted, and results were analyzed and are discussed in this report.

FRP dowel bars with 3.81-cm (1.5-inch) diameters were installed for pavement rehabilitation near the intersection of Routes 857 and 119, University Avenue, Morgantown, WV. Dowel strains due to regular traffic were analyzed and are discussed in this report.

Analysis and discussions corresponding to theoretical calculations are provided for four different examples of pavements with FRP and steel dowels in terms of dowel diameter, spacing, dowel material properties, joint width, and base material properties.

The remainder of this report is organized into the following chapters and appendices:

- Chapter 2 deals with the literature review.
- Chapter 3 describes materials and laboratory test setup used in this research.
- Chapter 4 discusses experimental results from laboratory tests.
- Chapter 5 presents field installation, field load test results, and discussions.
- Chapter 6 presents theoretical evaluations.
- Chapter 7 provides the summary and conclusions of this research, including suggestions for future research.
- Appendix A describes a preliminary test on timber ties consisting of an FRP dowel as the load transfer device.
- Appendix B analyzes and evaluates the effects of FRP dowel shear modulus on pavement RD.
- Appendix C describes the details of burnout tests for determining fiber weight fraction (FWF) and fiber volume fraction (FVF) of FRP dowels with 2.54- and 3.81-cm (1.0- and 1.5-inch) diameters.

CHAPTER 2. LITERATURE REVIEW

INTRODUCTION

In JPCP highways and roads, inadequate load transfer across the joint will cause substantially higher stresses and deflections due to joint loading than those due to interior loading. A dowel bar transfers part of an applied wheel load from the loaded slab across the joint to the adjacent unloaded slab. Load transfer through dowel bars significantly reduces stresses and deflections due to joint loading, leading to minimized faulting and pumping (figure 2). Faulting is a difference in elevation across the joint of two slabs, while pumping is defined as the expulsion of subgrade material through joints and along the edges of the pavement.⁽⁵⁾

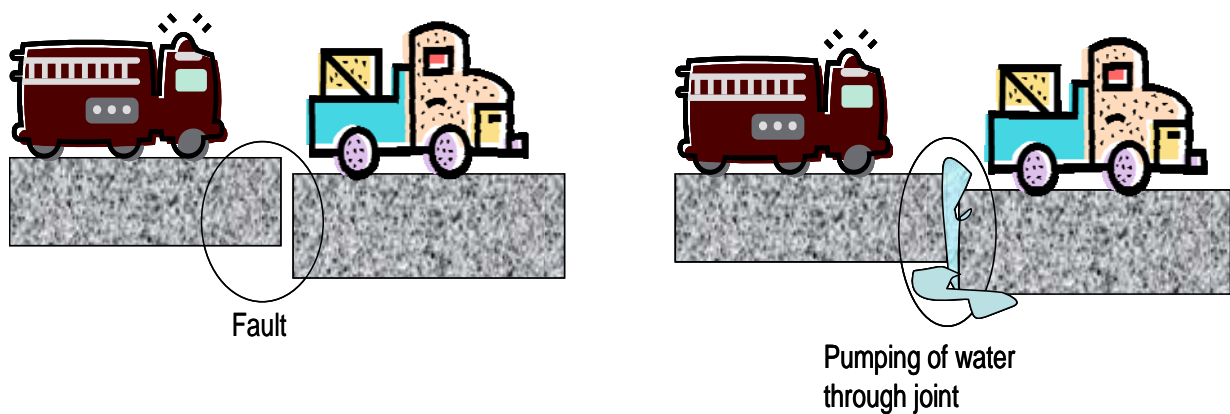


Figure 2. Typical pavement problems—faulting and pumping.

LITERATURE REVIEW FINDINGS

FRP dowels have not been widely used in concrete pavements for highways. However, a number of projects in the United States and Canada have used these composite materials for highway pavement on an experimental basis.

In 1983, the Ohio Department of Transportation installed several FRP dowel bars to evaluate long-term performance in sections of Interstate 77 in Guernsey County and Ohio State Route 7 in Belmont County. In 1998, the Market Development Alliance of the composites industry organized the extraction and testing of samples of these dowel bars. Glass fiber reinforced polymer (GFRP) dowel bars were found to be virtually unaffected by approximately 15 years of field service and exposure in pavement service.

In 1997, FRP dowel bars were installed in a high-performance pavement project on the U.S. Route 65 bypass near Des Moines, IA. Lengths of the pavement sections with FRP dowels were 134.11 and 127.10 m (440 and 417 ft) with 6.10-m (20-ft) joint spacing (skewed) and dowel bars on 30.48- and 20.32-cm (12- and 8-inch) spacing, respectively. Indications are that the FRP dowels have been performing well. Additional alternative dowel bar projects utilizing FRP dowels have been installed in Illinois, Iowa, Kansas, Minnesota, Ohio, Wisconsin, and Manitoba.

Brown and Bartholomew found that FRP dowels made of vinyl ester resins compared well with steel dowels in the scaled model tests.⁽⁶⁾ Experimental load transfer percentages were in agreement with theoretical values and fell within the 35–40 percent range predicted for standard joints under typical subgrade conditions. They recommend an approximately 20–30 percent increase in dowel diameter to maintain deflections, concrete bearing stresses, and load transfer percentages at comparable levels with joints containing steel dowels.⁽⁶⁾

Ahmed et al. from the University of Manitoba, Canada, have conducted research on GFRP dowels.⁽⁷⁾ In their experimental program, a round GFRP dowel bar having a 38-mm (1.5-inch) diameter and a concrete-filled GFRP pipe having a 60-mm (2.36-inch) outside diameter were evaluated in a laboratory setting and in a field implementation. The field test section was constructed on a regional highway in Winnipeg, Manitoba.⁽⁷⁾

They concluded that GFRP dowels subjected to Falling Weight Deflectometer tests in the field showed that LTEs of GFRP dowels were comparable to those produced by steel dowels, provided that the diameter of the GFRP dowel was 20–30 percent larger than the steel dowel. The larger diameter resulted in a reduction in bearing stresses that in turn reduced the potential for faulting.

Tests conducted by Eddie et al. showed the joint effectiveness of GFRP dowels to be in the range of 86–100 percent using a weak subgrade, and 90–97 percent using a stiff subgrade.⁽⁸⁾ An American Concrete Pavement Association (ACPA) criterion for successful joint load transfer is 75 percent.⁽⁸⁾

Porter and other researchers at Iowa State University studied the use of GFPR dowels for JPCP with contraction.⁽⁹⁾ They concluded the following:

- The 3.81-cm (1.5-inch)-diameter GFRP dowels spaced at 30.48-cm (12-inch) centers were inadequate in transferring load for the anticipated design life of the pavement.
- The 3.81-cm (1.5-inch)-diameter GFRP dowels spaced at 15.24-cm (6-inch) centers were effective in transferring load over the anticipated design life of the pavement.⁽⁹⁾

The literature review indicates contradictory conclusions on the LTE of 3.81-cm (1.5-inch) FRP dowels. Suggestions are also provided by the researcher to increase dowel bar diameter from 3.81 cm (1.5 inches) to 4.45 cm (1.75 inches). Some researchers have noted increased RD with an increased diameter. Hence, it was decided to utilize 3.81- and 2.54-cm (1.5- and 1.0-inch) dowel diameters in this research with 69.47 percent and 72 percent FWF, respectively. Chapter 3 describes materials and laboratory test setup used in this research.

CHAPTER 3. MATERIALS, EQUIPMENT, AND LABORATORY TESTING PROCEDURES

INTRODUCTION

Mechanical properties of dowel bars affect the behavior and performance of JPCP provided with FRP and steel dowels. This chapter discusses mechanical properties of FRP and steel dowels and test setup in the Major Units Laboratory of WVU. Seven full-scale JPCPs (two with a dimension of 30.48 by 30.48 by 304.8 cm (12 by 12 by 120 inches) and five with a dimension of 30.48 by 27.94 by 304.8 cm (12 by 11 by 120 inches) were cast with simulated contraction or sawcut joints. The specimens were subjected to both static load and fatigue load with a frequency of about 4.0 Hz.

MATERIAL PROPERTIES

Class K concrete (25.856 and 31.026 MPa (3,750 and 4,500 psi) and two different diameters (3.81 and 2.54 cm (1.5 and 1.0 inch)) of GFRP dowel and epoxy-coated steel dowels were used for casting the concrete pavements in the structural laboratory. Relevant material properties are provided in this section.

The two slabs that were used for preliminary testing consisted of f'_c of 25.856 MPa (3,750 psi); the remainder of the five slabs consisted of f'_c of 31.026 MPa (4,500 psi), as found through cylinder tests.

GFRP Dowels

GFRP dowels provided by independent manufacturers are pultruded with continuous E glass filaments and polyester resin. Typically, filaments are drawn through a resin bath, sized by an appropriate die, to form the dowel bar. An ultraviolet inhibitor is added to the resin to resist effects of sunlight. Dowels with 3.81- and 2.54-cm (1.5- and 1.0-inch) diameters were used in this project. Other researchers have commented on using 4.45-cm (1.75-inch)-diameter FRP dowel bars instead of 3.81-cm (1.5-inch)-diameter dowel bars. However, researchers have noted that increased bar diameter result in larger RD. Hence, it was decided to use lower diameter bars in this research.⁽⁹⁾

Figure 3 shows two types of GFRP dowels used in this research. Table 1 and table 2 show properties of FRP bars listed by the manufacturer.



Figure 3. Photo. FRP dowels (2.54 and 3.81 cm (1.0 and 1.5 inches) in diameter).

Table 1. Modulus of elasticity (MOE) test results of FRP rod specimens—ASTM D3916

Type	Nominal Diameter (inches)	Actual Diameter (inches)	Area Square (inches)	Ultimate Load (lbs)	Tensile Stress (psi)	Elongation (percent)	MOE (Msi)
A	1.0000	0.9713	0.7394	66,539	89,986	0.094	6.0
	1.0000	0.9700	0.7390	65,204	88,235	0.091	6.0
Average	1.0000	0.9707	0.7392	65,872	89,111	0.093	6.0
B	1.5000	1.4932	1.7512	134,440	76,772	0.219	5.2
	1.5000	1.4933	1.7514	137,000	78,226	0.179	5.0
Average	1.5000	1.4933	1.7513	135,720	77,499	0.199	5.1

1 inch = 2.54 cm

1 inch² = 2.54 cm²

1 psi = 0.006895 MPa

1 million psi (Msi) = 6.895 GPa

Table 2. Shear test results of FRP rod specimens—single-shear fixture.

Type	Nominal Diameter (inches)	Actual Diameter (inches)	Area Square (inches)	Ultimate Load (lbs)	Shear Stress (psi)
A	1.0000	0.9703	0.7390	28,600	38,700
	1.0000	0.9700	0.7380	30,300	41,060
	1.0000	0.9702	0.7390	27,200	36,810
Average	1.0000	0.9702	0.7387	28,700	38,857
B	1.5000	1.4923	1.7490	33,982	19,429
	1.5000	1.4935	1.7519	31,782	18,142
Average	1.5000	1.4929	1.7505	32,882	18,786

1 inch = 2.54 cm

1 inch² = 2.54 cm²

1 lb = 0.454 kg

1 psi = 0.006895 MPa

Steel Dowels

The steel dowels used in this research, shown in figure 4, were grade 40 plain uncoated steel or epoxy-coated steel. Dowels with 3.81- and 2.54-cm (1.5- and 1.0-inch) diameters were used for laboratory experiments and field installation.



Figure 4. Photo. Steel dowels 3.81 and 2.54 cm (1.5 and 1.0 inches) in diameter.

Concrete

Class K ready-mixed concrete was used for laboratory slab casting. The compressive strength of the concrete was 25.856 MPa (3,750 psi) for 30.48-cm (12-inch)-thick slabs and 31.026 MPa (4,500 psi) for 27.94-cm (11-inch)-thick slabs. Concrete was poured in formwork, and forms were removed after 24 hours. The concrete beams were cured 28 days by wet burlap and plastic sheet covering.

Base

To simulate a stiff subgrade used in the field, a base layer of limestone aggregates was prepared and compacted to a depth of 40.64 cm (16 inches) in a wood-framed bin shown in figure 5. The modulus of subgrade reaction k was determined from plate loading tests in the laboratory. Based on the measured values, an average of 11.072 kg/cm³ (400 lbs/pci) was used for all tests employing aggregate base. The value was also applied to the theoretical calculations.

FORMWORK

Figure 5 and figure 6 show wood formworks made for casting concrete slabs in the laboratory.

TEST SETUP

Specimen Fabrication

Seven different slabs were cast with FRP and steel dowels using different spacing and diameters.

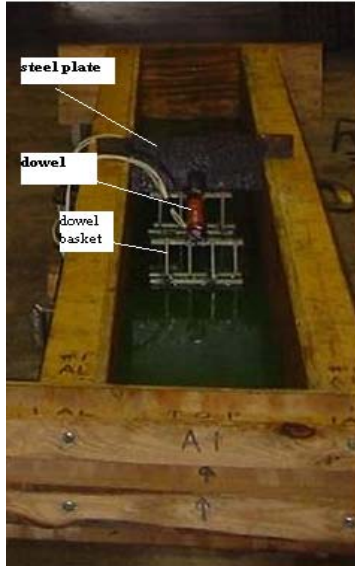
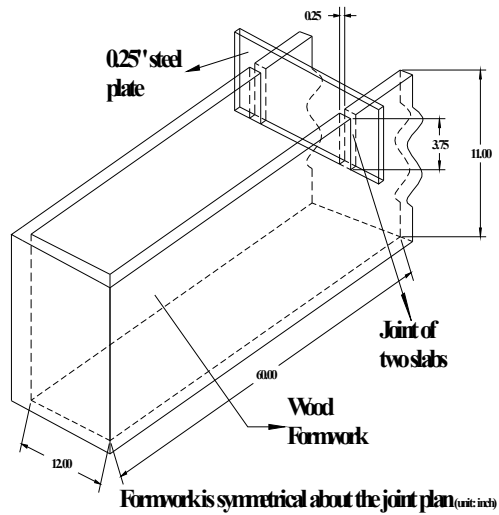


Figure 5. Photo. Wood formwork.



1 inch = 2.54 cm

Figure 6. Diagram. Dimensions of formwork.

Material Preparations

FRP and steel dowels were prepared with slots at locations where strain gauges were going to be placed.

Uniaxial strain gauges were bonded to dowels at the slot position shown in figure 7. Strain gauges were protected using M-Coat-J (polysulfide liquid polymer).

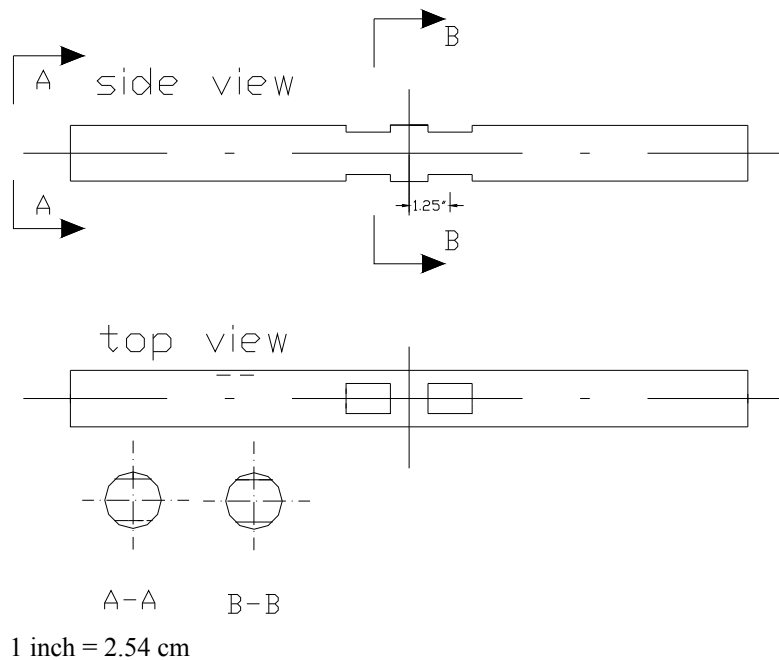


Figure 7. Diagram. Trimmed dowel bar.

Pavement Slab Casting

The inside walls of the wood formworks were oiled so that the concrete pavement slabs could be easily demolded. Strain gauge instrumented dowels were then placed in dowel baskets to properly center them in the joint (figure 8). A steel plate with 0.635-cm (0.25-inch) thickness was placed in the middle to simulate a contraction or sawcut joint in the concrete pavement (figure 5, figure 6, and figure 8).

Figure 9 through figure 12 show the slab casting. Class K concrete conforming to the West Virginia Department of Transportation (WVDOT), Department of Highway (DOH) specification was used for casting (figure 11). Concrete cylinders were cast simultaneously to obtain concrete compressive strength. Twenty-four hours after casting the beams and cylinders, curing was carried out using wet burlaps.



Figure 8. Photo. Instrumented dowels and steel plate positioned in the wood formwork.



Figure 9. Photo. Placing concrete into the formwork.



Figure 10. Photo. Dowel being covered by concrete.



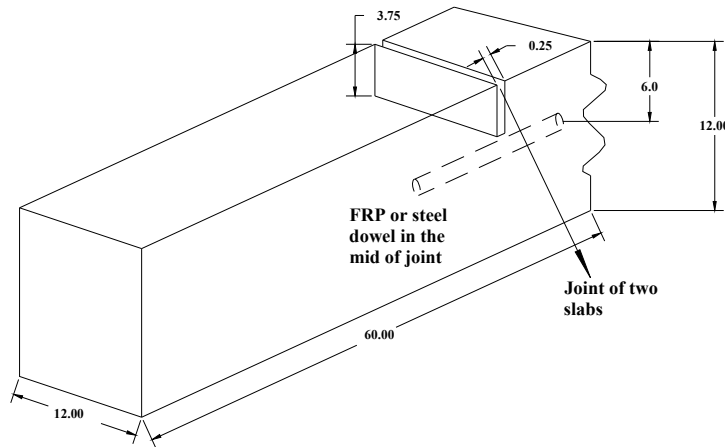
Figure 11. Photo. Casting concrete cylinders.



Figure 12. Photo. Surface finished specimens.

Test Specimens

Two specimens with dimensions of 30.48 by 30.48 by 304.8 cm (12 by 12 by 120 inches) (figure 13) were cast for preliminary tests. Only FRP or steel dowels were used as load transfer devices in these two specimens.



specimen is symmetrical about the joint plan (unit: inch)

1 inch = 2.54 cm

Figure 13. Diagram. Concrete slabs for preliminary tests.

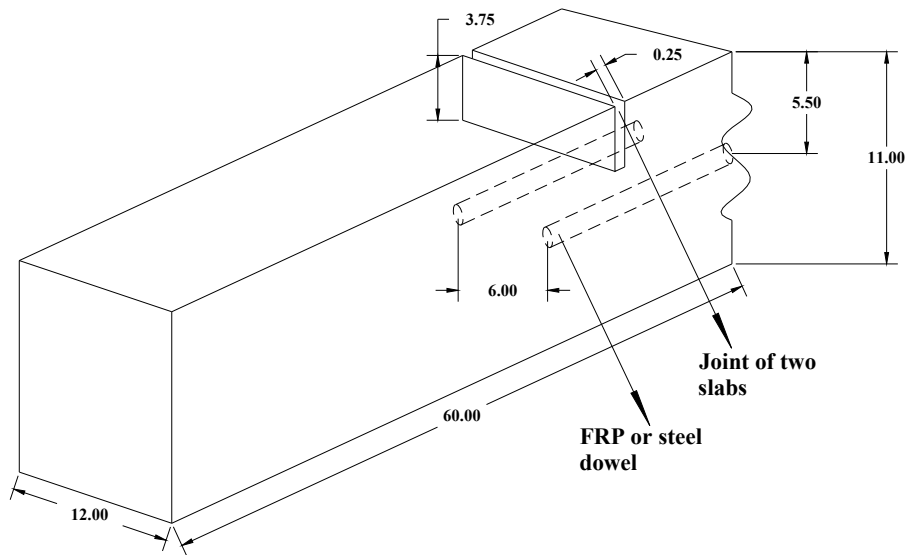
Five different concrete slabs were cast with FRP and steel dowels with different spacings and diameters (table 3). Two embeddable strain gauges were positioned vertically on both sides of a dowel across the joint to measure concrete strain at loaded side and unloaded side. Details of concrete specimens and dowels are provided in figure 14, figure 15, and table 3.

Table 3. Dowel details in specimens.

	Specimen Number	Slab Depth (inches)	Dowel Material	Dowel Diameter (inches)	Spacing (inches) c/c	Number of Dowels in Each Specimen
Preliminary group	PG-1	12	FRP	1.5	12	1
	PG-2		FRP	1.5		
Group 1	1	11	Steel	1.0	6	2
	2		FRP	1.0		
	3		FRP	1.5		
Group 2	4	11	FRP	1.5	12	1
	5		Steel	1.5		

c/c = Center to center

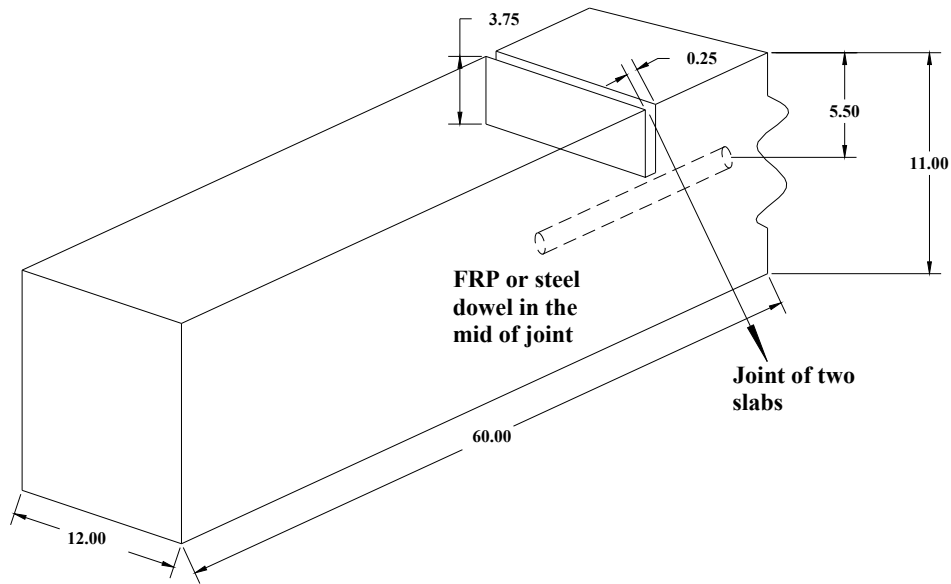
1 inch = 2.54 cm



specimen is symmetrical about the joint plan (unit: inch)

1 inch = 2.54 cm

Figure 14. Diagram. Concrete slabs containing two dowels.



specimen is symmetrical about the joint plan (unit: inch)

1 inch = 2.54 cm

Figure 15. Diagram. Concrete slabs containing only one dowel.

Test Setup and Instrumentation

Jointed concrete slabs were placed on an aggregate base inside a wooden box to simulate field conditions. The base was 15.24 cm (6 inches) high, 45.72 cm (18 inches) wide, and 304.8 cm (120 inches) in length. The modulus of subgrade reaction k was obtained from tests on this base through load application on a standard steel plate.⁽¹⁰⁾

Pavement load was applied on one side of the joint (figure 16 and figure 17) using a 244.65-kN (55-kip) hydraulic actuator system through a controller. A 0.635-cm (0.25-inch)-thick steel plate 25.4 by 40.64 cm (10 by 16 inches) was connected to the actuator to simulate the load from a dual tire wheel load. An additional neoprene pad was used between the steel plate and the concrete surface to prevent any local damage during the test. Two calibrated linear variable differential transformers (LVDTs) were used to measure joint deflections at the loaded and unloaded sides of the joint. Strain gauges, LVDTs, and the load cell from the actuator were connected to a data acquisition system to automatically record data during the tests.



Figure 16. Photo. Experimental setup.



Figure 17. Photo. LVDTs positioned on both sides of the joint.

Static Testing

Load was applied at different increments to simulate an HS25 wheel load and/or higher load. Deflections and strains were recorded automatically by the data acquisition system. Details of the load applied on different concrete slabs are shown in table 4.

Table 4. Details of static testing.

Specimen Number	Load Range
Slab number 1	0–12.5 kips
Slab number 2	0–12.5 kips
Slab number 3	0–12.5 kips
Slab number 4	0–11 kips
Slab number 5	0–11 kips

1 kip = 4.448 kN

Fatigue Testing

The load from the hydraulic actuator system was set at the required range of fatigue cycles (table 5) and was applied using a sine wave. After every 1 million cycles, a static test was conducted on the pavement system to measure strain and deflections. Details of fatigue tests are provided in table 5.

Table 5. Details of fatigue testing.

Specimen Number	Load and Range (kips)					
	0–1	1–1.25	1.25–2	2–3	3–4	4–5
Number of cycles (million)	0–1	1–1.25	1.25–2	2–3	3–4	4–5
Slab number 1	2–12.5	2–18.75	2–18.75	2–18.75	2–18.75	2–18.75
Slab number 2	2–12.5	2–18.75	2–18.75	—	—	—
Slab number 3	2–12.5	2–12.5	—	—	—	—
Slab number 4	2–11	2–11	2–11	2–11	2–11	2–11
Slab number 5	2–11	2–11	2–11	2–11	2–11	2–11

— No loading at corresponding cycles.

For specimens 1, 2, and 3, an overload factor of 1.5 (i.e., 1.5 by HS25) was used to apply higher load during fatigue tests after 1 million cycles.

1 kip = 4.448 kN

It should be noted that slabs number 1 through 3 had 55.60 kN (12.5 kips), and slabs number 4 and 5 had 48.93 kN (11 kips) of loading corresponding to HS25 loading as described in chapter 6 of this report.

CHAPTER 4. EXPERIMENTAL RESULTS AND DISCUSSION

INTRODUCTION

Experimental setup used in the Major Units Laboratory was previously discussed in chapter 3. This chapter discusses the experimental results of five jointed concrete slabs with FRP or steel dowels. Parameters evaluated in these tests under static and fatigue loads included the following:

- LTE.
- RD between loaded and unloaded pavement.
- Strain on dowels.

Before discussing these three parameters, joint crack patterns observed in the tests are presented. Joint crack patterns have significant effects on LTE, RD, and dowel strains.

Parameters of two preliminary tests conducted on two pavement slabs with FRP dowels and actual main tests are listed in table 6. Slabs with 15.24-cm (6-inch) spacing were placed in group 1, whereas slabs with 30.48-cm (12-inch) spacing were placed in group 2.

Table 6. Parameters of dowel groups.

Group	Slab Number	Center-to-Center Spacing (inches)	Number of Dowels in Slab	Concrete Strength (psi)	Dowel Material	Dowel Diameter (inches)
Preliminary group	PG-1	12	1	3,500	FRP	1.5
	PG-2					
Group 1	1	6	2	4,500	FRP	1.0
	2				Steel	1.0
	3				FRP	1.5
Group 2	4	12	1	4,500	FRP	1.5
	5				Steel	1.5

1 inch = 2.54 cm

1 psi = 0.006 895 MPa

JOINT CRACK PATTERNS OBSERVED IN LABORATORY TESTS

Cracks in JPCP specimens occurred at two locations: one was right at the joint, and the other was directly under the loading zone, close to dowel edge. Figure 18 through figure 20 show the following three types of crack patterns observed in tests (also refer to table 7):

- Type I—Crack occurred only in the joint (figure 18).
- Type II—Cracks occurred at joint and loading zone close to dowel edge (figure 19).

- Type III—Crack occurred away from the joint at the dowel edge in the loading zone (figure 20).



Figure 18. Photo. Typical crack observed in slabs number 1, 4, and 5 (table 7).



Figure 19. Photo. Crack observed in slab number 2 (table 7).



Figure 20. Photo. Typical crack observed in slab number 3 (table 7).

Table 7. Cracks in the tested slabs.

Group Number	Specimen	Dowel Material	Concrete Strength (psi)	Dowel Diameter/ Spacing (inches)	Number of Dowels in Specimen	Crack Pattern
Preliminary group	PG-1	FRP	3,500	1.5 at 12 c/c	1	I
	PG-2					
Group 1	Slab number 1	FRP	4,500	1.0 at 6 c/c	2	I
	Slab number 2	Steel		1.0 at 6 c/c		II
	Slab number 3	FRP		1.5 at 6 c/c		III
Group 2	Slab number 4	FRP	4,500	1.5 at 12 c/c	1	I
	Slab number 5	Steel				I

c/c = Center to center
 1 inch = 2.54 cm
 1 psi = 0.006 895 MPa

According to table 7, specimens PG-1 and PG-2 and slabs number 1, 4, and 5 had crack formation at the joints. In these cases, dowels provided maximum load transfer across the joints. This was the scenario expected to occur in the field.

In slab number 3, a crack occurred at the loaded zone only, away from the sawcut junction of two slabs. Under field conditions, such joint formation would not contribute to effective load transfer. At most, it would be expected that only a very small portion of the applied load would be transferred across this crack. Joint formation at unintended locations may facilitate concrete expansion or contraction due to field thermal variations. In slab number 2, cracks occurred at both joint and load zone locations.

The reason for cracks occurring away from mid-joint and under the loading zone could possibly be attributed to the uneven base surface under the loaded side of the slab. Because the slabs were not cast directly on the aggregates as in the field construction method, when the load was applied, the uneven surface including possible gradients could cause enough stress concentration at the dowel edge to lead to concrete cracking prior to load transfer.

PRELIMINARY TESTS

Preliminary static tests were conducted on two slabs consisting of one 3.8-cm (1.5-inch)-diameter FRP dowel at 30.48 cm (12 inches) center to center (c/c). LTEs obtained from these static tests were both greater than 90 percent, i.e., much higher than 60 percent of LTE as recommended by ACPA (corresponding to 75 percent of joint effectiveness, E).⁽¹¹⁾

JOINT DEFLECTIONS AND JOINT LTE

Deflections of dowel-connected slabs were measured using LVDTs positioned at both loaded and unloaded sides of joints. LTE and RDs were then calculated from measured deflections.

Joint RD

Joint RD of Group 1

Slab number 1 consisted of two 2.54-cm (1.0-inch)-diameter FRP dowels with spacing of 15.24 cm (6 inches) (refer to figure 8, figure 14, and table 7). Static tests were conducted according to table 8. RD versus applied load is shown in figure 21.

Table 8. Static load applied for specimen 1.

Specimen Number	Load Range
1	0 to 55.603 kN (0 to 12.5 kips)

Note: 55.603 kN (12.5 kips) was applied corresponding to HS25 load.

After static testing, fatigue tests were conducted up to 5 million cycles (table 9). Figure 21, figure 22, and figure 23 show the RDs obtained from tests. It should be noted that 83.404 kN (18.75 kips) (1.5 times HS25 loading) was applied to the joint after 1 million cycles.

Table 9. Load applied for fatigue tests on slab number 1.

Slab Number	Wave Shape	Frequency (Hz)	0 to 1 Million Cycles	1 to 5 Million Cycles
1	Sine	4.0	2–12.5 kips	2–18.75 kips

Note: 55.603 kN (12.5 kips) was applied corresponding to HS25 load, and 83.404 kN (18.75 kips) corresponds to 1.5 times HS25 load.

1 kip = 4.448 kN

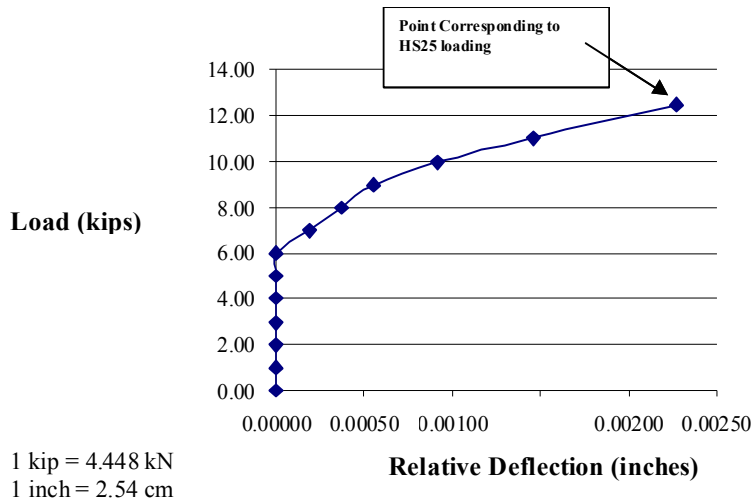
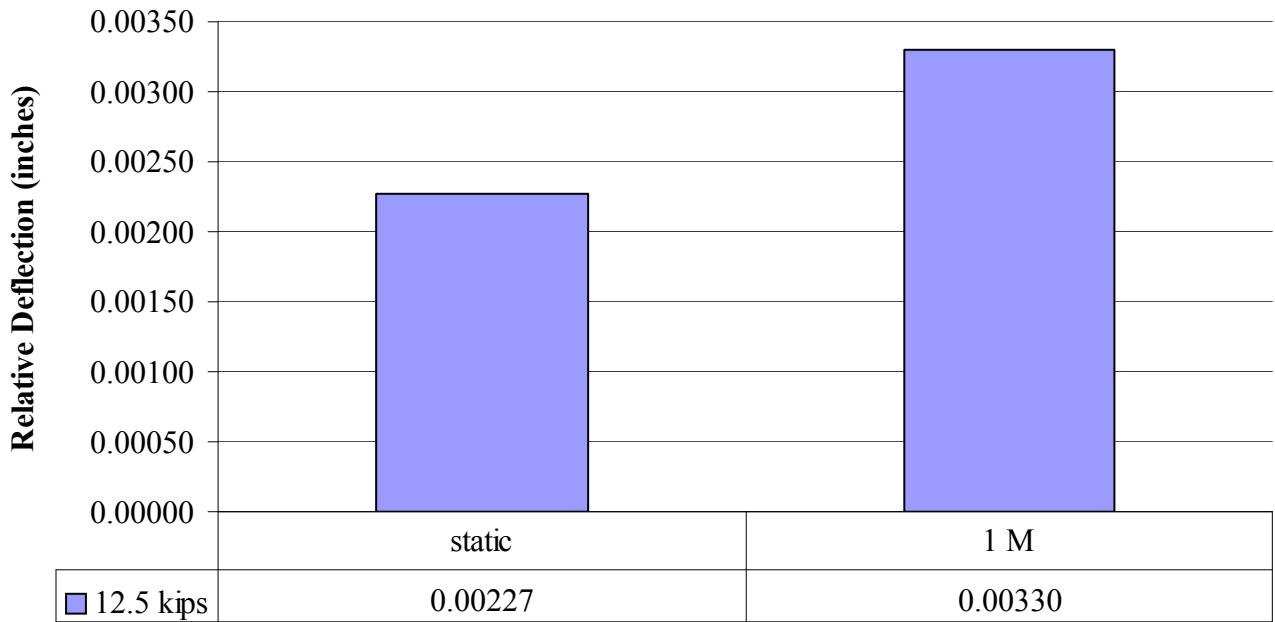
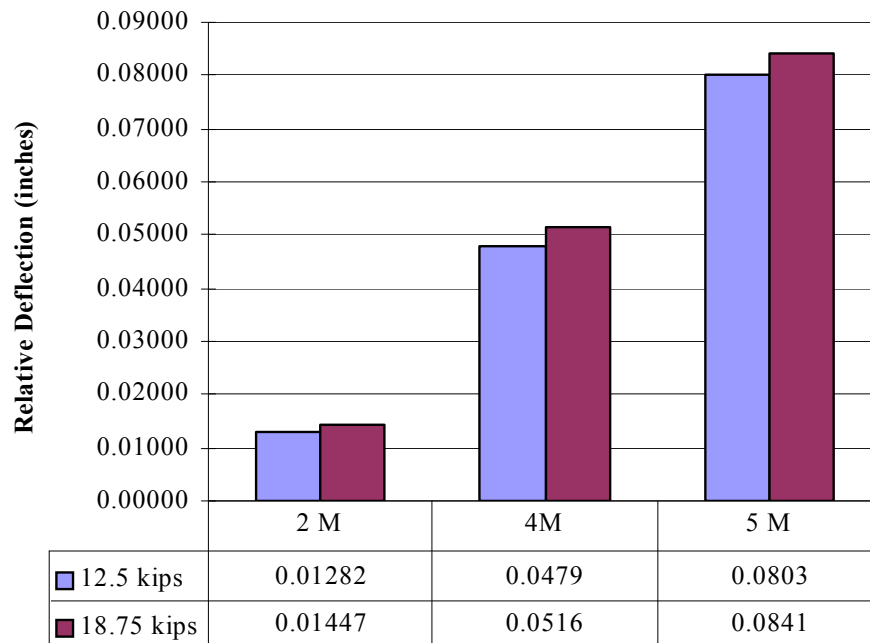


Figure 21. Chart. Joint RD for slab number 1 under static test.



1 kip = 4.448 kN
1 inch = 2.54 cm

Figure 22. Graph. RDs under HS25 loading for slab number 1 at joint width of 0.635 mm (0.25 inch) (static and 1 million cycles).

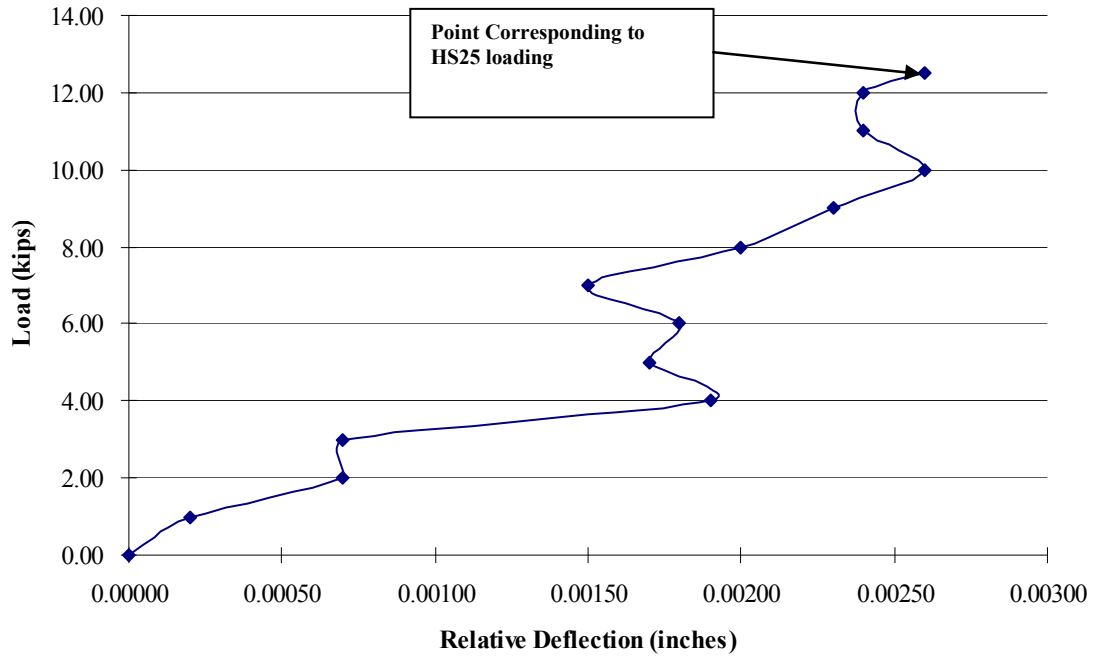


1 kip = 4.448 kN
1 inch = 2.54 cm

Figure 23. Graph. RDs for slab number 1 under fatigue tests (joint width increased from 0.635 cm (0.25 inch) to 1.016 mm (0.4 inch) from 2 to 5 million cycles).

In figure 23, the 55.603-kN (12.5-kips) load corresponds to HS25 loading and was applied up to 1 million cycles; 83.404 kN (18.75 kips) corresponds to 1.5 times HS25 loading and was applied for fatigue tests after 1 million cycles and up to 5 million cycles. Also, joint width increased from 0.635 mm (0.25 inch) to 10.16 mm (0.4 inch) during bin and slab repositioning. Thus, the RDs after 1 million cycles due to increased joint width were much greater than those from static and 1 million cycle tests (0.3256 mm (0.01282 inch) at 2 million cycles versus 0.0838 mm (0.0033 inch) at 1 million cycles).

Slab number 2 consisted of two 2.54-cm (1-inch)-diameter steel dowels with 15.24-cm (6-inch) spacing. A static test was conducted on this slab with a load range of 0 to 55.603 kN (0 to 12.5 kips), and crack formation was noticed at the dowel edge under the loading plate. Load versus RD results are shown in figure 24. After static testing, fatigue tests were conducted according to table 10. Because cracks occurred at locations away from the joint, fatigue cycles up to 2 million were applied. Figure 25 shows RDs under fatigue tests. It should be noted that when cracks occur away from mid-joints, only a small portion of the load would be transferred across the joint.



1 kip = 4.448 kN
 1 inch = 2.54 cm

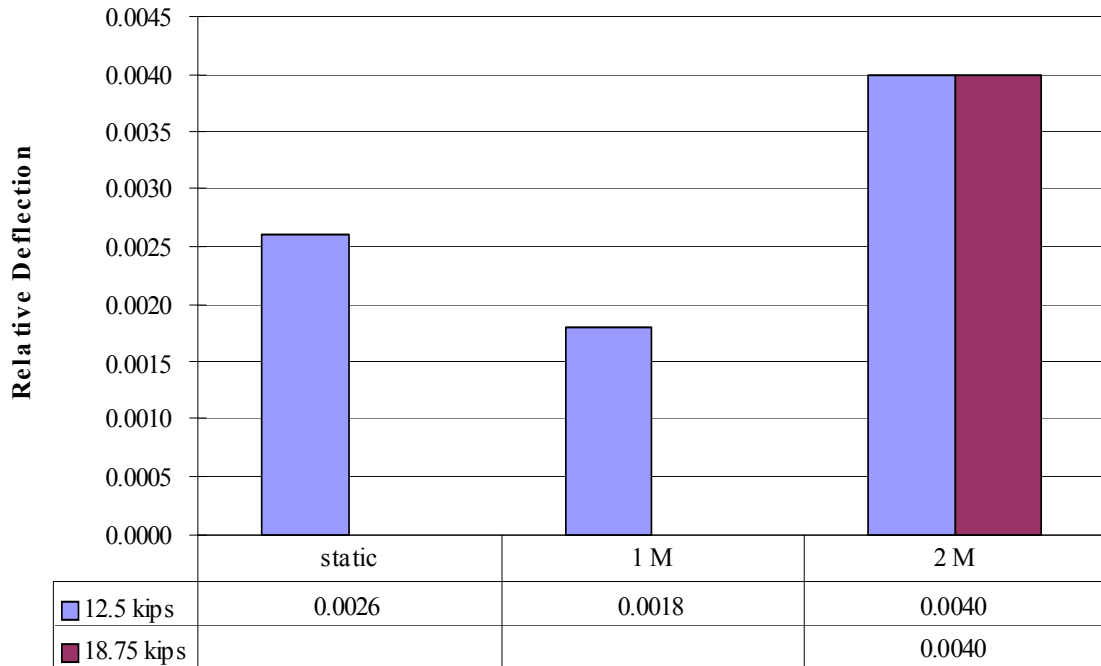
Figure 24. Chart. Joint RD for slab number 2 under static test.

Table 10. Load applied for fatigue tests on slab number 2.

Slab Number	Frequency (Hz)	0–1 Million Cycles	> 1–2 Million Cycles
2	4.0	2–12.5 kips	2–18.75 kips

Note: 55.603 kN (12.5 kips) was applied corresponding to HS25 load, and 83.404 kN (18.75 kips) corresponded to 1.5 times HS25 load.

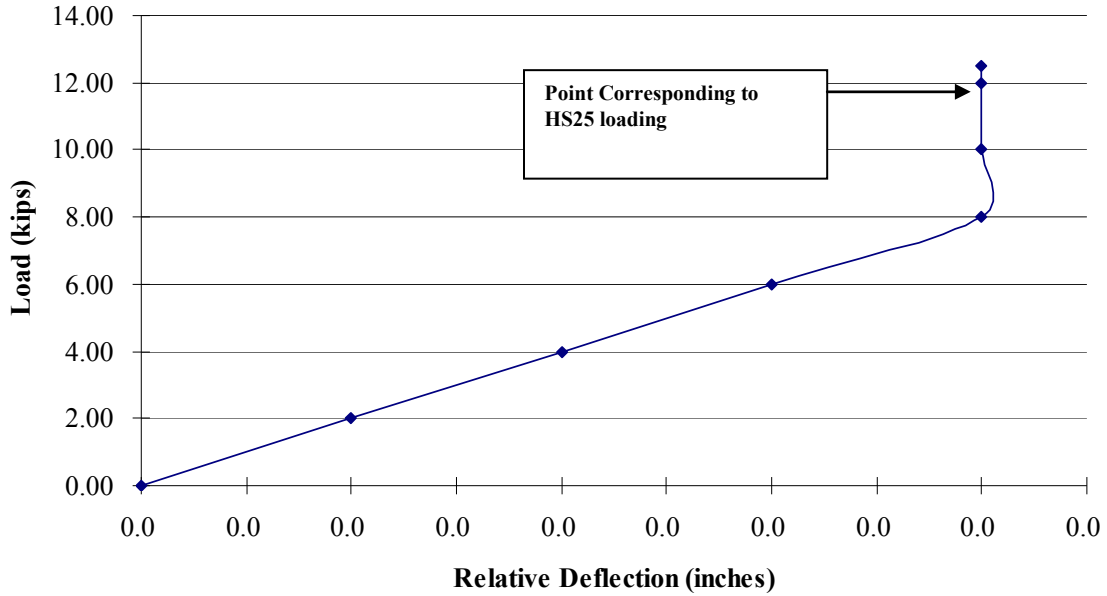
1 kip = 4.448 kN



1 kip = 4.448 kN
 1 inch = 2.54 cm

Figure 25. Graph. RDs for specimen 2 (0 to 2 million cycles).

Slab number 3 consisted of two 3.81-cm (1.5-inch)-diameter FRP dowels with 15.24-cm (6-inch) spacing. Static deflections were measured for a load range from 0 to 55.603 kN (0 to 12.5 kips), and the details are shown in figure 26. Crack locations were away from the mid-joint; hence, fatigue tests were conducted up to only 1.25 million cycles (refer to table 11). Table 11 details the load applied for fatigue tests on slab number 3. Figure 27 shows the RDs under fatigue tests. Deviations observed in RD values from slab number 3 were due to crack formation under the loading plate at the dowel edge.



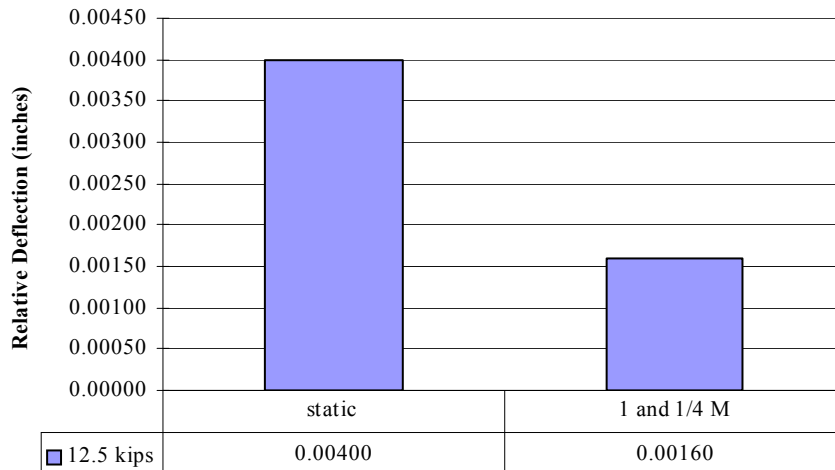
1 kip = 4.448 kN
 1 inch = 2.54 cm

Figure 26. Chart. Joint RD for specimen 3 under static test.

Table 11. Load applied for fatigue tests on slab number 3.

Slab Number	Frequency (Hz)	0–1.25 Million Cycles
3	4.0	2 to 12.5 kips

1 kip = 4.448 kN

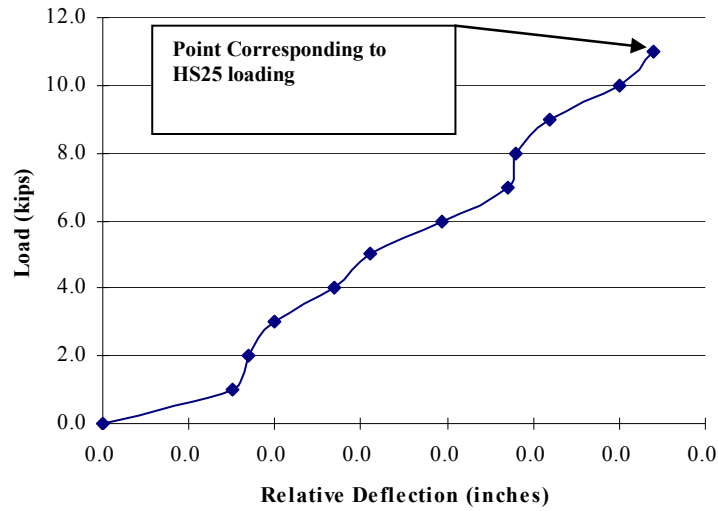


1 kip = 4.448 kN
 1 inch = 2.54 cm

Figure 27. Graph. RDs for specimen 3 (0 to 1.25 million cycles).

Joint RD of Group 2

Slab number 4 consisted of one 3.81-cm (1.5-inch)-diameter FRP dowel representing 30.48-cm (12-inch) spacing in actual pavement. The static test was conducted in the range from 0 to 48.930 kN (0 to 11 kips). Load versus RD results are shown in figure 28. After the static test, fatigue tests were conducted as per table 12 up to 5 million cycles. Figure 29 and figure 30 show pavement deflections and RDs under fatigue testing.



1 kip = 4.448 kN

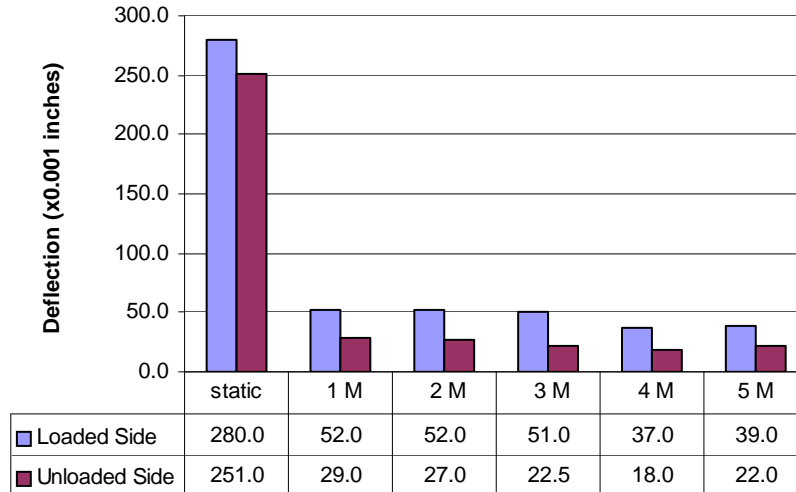
1 inch = 2.54 cm

Figure 28. Chart. Joint RD for specimen 4 under static test.

Table 12. Load applied for fatigue tests on slab number 4.

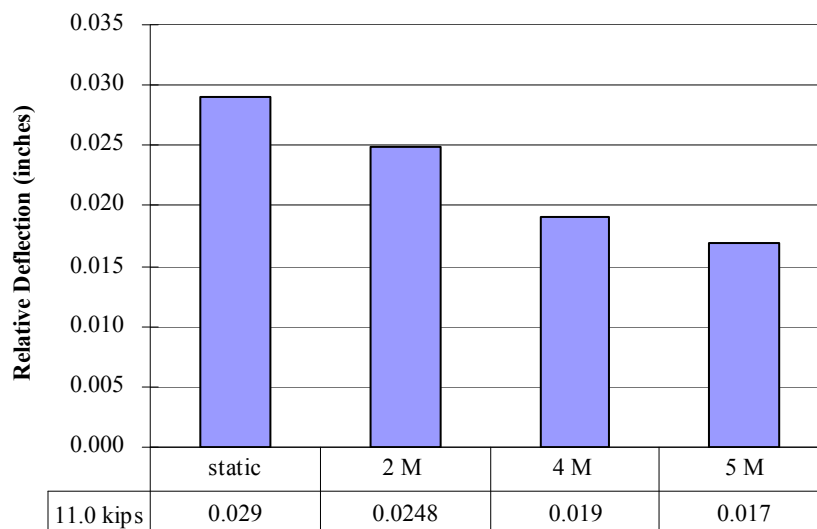
Slab Number	Frequency (Hz)	0 to 5 Million Cycles
4	4.0	2 to 11.0 kips

1 kip = 4.448 kN



1 inch = 2.54 cm

Figure 29. Graph. Pavement deflections under fatigue test for slab number 4 (0 to 5 million cycles, FRP dowel at 30.48 cm (12 inches) c/c).



1 kip = 4.448 kN

Figure 30. Graph. RDs under fatigue test for specimen 4 (0 to 5 million cycles).

Slab number 4 was the first slab tested in the laboratory. Base materials were compacted before starting the test, but, during laboratory fatigue cycles testing, base materials under both sides of the slabs became more compact and the deflections reduced (figure 29). Similar trends were observed under increased fatigue cycles in figure 30. The modulus of subgrade reaction k increased from 11.072 to 22.144 kg/cm³ (400 to 800 pci) after 5 million fatigue cycles.

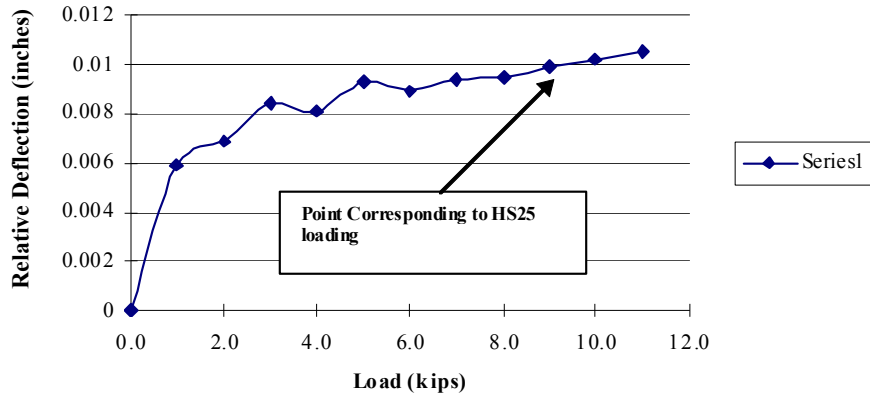
Slab number 5 consisted of one 3.81-cm (1.5-inch)-diameter steel dowel representing 30.48-cm (12-inch) spacing in the pavement. The static test was conducted in the range from 0 to 48.930 kN (0 to 11.0 kips). Fatigue tests were conducted as per table 13. Figure 31 shows the

load versus RD. After static testing, fatigue tests were conducted up to 5 million cycles. Figure 32 shows RDs for slab number 5 under fatigue tests.

Table 13. Load applied for fatigue tests on slab number 5.

Slab Number	Frequency (Hz)	0 to 5 Million Cycles
5	4.0	2 to 11.0 kips

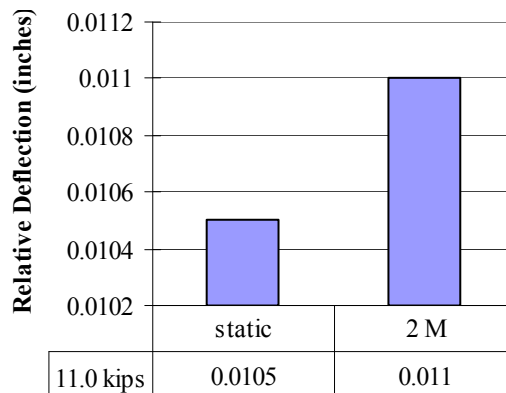
1 kip = 4.448 kN



1 kip = 4.448 kN

1 inch = 2.54 cm

Figure 31. Chart. Joint RD for specimen 5 under static test.



1 kip = 4.448 kN

1 inch = 2.54 cm

Figure 32. Graph. RDs under fatigue test for specimen 5 (0 to 5 million cycles).

Analysis of RD

Analysis for Specimen Group 1 as per Table 6 (15.24-cm (6-inch) Spacing):

For slabs number 1 through 3, static and fatigue test results are summarized in table 14 and table 15, respectively, and their behavior is discussed in following the tables.

Table 14. RD of group 1 from static tests.

Slab Number	Parameters	Static RD (inch)
1	FRP dowel, 1.0 inch at 6 inches c/c	0.00227
2	Steel dowel, 1.0 inch at 6 inches c/c	0.00260
3	FRP dowel, 1.5 inches at 6 inches c/c	0.00400

1 kip = 4.448 kN
1 inch = 2.54 cm

Table 15. RD of group 1 from fatigue tests.

Slab Number	Relative Deflection (inch)				Proper Crack at Mid-joint
	1 M	2 M	4 M	5 M	
1	0.0033 (Joint width = 0.25 inch)	0.0128* [†]	0.0479* [†]	0.0803* [†]	Yes
2	0.0018	0.0040 [†]	—	—	No
3	0.0001	—	—	—	No

* Joint width increased to 1.016 cm (0.4 inch).

[†] An overload factor of 1.5 was used so that 1.5 times HS25 load was applied for specimens 1 and 2 during fatigue tests started after 1 million cycles.

— No loading at corresponding cycles.

1 inch = 2.54 cm

The following results were found:

- The larger RD (0.00660 cm (0.00260 inch)) in slab number 2 with steel dowels compared to that of slab number 1 with FRP dowel (0.00577 cm (0.00227 inch)) can be attributed to the cracking pattern in slab number 2 where joint crack occurred at a place other than the mid-joint.
- Slab number 3 had a much larger RD possibly because the crack formation was close to the edge of the dowel under the steel plate rather than at mid-joint. Therefore, the load transferred by the dowel was less, including a higher RD.
- When a crack occurred at a joint location where it was expected to occur, the RD data from the tests seemed to be more consistent; for example, the RD for slab number 1 increased from 0.00584 to 0.0204 cm (0.0023 to 0.0803 inch).
- Experimental results on RD were sensitive to supporting base stiffness (k). Therefore, base property should be considered before and after each fatigue test.

Analysis for Specimen Group 2 (30.48-cm (12-inch) Spacing):

Test results are summarized in table 16 and table 17.

Table 16. RD of group 2 from static tests.

Slab	Static RD (inch)	Proper Crack at Mid-joint
Number 4 (FRP dowel, 3.81 cm (1.5 inch) at 30.48 cm (12 inches) c/c)	0.029	Yes
Number 5 (steel dowel, 3.81 cm (1.5 inch) at 30.48 cm (12 inches) c/c)	0.011	Yes

1 inch = 2.54 cm

Table 17. RD of group 2 from fatigue tests.

Slab Number	Relative Deflection (inch)		
	2 M	4 M	5M
4	0.025	0.019	0.017
5	0.011	—	—

— No loading at corresponding cycles.

The following was noted:

- Both slabs number 4 and 5 had proper crack occurrence at the joint.
- In static tests (table 17), slab number 4 (3.81-cm (1.5-inch)-diameter FRP dowel) had a larger difference in deflection between loaded and unloaded sides of the pavement (RD) than slab number 5 (3.81-cm (1.5-inch)-diameter steel dowel).
- The RD for both slabs reduced with progression of fatigue load from 0 to 5 million cycles. This was partly attributed to compaction/settlement of aggregate base underneath the pavement slabs with increasing fatigue cycles.
- RD decreased more in slabs with FRP dowels than with steel dowels, which can be partly attributed to simulation in stiffness between FRP and concrete. Benefits of these reductions may be more evident with freeze-thaw variations.
- Experimental results on RD were sensitive to supporting base stiffness (k). It was found that the base property (modulus of subgrade reaction, k) value changed from 11.072 to 22.144 kg/cm³ (400 to 800 pci) after 5 million fatigue cycles.

Joint LTE

Joint LTE (figure 33 through figure 38) was calculated from the results of static and fatigue tests by using equation 1 as follows:⁽¹⁾

$$LTE = \frac{d_U}{d_L} \times 100\% \quad (1)$$

Where:

d_U = Deflection at unloaded side.

d_L = Deflection at loaded side.

ACPA gives joint effectiveness, E , to measure the performance of joints (equation 2):⁽¹¹⁾

$$E = \frac{2d_U}{d_L + d_U} \times 100\% \quad (2)$$

Where:

d_U = Deflection at unloaded side.

d_L = Deflection at loaded side.

ACPA recommends that a pavement joint be considered adequate if the effectiveness is 75 percent or greater. However, LTE and E are related by equation 3:⁽³⁾

$$\text{LTE} = \left(\frac{2}{2 - E} - 1 \right) \times 100\% \quad (3)$$

According to equation 3, an LTE of 60 percent corresponds to an E of 75 percent. When the value of LTE is between 70 and 100 percent, the joint provides sufficient load transfer for heavy loads.

LTE of Group 1

Slab Number 1:

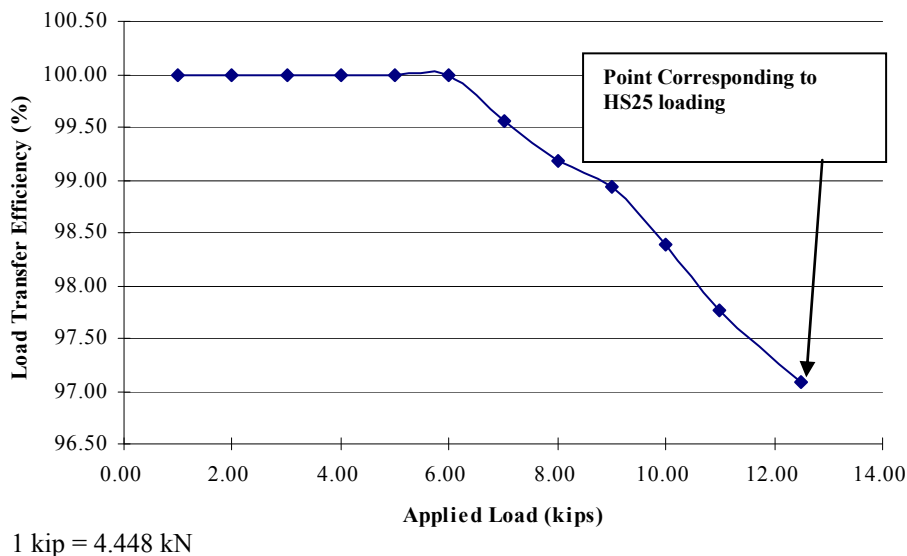
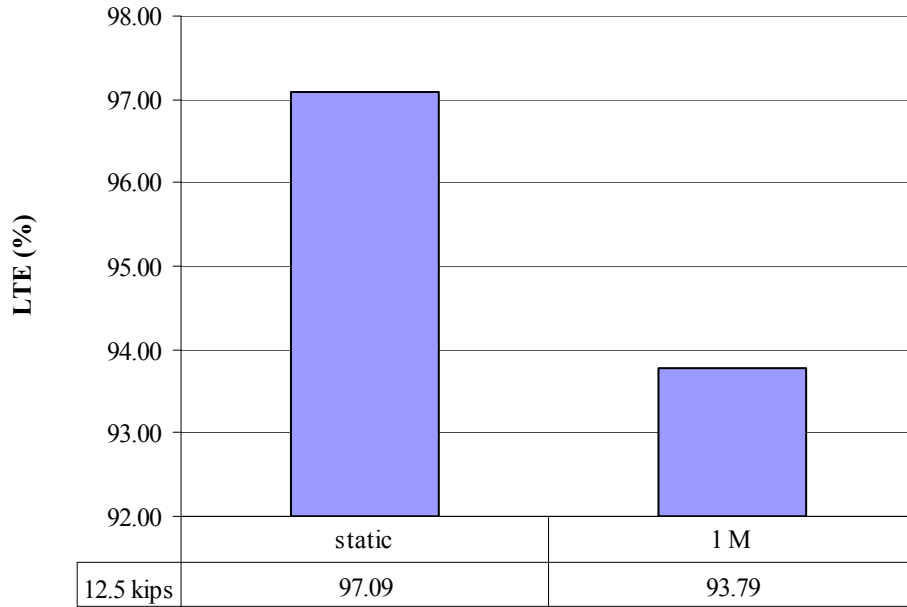


Figure 33. Chart. Joint LTE for slab number 1.



1 kip = 4.448 kN

Figure 34. Graph. LTE corresponding to HS25 loading for slab number 1 (2.54-cm (1.0-inch) diameter at 15.24 cm (6 inches) c/c), static and 1 million cycles.

In figure 35, a load of 55.603 kN (12.5 kips) corresponding to HS25 loading was applied for the static test and 1 million cycles; 83.404 kN (18.75 kips) corresponding to 1.5 times HS25 loading was applied for fatigue tests from 2 to 5 million cycles. Also, joint width was intentionally separated from to 0.635 to 1.016 cm (0.25 to 0.4 inch).

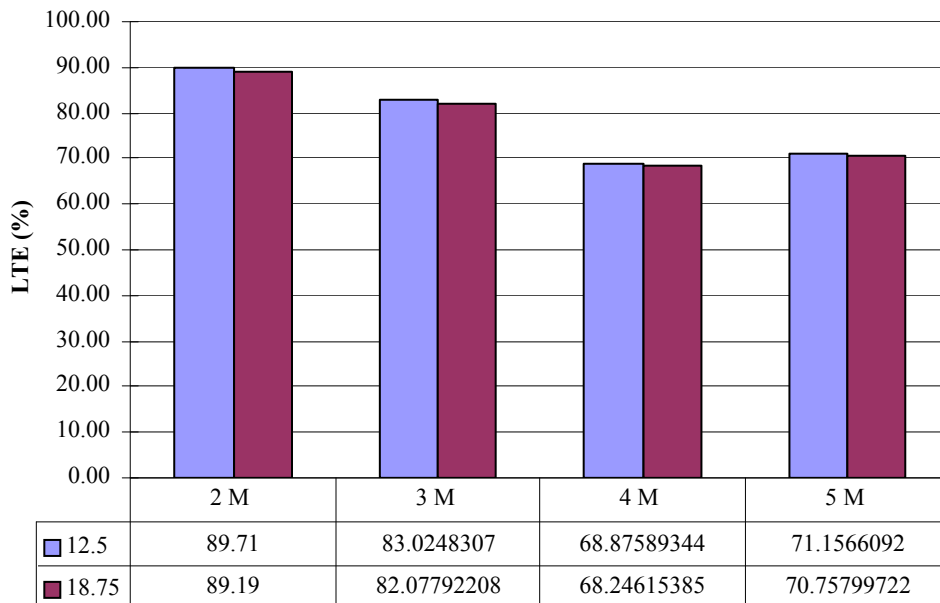


Figure 35. Graph. LTE for slab number 1 under fatigue tests (> 1 million cycles and joint width increased from 0.635 to 1.016 cm (0.25 to 0.4 inch)).

To find the condition of the interface between the FRP dowel and concrete, slab number 1 was separated by cutting the FRP dowel after 5 million cycles of HS25 and higher loading. The dowel-concrete interface was found to be in good shape with no visible microcracks (figure 36).

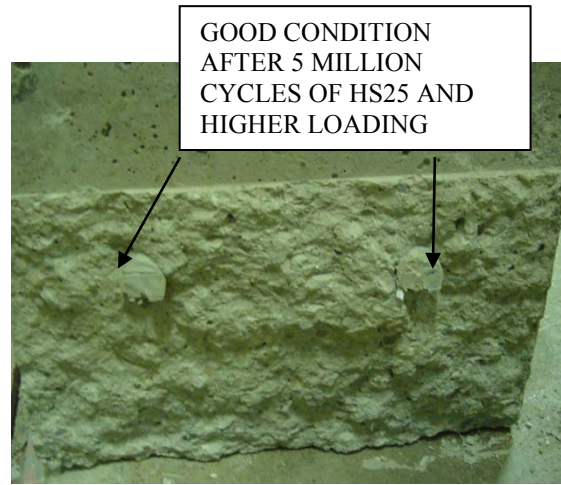
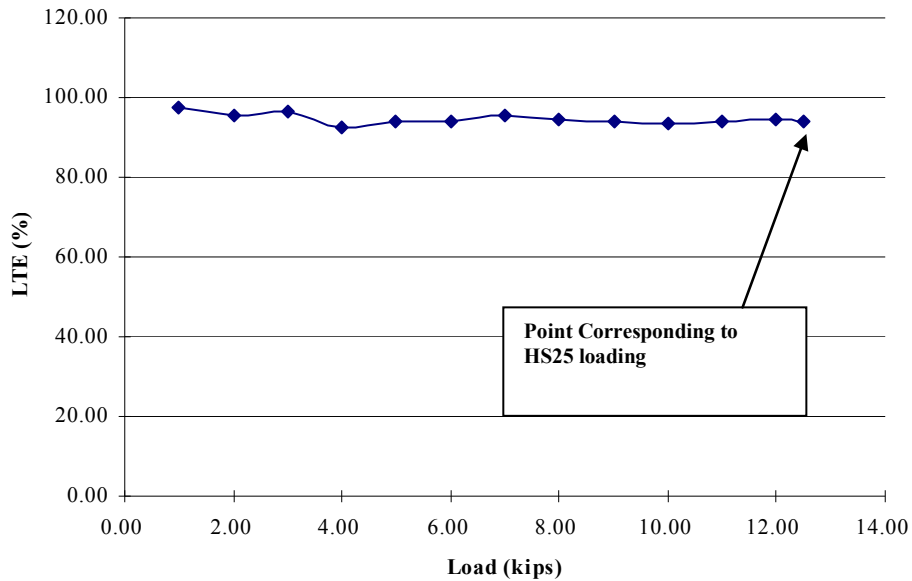


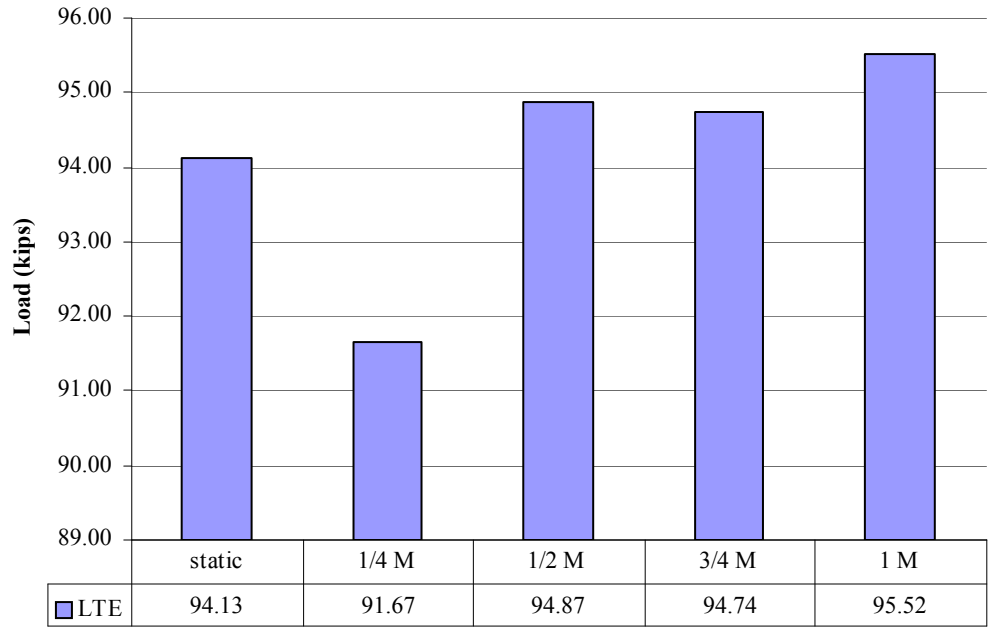
Figure 36. Photo. Dowel-concrete interface condition in slab number 1 after 5 million load cycles.

Slab Number 2:



1 kip = 4.448 kN

Figure 37. Chart. Joint LTE for slab number 2.

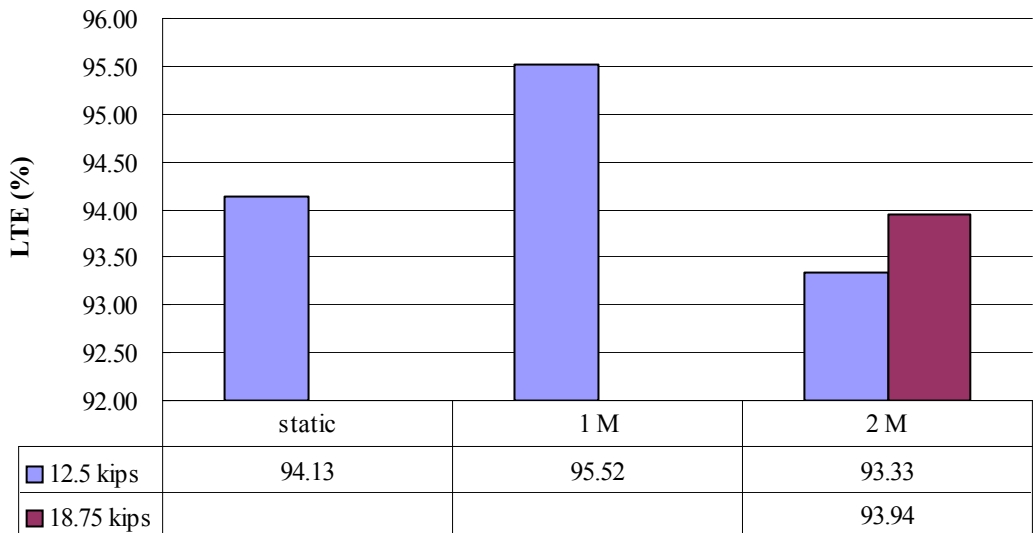


1 kip = 4.448 kN

Figure 38. Graph. LTE under fatigue tests (HS25 loading) for slab number 2 (0 to 1 million cycles).

In figure 39, a load of 55.603 kN (12.5 kips) corresponding to HS25 loading was applied for the static test and up to 1 million cycles; 83.404 kN (18.75 kips) corresponding to 1.5 times HS25 loading was applied for fatigue tests after 1 million cycles.

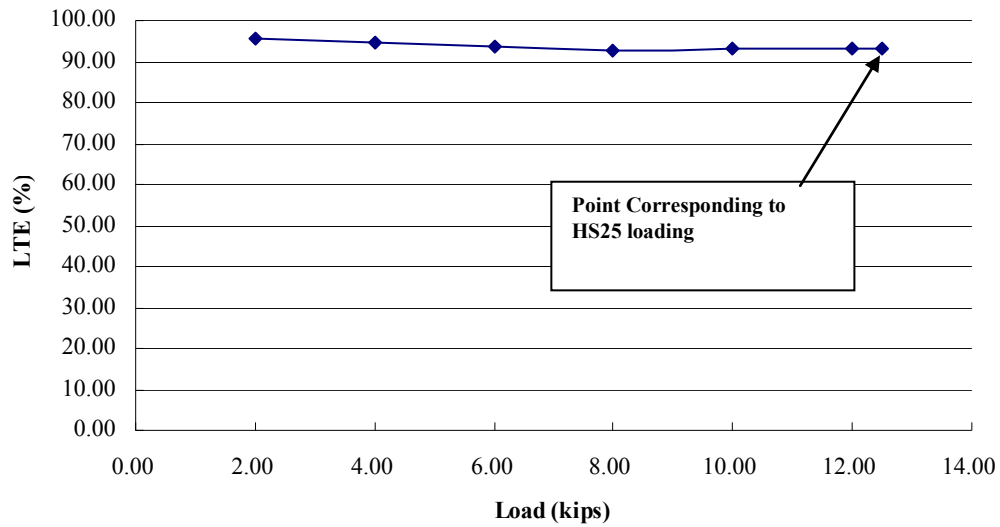
LTE Under Fatigue Load



1 kip = 4.448 kN

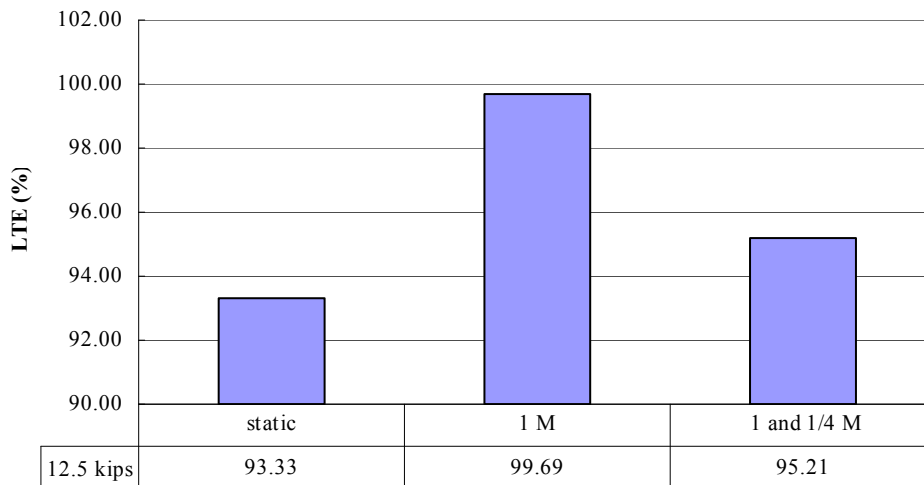
Figure 39. Graph. LTE under fatigue test for slab number 2 (1 to 2 million cycles).

Slab Number 3:



1 kip = 4.448 kN

Figure 40. Chart. Joint LTE for slab number 3.



1 kip = 4.448 kN

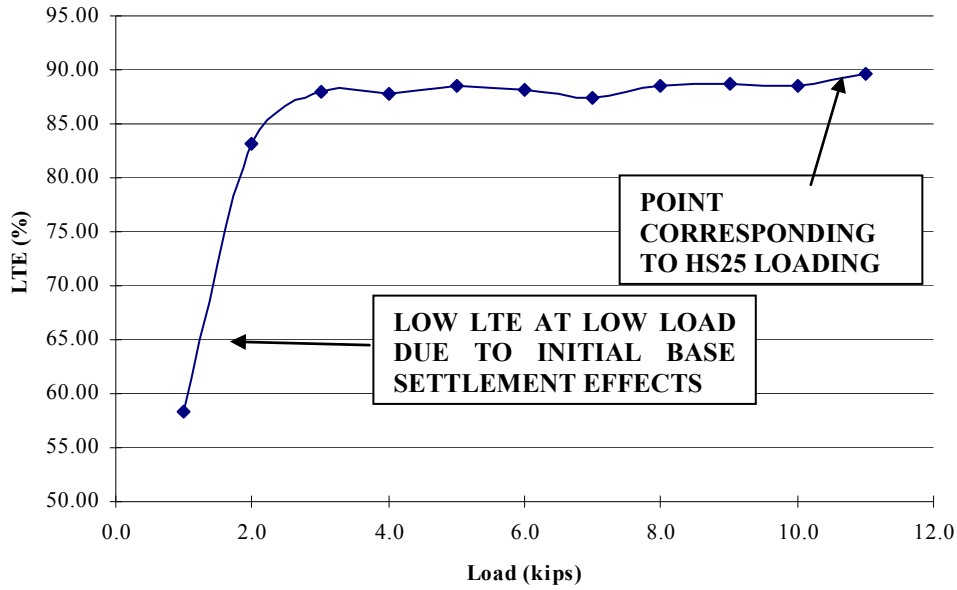
Figure 41. Graph. LTE under fatigue test for slab number 3 (0 to 1.25 million cycles).

The crack that occurred in slab number 3 was away from mid-joint; hence, these results (figure 40 and figure 41) did not have much significance.

Joint LTE of Group 2

Slab Number 4:

During static testing, slab number 4 was subjected to loading up to 48.930 kN (11 kips) corresponding to HS25 loading, and the response is shown in figure 42.



1 kip = 4.448 kN

Figure 42. Chart. Joint LTE for slab number 4.

In fatigue tests, slab number 4 provided good LTE—greater than 80.5 percent after 5 million fatigue load cycles when the base surface and base material under this slab remained in good condition. When base aggregates were not in contact with the slab due to aggregate compaction or slight sideways flexing of the aggregate bin, LTE was found to have been decreased to about 55 percent, which was still around 92.1 percent of the 60 percent LTE which corresponded to the ACPA-recommended value on joint effectiveness (*E*) of 75 percent. Detailed data are shown in figure 43.

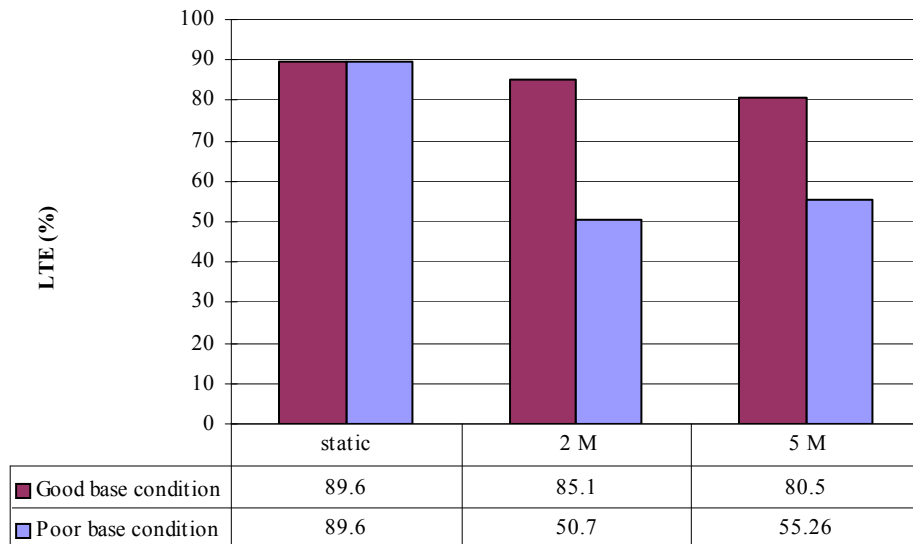


Figure 43. Graph. LTE under fatigue test for slab number 4 (0 to 5 million cycles).

From figure 43, LTE of slab number 4 containing FRP dowels remained at about 80 percent with good base condition. With poor base condition, LTE reduced from 88 percent to 55 percent (92.1 percent of the 60 percent LTE which corresponded to the ACPA-recommended value on joint effectiveness (E) of 75 percent). The poor base condition was observed with a concave slab-base surface due to aggregate compaction and base settlement. Also, it should be noted that the slabs were not cast directly on top of the aggregates, which led to some aggregate repositioning under fatigue loading. The modulus of subgrade reaction k was found changed from 11.072 to 22.144 kg/cm³ (400 to 800 pci) after 5 million cycles in poor base condition.

To find the condition of the interface between the FRP dowel and the concrete, slab number 4 was separated by cutting the FRP dowels after 5 million cycles of HS25 and higher loading. The dowel-concrete interface was found to be in good shape with no visible microcracks (figure 44).

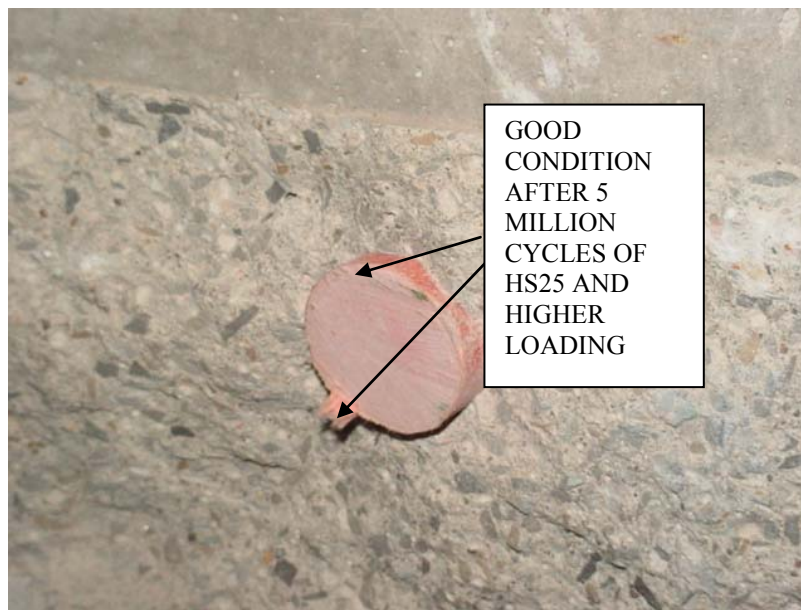
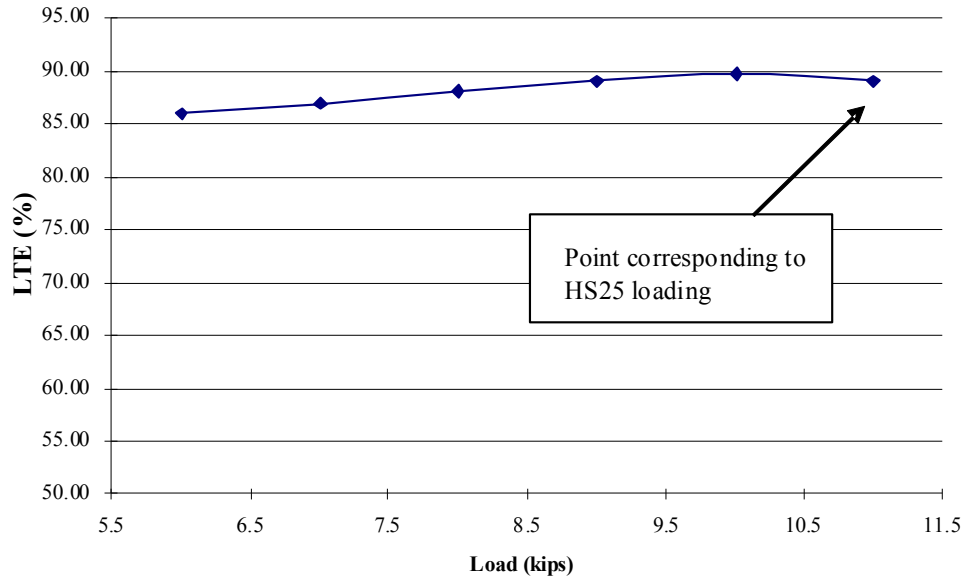


Figure 44. Photo. Dowel-concrete interface condition in slab number 4 after 5 million load cycles.

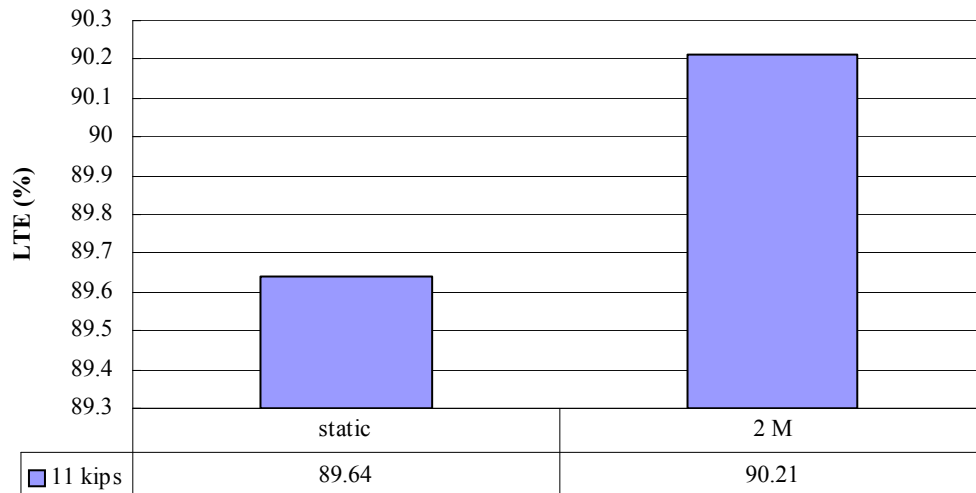
Slab Number 5:

LTE of slab number 5 under static and fatigue loads are shown in figure 45 and figure 46, respectively.



1 kip = 4.448 kN

Figure 45. Chart. Joint LTE for slab number 5.



1 kip = 4.448 kN

Figure 46. Graph. LTE under fatigue test for slab number 5 (0 to 5 million cycles).

Analysis and Discussion for Joint LTE

Analysis and Discussion for Slab Group 1 (15.24-cm (6-inch) Spacing):

Test results are summarized in table 18 and table 19.

Table 18. LTE of group 1 from static tests.

Slab Number	LTE (percent)
1	97.79
2	94.13
3	93.33

Table 19. LTE of group 1 during fatigue tests.

Specimen Number	LTE (percent)				Proper Crack at Mid-joint
	1 M	2 M	4 M	5 M	
1	93.79 (joint width = 0.25 inch)	89.71* [†]	68.88* [†]	71.57* [†]	Yes
2	95.52	93.33 [†]	—	—	No
3	99.69	—	—	—	No

* Joint width was increased to 1.016 cm (0.4 inch).

[†] An overload factor of 1.5 was used so that 1.5 times HS25 load was applied for specimens 1 and 2 during fatigue tests and started from 2 million cycles.

— No loading at corresponding cycles.

1 kip = 4.448 kN

The following can be said:

- In static tests, all slabs provided good LTE, which was greater than 60 percent of LTE (corresponding to 75 percent of joint effectiveness, E).⁽⁹⁾ Slab number 1 (2.54-cm (1.0-inch)-diameter FRP dowel with 15.24-cm (6-inch) spacing) with proper crack formation at the mid-joint had a greater than 90 percent LTE, which was slightly larger than the LTE for slab number 2 (2.54-cm (1.0-inch)-diameter steel dowel with 15.24-cm (6-inch) spacing) and slab number 3 (3.81-cm (1.5-inch)-diameter FRP dowel with 15.24-cm (6-inch) spacing). Slabs number 2 and 3 had crack formation away from the mid-joint (table 7). In slab number 1, the dowel worked as per design to transfer maximum load.⁽¹¹⁾
- Even when 1.5 times the design load (HS25 loading) and an influence of increased joint width (increased from 0.635 to 1.016 cm (0.25 to 0.4 inch) were considered, the observed LTE in slab number 1 was consistent (reduced from 93.79 to 71.57 percent) due to the right crack position and still higher than 60 percent of LTE (corresponding to 75 percent of joint effectiveness, E).⁽¹¹⁾
- Pumping and erosion under the loaded side of the slabs was observed during the tests. This could be the main reason that LTE of slab number 1 was reduced. Base settlement was also a reason for reduced LTE. Therefore, base property (such as k , modulus of subgrade reaction) should be checked before and after each fatigue test.

Analysis and Discussion for Slab Group 2 (30.48 cm (12-inch) Spacing):

Tests results are summarized in table 20 and table 21.

Table 20. LTE of group 2 from static tests under corresponding HS25 load.

Slab Number	LTE (percent)
4	88.48
5	89.00

Table 21. LTE of group 2 from fatigue tests.

Slab Number	LTE (percent)		
	2 M	4 M	5 M
4	85.1	—	80.5
	50.70*	47.22	55.26*
5	90.21	—	—

— No loading at corresponding cycles.

* Results from tests conducted on poor base condition.

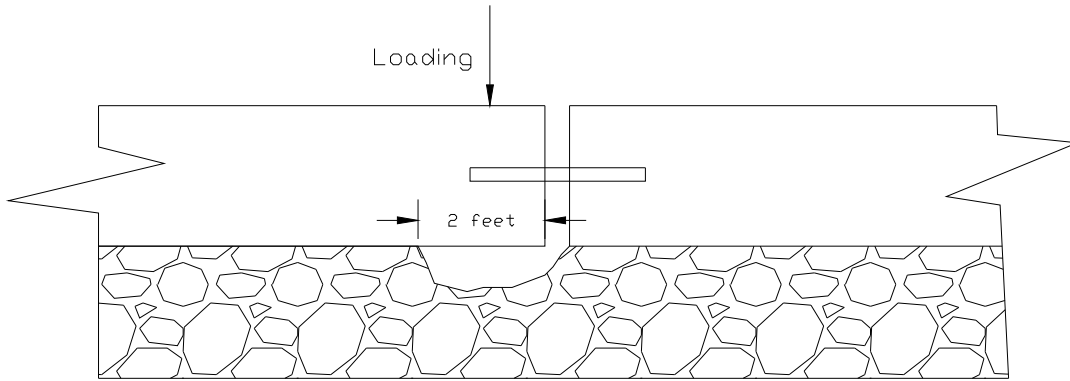
The following can be found:

- Both slab number 4 and slab number 5 had proper crack occurrence at the joint.
- In static tests, both slabs had very good LTE, more than 88 percent, which was much greater than 60 percent of LTE (corresponding to 75 percent of joint effectiveness, E). Thus, FRP dowels performed as well as steel dowels and showed LTE as good as steel dowels in the static tests.⁽¹¹⁾
- After 2 million HS25 fatigue loading cycles, for the same dowel diameters and spacing, the concrete pavement containing FRP dowels provided slightly lower LTE (85.1 percent versus 90.21 percent) than pavement containing steel dowels (table 21). With poor base condition, the LTE of slabs with FRP dowels over steel dowels was 50.71 percent versus 90.21 percent.
- The LTE of slabs with FRP dowels remained greater than 80 percent after 5 million loading cycles.

Investigations on Pavement Pumping Problem

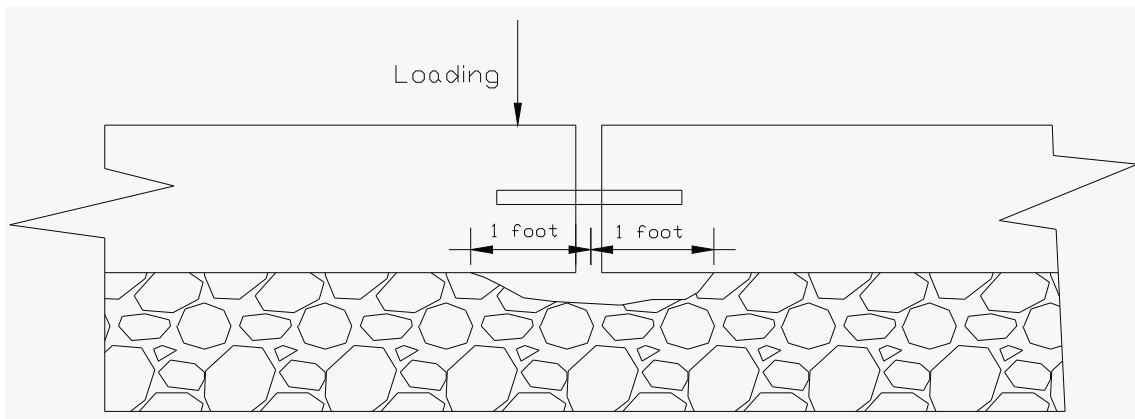
Pumping is a common problem occurring in concrete pavements due to the movement of material underneath the slab or ejection of material from underneath the slab as a result of water pressure. Pumping will cause decreased structural support of the slab, which can lead to linear cracking, corner breaks, and faulting.

Two cases of pumping tests were conducted (figure 47 and figure 48). In case one, base material under the loaded side of the slabs was removed for a 60.96-cm (2-ft) range to simulate the pumping problem occurring in the field (figure 47). These tests were conducted only on slab number 4 (3.81-cm (1.5-inch)-diameter FRP dowel at 30.48 cm (12 inches) c/c) and slab number 5 (3.81-cm (1.5-inch)-diameter steel dowel at 30.48 cm (12 inches) c/c) up to 44.482 kN (10 kips). Test results are shown in figure 49 and figure 50 and in table 22 and table 23.



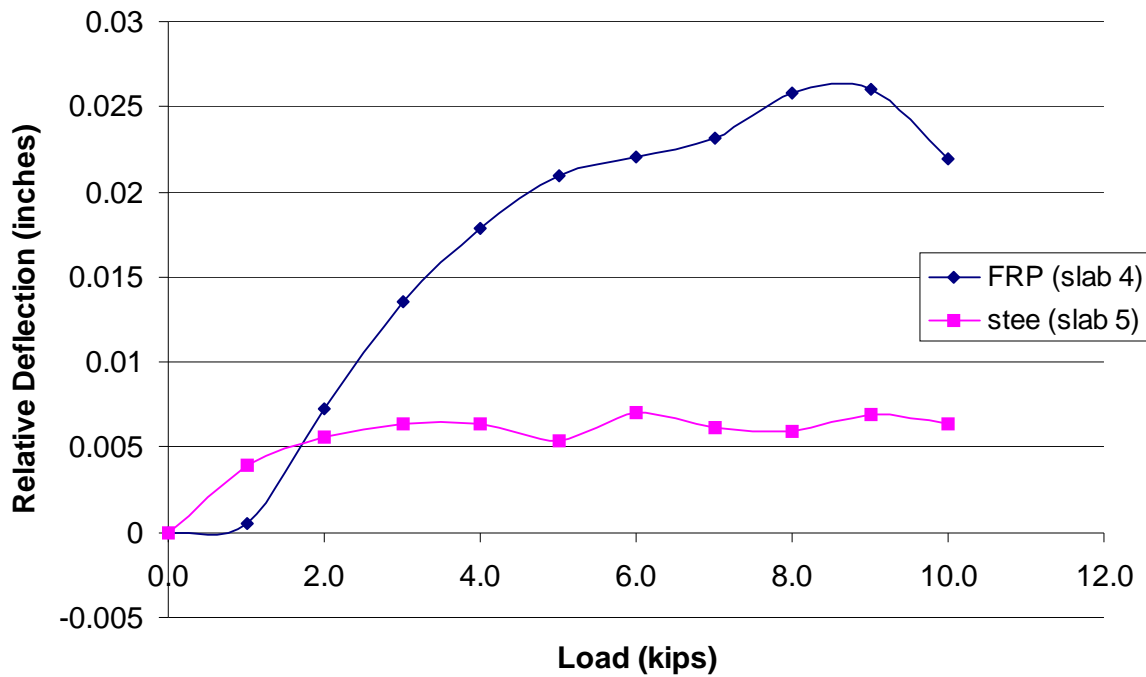
1 inch = 2.54 cm

Figure 47. Diagram. Case one—60.96-cm (2-ft) base material removal under loaded side of slabs.



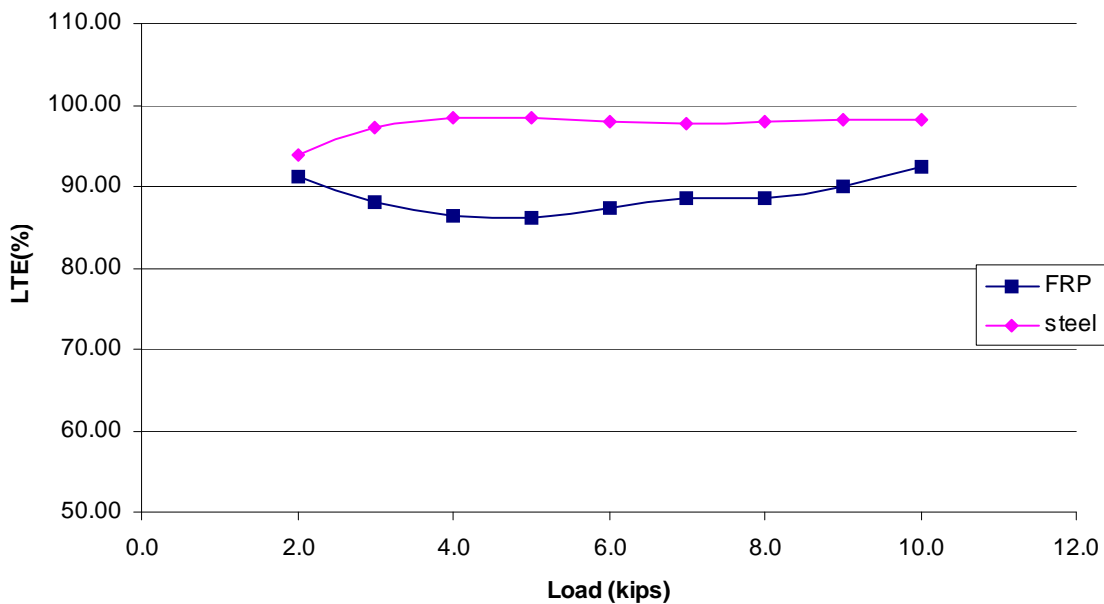
1 inch = 2.54 cm

Figure 48. Diagram. Case two—30.48-cm (1-ft) base material removal under both sides of slabs.



1 kip = 4.448 kN
 1 inch = 2.54 cm

Figure 49. Chart. RD for pumping tests (case one—60.96-cm (2-ft) base removal).



1 kip = 4.448 kN

Figure 50. Chart. LTE for pumping tests (case one—60.96-cm (2-ft) base removal).

Table 22. Evaluation of pumping issue under 44.482 kN (10 kips) loading.

Test Case Number	Dowel Material	Relative Deflection ($\times 10^{-3}$ inch)	LTE (percent)
Case one (2-ft base removal under loaded slab)	FRP (slab number 4)	21.9	92.42
	Steel (slab number 5)	6.4	98.21
Case two (1-ft base removal under both slabs)	FRP (slab number 4)	—	—
	Steel (slab number 5)	—	—

— No loading at corresponding cycles.

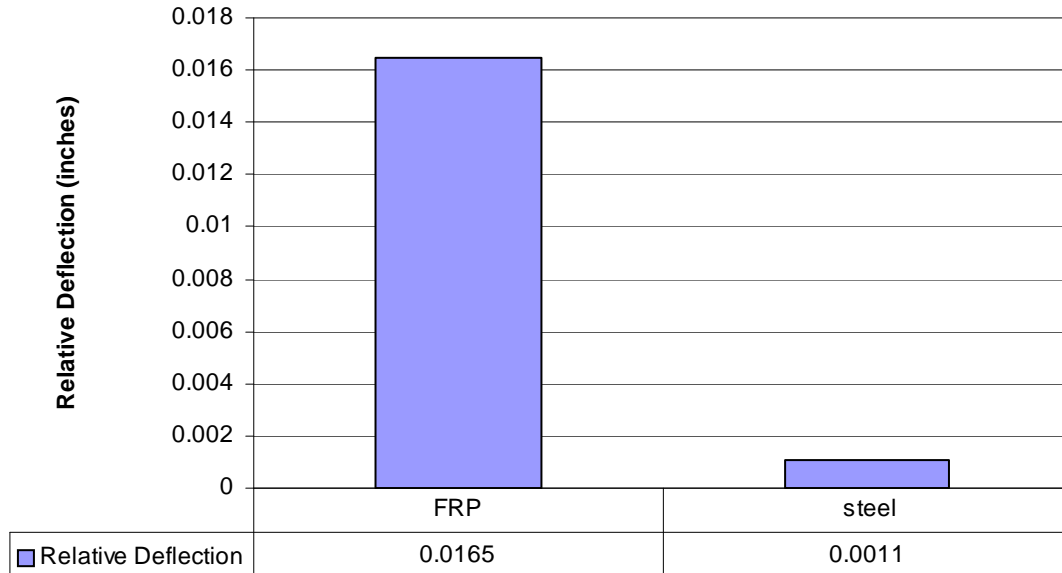
1 inch = 2.54 cm

Table 23. Evaluation of pumping issue under 13.345 kN (3 kips) loading.

Test Case Number	Dowel Material	Relative Deflection ($\times 10^{-3}$ inch)	LTE (percent)
Case one (2-ft base removal under loaded slab)	FRP (slab number 4)	13.5	88.00
	Steel (slab number 5)	6.4	97.15
Case two (1-ft base removal under both slabs)	FRP (slab number 4)	16.5	91.95
	Steel (slab number 5)	1.1	99.09

1 inch = 2.54 cm

In case two, base material under each side of the slabs was removed for a 30.48-cm (1-ft) range (figure 50). When loading exceeded 13.345 kN (3 kips), the joint opening closed, and the two faces of the joint bore against each other. Hence, tests were conducted only on slabs number 4 and 5 up to 13.345 kN (3 kips) in case two. Test results are shown in figure 51 and figure 52.



1 inch = 2.54 cm

Figure 51. Graph. RD for pumping tests under 13.345 kN (3 kips) loading (case two—30.48-cm (1-ft) base removal under both slabs).

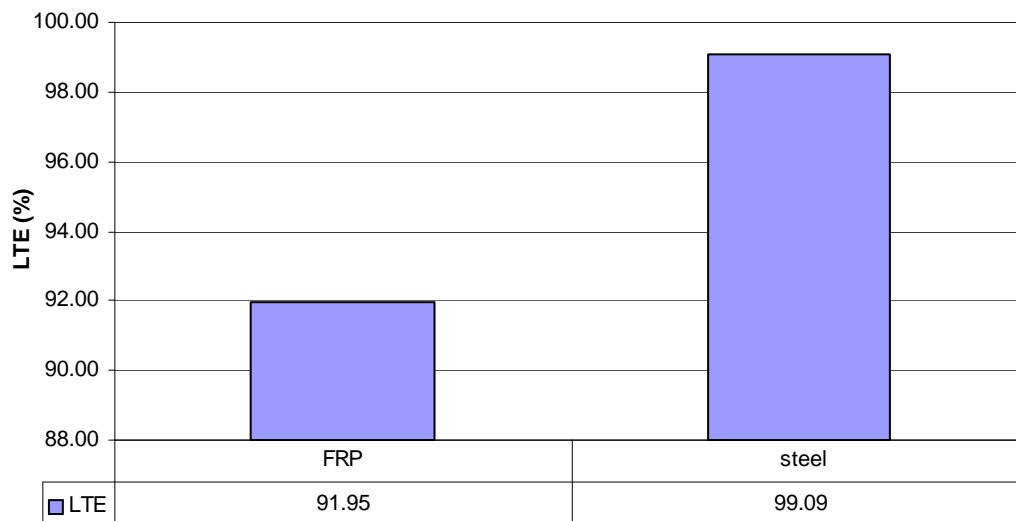


Figure 52. Graph. LTE for pumping tests under 13.345 kN (3 kips) loading (case two—30.48-cm (1-ft) base removal under both slabs).

Test results from cases one and two are compared and summarized in table 22 and table 23.

The following can be found:

- LTEs were observed in cases investigated for the simulated pavement pumping problem with supporting base removal up to a certain length near the joint (figure 47 and figure 48). LTEs were not less than the LTEs obtained from intact base condition (table 20). However, under

fatigue load cycles, LTE was expected to reduce significantly for specimens without support near the joint.

- LTE obtained in case two (30.48-cm (1-ft) base material removal under both sides of slabs) was greater than 90 percent at 13.345 kN (3 kips) loading, and, after loading exceeded 13.345 kN (3 kips), two joint faces would bear against each other. Thus, case two (30.48-cm (1-ft) base removal under both slabs) with unsupported slab areas on both sides of the slab was more detrimental than case one (60.96-cm (2-ft) base removal under the loaded slab).

Strains on Dowels

Most of the strain gauges installed on dowels survived before fatigue tests. However, some of them did not function properly after fatigue tests. Strain readings shown in this section are only from slab number 1 (2.54-cm (1.0-inch) diameter at 15.24-cm (6-inch) spacing c/c) (figure 53) and slab number 4 (3.81-cm (1.5-inch) diameter at 30.48-cm (12-inch) spacing c/c) (figure 54).

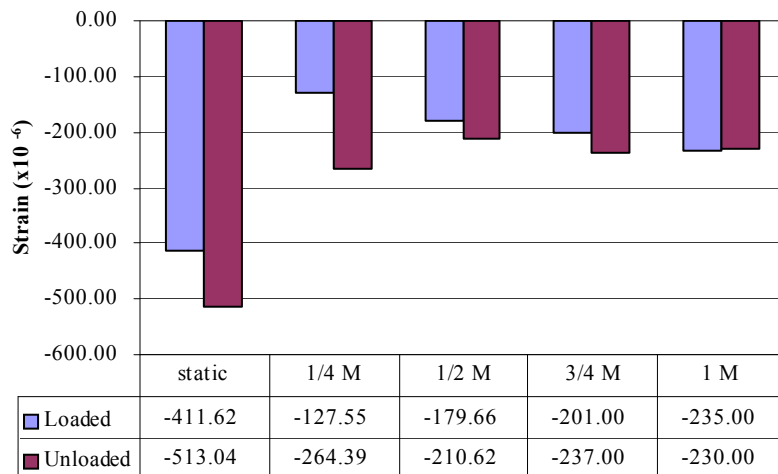
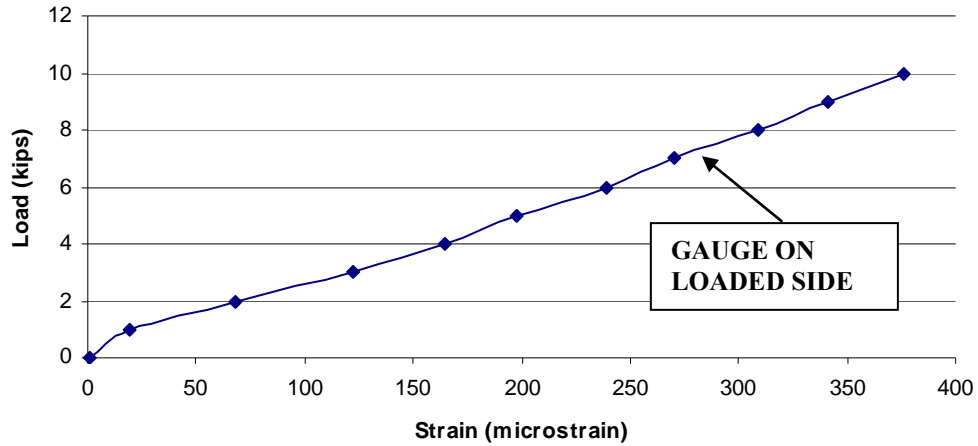


Figure 53. Graph. Strain gauge reading in slab 1 (2.54-cm (1.0-inch) diameter at 15.24-cm (6-inch) spacing c/c) from static test to 1 million cycles under HS25 loading).



1 kip = 4.448 kN

Figure 54. Chart. Strain gauge reading in slab number 4 (3.81-cm (1.5-inch) diameter at 30.48-cm (12-inch) spacing c/c) from static test under HS25 loading.

Strain values at the unloaded side of dowels during static tests from slabs number 1 and 4 were 513.04 and 376.43 microstrains, respectively. Both values were less than those from analytical evaluation (ranges from 1,000 to 1,200 microstrains), but strain values were typically not used for LTE calculation.

CHAPTER 5. FIELD APPLICATIONS AND TEST RESULTS

INTRODUCTION

Experimental tests and results discussed in chapter 4 show that FRP dowels can provide sufficient LTE under heavy traffic load rating (HS25 load and 1.5 times HS25). The purpose of the field test program was to investigate FRP dowel performance and FRP-concrete interaction in full-scale highway pavement slabs under realistic loading and field exposure conditions.

Field application and tests were done in collaboration with the WVDOT DOH. FRP dowels were used for new pavement construction and rehabilitation of damaged pavement sections. FRP dowel joints were used for new highway pavement construction on Route 219 and Route 33 East in Elkins, WV, from September to November 2001. Field tests were conducted in July 2002 and June 2003. FRP dowels were used for pavement rehabilitation at the junction of Routes 119 and 857, University Avenue, Morgantown, WV, during October 2002.

FRP DOWELS FOR NEW HIGHWAY PAVEMENT CONSTRUCTION

FRP dowels were used during the construction of new highway Route 219 and Route 33 East in Elkins, WV. The installation and field test setup are discussed in this section. Field test results are also analyzed and discussed.

Field Locations

Two locations separated by about 6.4 km (4 mi) were selected for field installations in corridor H highway at Route 219 and Route 33 in Elkins, WV. Location 1 (figure 55 and figure 56) was westbound, and location 2 (figure 57 and figure 58) was eastbound.



Figure 55. Photo. Dowel installation at location 1 of corridor H, Route 250, Elkins, WV.

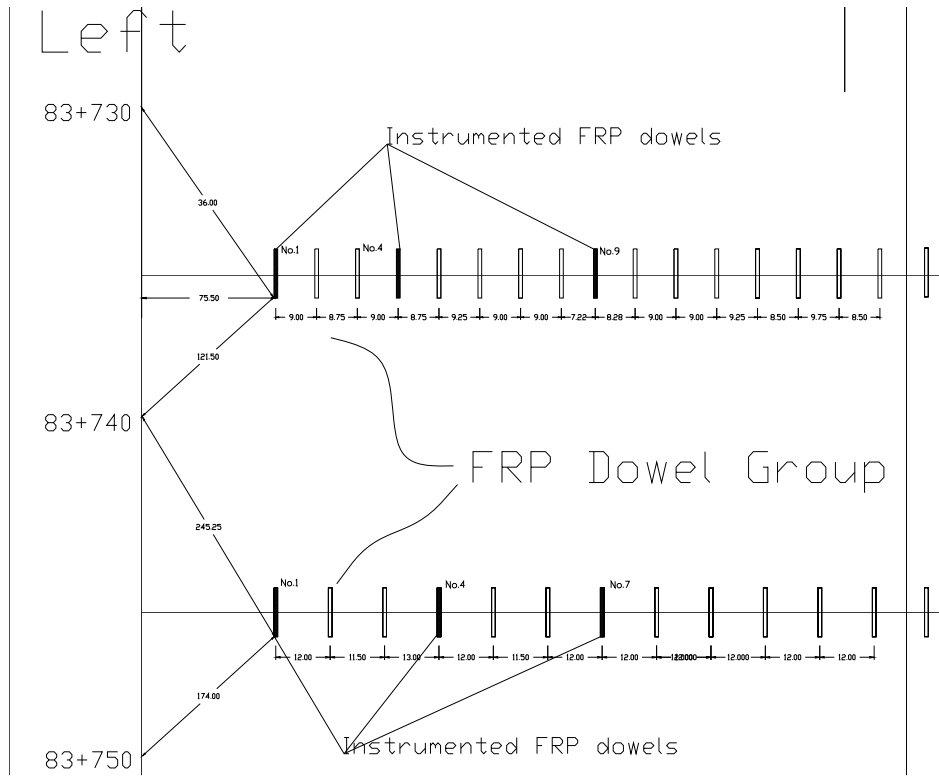


Figure 56. Diagram. FRP dowel positions at location 1 of corridor H, Route 250, Elkins, WV.

Only dowels with shading in figure 56 were instrumented.



Figure 57. Photo. FRP dowel bars at location 2 of corridor H, Route 219, Elkins, WV.

Side pipes carried wires from instrumented dowels to the outside of the shoulder region (figure 57).

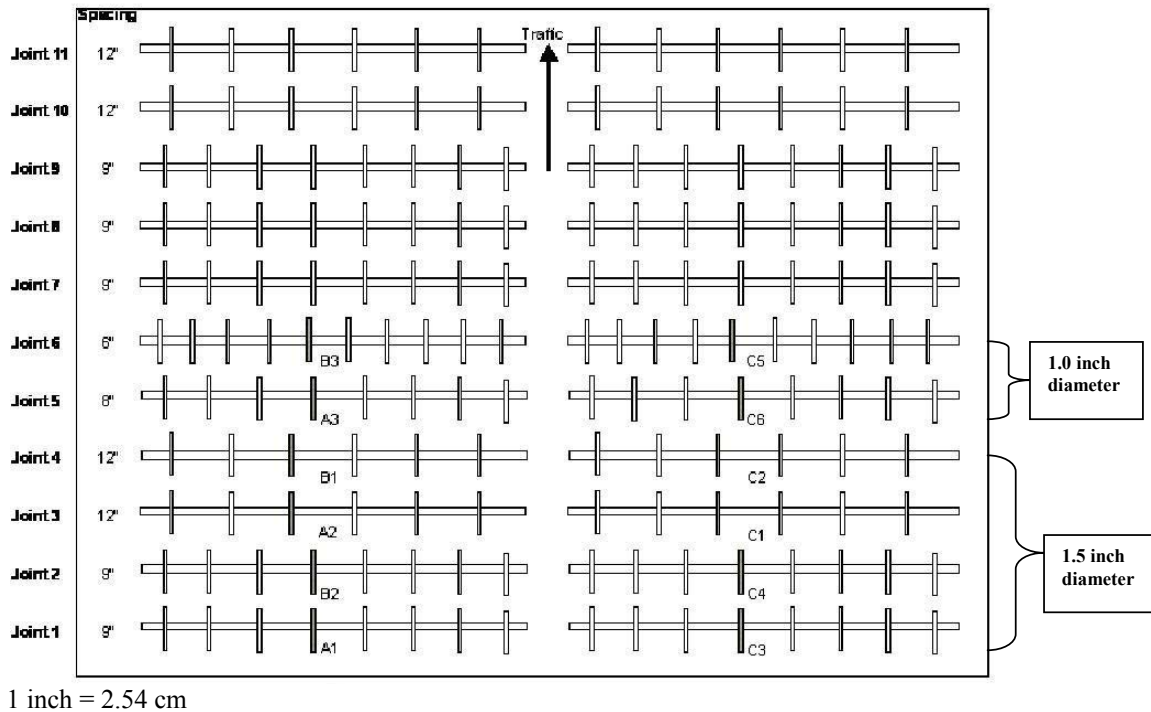


Figure 58. Diagram. FRP dowel positions at location 2 of corridor H, Route 219, Elkins, WV.

Only dowels with shading in figure 58 were instrumented.

Field Installation

FRP dowels were instrumented with strain gauges (figure 59) to monitor strains in dowel bars installed in the field. Embeddable concrete strain gauges (figure 60) were also installed to monitor strains in the pavement.

Dowel bars with 2.54-cm (1.0-inch) diameter (figure 60) and 3.81-cm (1.5-inch) diameter (figure 61) were supported by plastic baskets at design spacings of 30.48, 22.86, 20.32, or 15.24 cm (12, 9, 8, or 6 inches) (figure 56 and figure 58). Plastic baskets were anchored by either steel stakes (figure 60) or plastic stakes (figure 61).

Construction was carried out as shown in figure 62 and figure 63. Wires from instrumented dowels were carried through hollow polyvinyl chloride pipes to the outside of the pavement shoulder (figure 63).



Figure 59. Photo. FRP dowel bars bonded with strain gauges at loaded and unloaded sides.

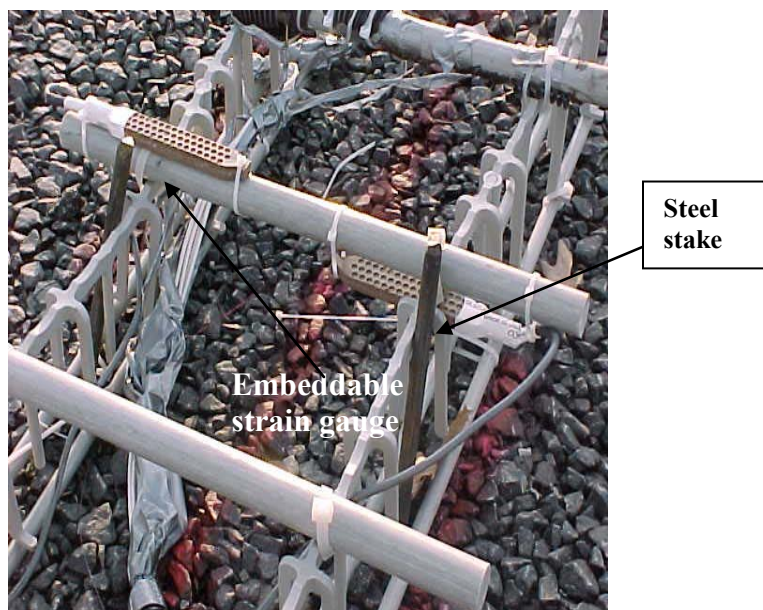


Figure 60. Photo. Embeddable concrete strain gauge with dowels.

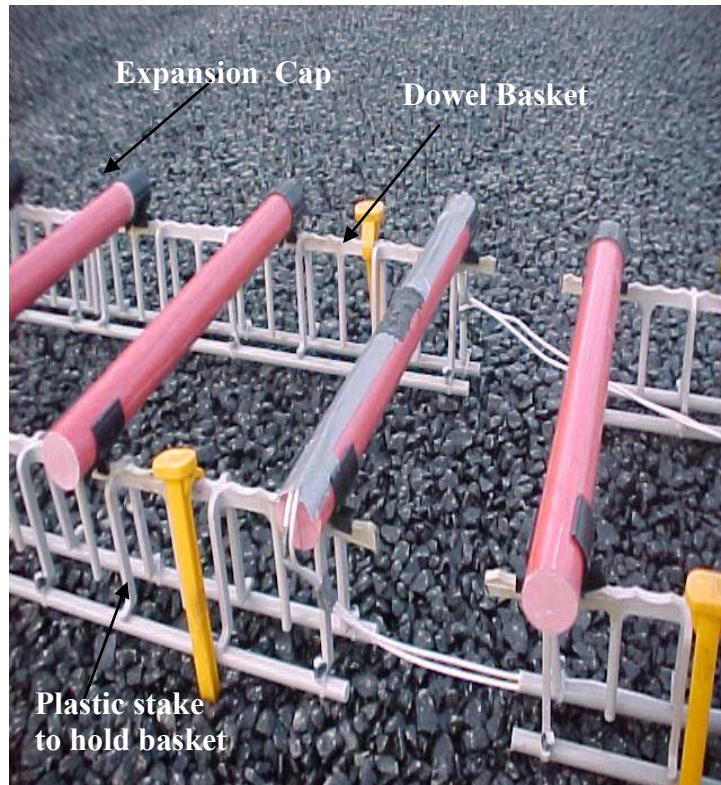


Figure 61. Photo. FRP dowels in dowel basket.



Figure 62. Photo. Paving operation in progress.



Figure 63. Photo. FRP dowel bars being covered by concrete.

FIELD TESTS

Figure 64 shows a standard AASHTO Type 3 truck load that was used to carry out field evaluations before and after opening the pavement to the traffic.⁽¹²⁾ Strain gauge readings were recorded prior to and after pavement construction (November 2001) and also during the field testing conducted in July 2002 and June 2003. The automatic data acquisition system was used to collect test data.

Field Test Before Opening Highway to Traffic in July 2002

A field test was completed before opening the pavement to traffic in July 2002. Static and dynamic tests including brake tests were conducted during this test. Parameters used for field testing are provided in table 24.

Table 24. Parameters of the field test at location 2, July 2002.

Dowel material	FRP
Dowel diameter	3.81 cm, 2.54 cm (1.5 inches, 1.0 inch)
f'_c	24.132 MPa (3,500 psi)
Dowel spacing	30.48 cm (12 inches), 3.81-cm (1.5-inch) diameter 22.86 cm (9 inches), 3.81-cm (1.5-inch) diameter 20.32 cm (8 inches), 2.54-cm (1.0-inch) diameter 15.24 cm (6 inches), 2.54-cm (1.0-inch) diameter
Type of loading	Truck type: AASHTO Type 3 (regular two-axle truck) Gross weight: 22.680 metric tons (50,000 lb) (AASHTO) Gross weight: 24.385 metric tons (53,760 lb) (actual) Front axle: 7.257 metric tons (16,000 lb) (AASHTO) Front axle: 7.158 metric tons (15,780 lb) (actual) Rear axle: 15.422 metric tons (34,000 lb) (AASHTO) Rear axle: 17.227 metric tons (37,980 lb) (actual) Wheel load: 3.856 metric tons (8,500 lb) (AASHTO) Wheel load: 4.307 metric tons (9,495 lb) (actual)
Types of tests	Static Dynamic: 16.1, 32.2, 48.3, 80.5 km/h (10, 20, 30, 50 mi/h) Brake test: speed of 80.5 km/h (50 mi/h)
Instrumentations	Strain gauges Dial gauges for measuring pavement deflection Data acquisition system
Measurements	Strain gauge reading Pavement deflection
Computation	Strain versus loading history LTE RD

Test Setup

A WVDOT truck with calibrated loads was used in the tests (table 24). The truck was positioned at required locations to apply load on instrumented dowels (figure 58 and figure 64).

The loading test for a joint consisted of guiding a truck slowly toward the designated joint from about a 15.24-m (50-ft) distance. The unloading test for a joint consisted of guiding a truck initially placed on the pavement joint to leave the joint slowly.

All strain gauges on FRP dowels and embeddable concrete gauges were connected to data acquisition (figure 65). Dial gauges were fixed on a long, adjustable stand system. Dial gauges were positioned according to the spacing of dowels (figure 55 through figure 58) at the pavement joint considered for testing. The span of the dial gauge stand system was long enough to support it on adjacent pavement to avoid the influence of support deflections. Strains in dowels and deflection of pavement on loaded and unloaded sides of the joint were recorded.



Figure 64. Photo. Dial gauges for measuring pavement deflection under truck loading.



Figure 65. Photo. Data acquisition system used for field tests.

Test Results and Analysis

Strain Data from Field Static Tests:

About 60 percent of strain gauges installed on FRP dowels were found to be working properly after field installation and pavement construction. It was also found that some strain data recorded by the data acquisition system contained significant noise. Field test results of four cases of FRP dowels were analyzed.

Joints with different diameters and spacing have been described in this section. Data for brake tests and dynamic tests from different vehicle speeds are included.

Performance of FRP dowels with different diameters and/or spacings chosen from the field installation (table 25) are discussed in the next several sections with respect to the following:

- FRP 3.81-cm (1.5-inch) diameter at 22.86 cm (9 inches) c/c (dowel A1, figure 66 and figure 67).
- FRP 3.81-cm (1.5-inch) diameter at 30.48 cm (12 inches) c/c (dowel A2, figure 68 and figure 69).
- FRP 2.54-cm (1.0-inch) diameter at 15.24 cm (6 inches) c/c (dowel C5, figure 70 and figure 71).
- FRP 2.54-cm (1.0-inch) diameter at 20.32 cm (8 inches) c/c (dowel C6, figure 72 and figure 73).

Table 25. Joint details used for analysis.

Dowel Number	Diameter, cm (inches)	Spacing, cm (inches)
A1	3.81 (1.5)	22.86 (9)
A2	3.81 (1.5)	30.48 (12)
C5	2.54 (1.0)	15.24 (6)
C6	2.54 (1.0)	20.32 (8)

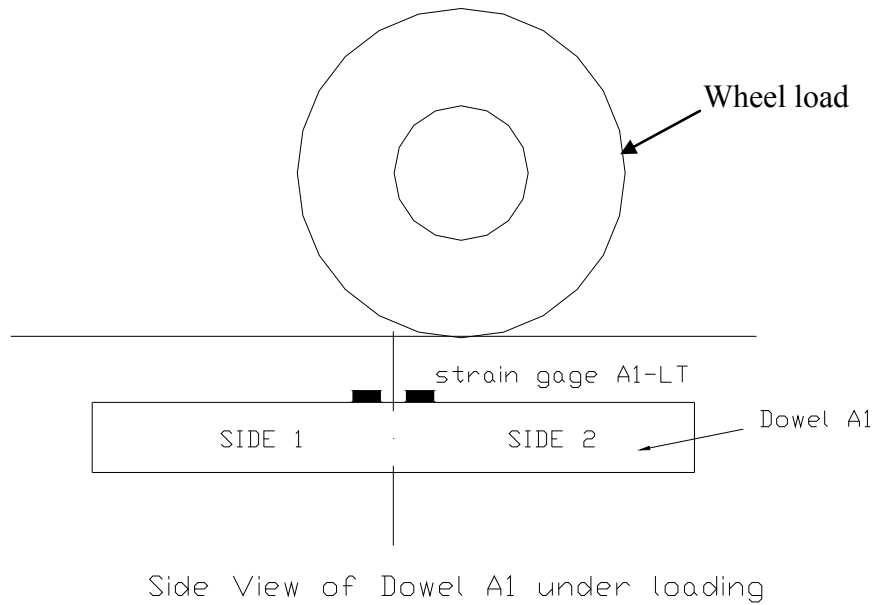


Figure 66. Diagram. Dowel A1 (3.81-cm (1.5-inch) diameter, 22.86-cm (9-inch) spacing); refer to figure 58.

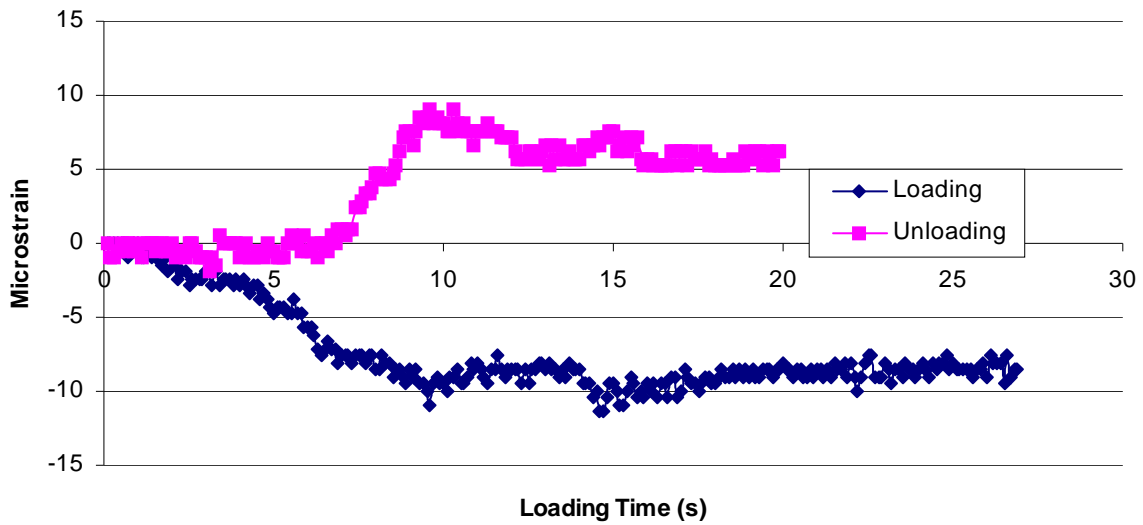
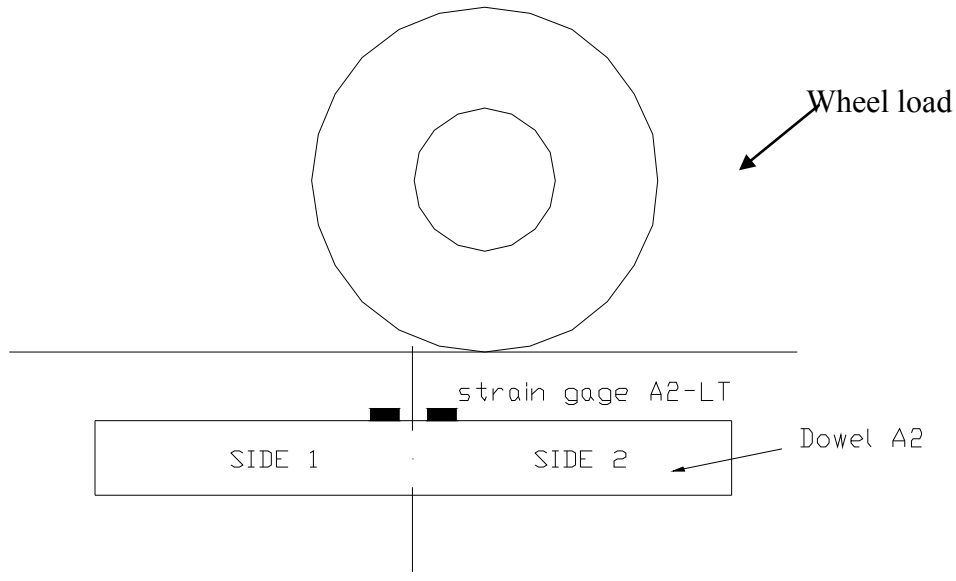


Figure 67. Chart. Strains in dowel during loading and unloading cases for gauge A1-LT (3.81-cm (1.5-inch) diameter, 22.86-cm (9-inch) spacing).



Side View of Dowel A2 under loading

Figure 68. Diagram. Dowel A2 (3.81-cm (1.5 inch) diameter, 30.48-cm (12-inch) spacing); refer to figure 58.

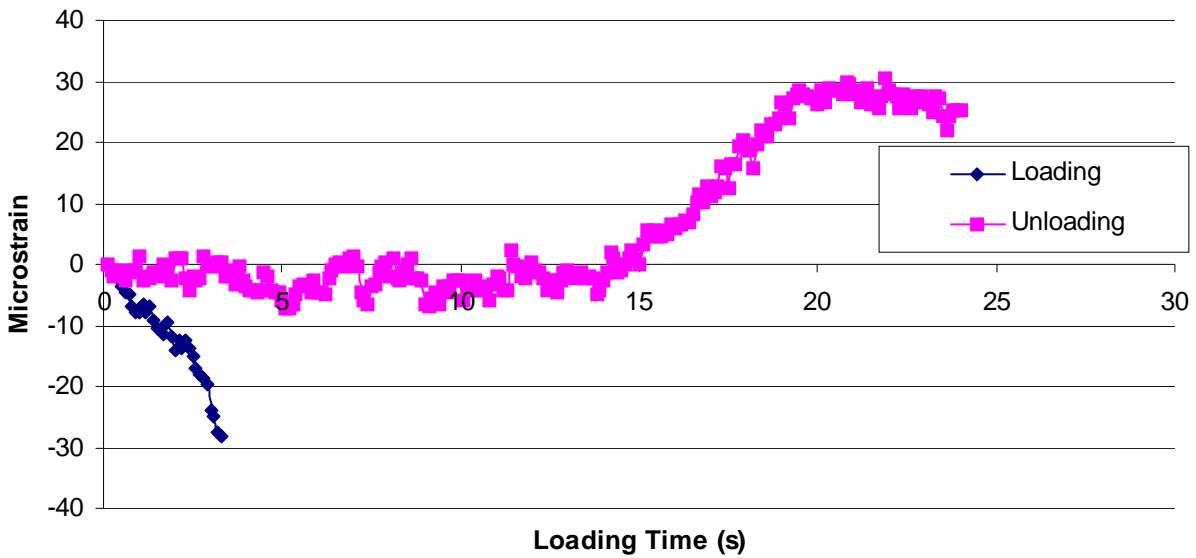


Figure 69. Chart. Strains in dowel during loading and unloading cases for gauge A2-LT (3.81-cm (1.5-inch) diameter, 30.48-cm (12-inch) spacing); refer to figure 58.

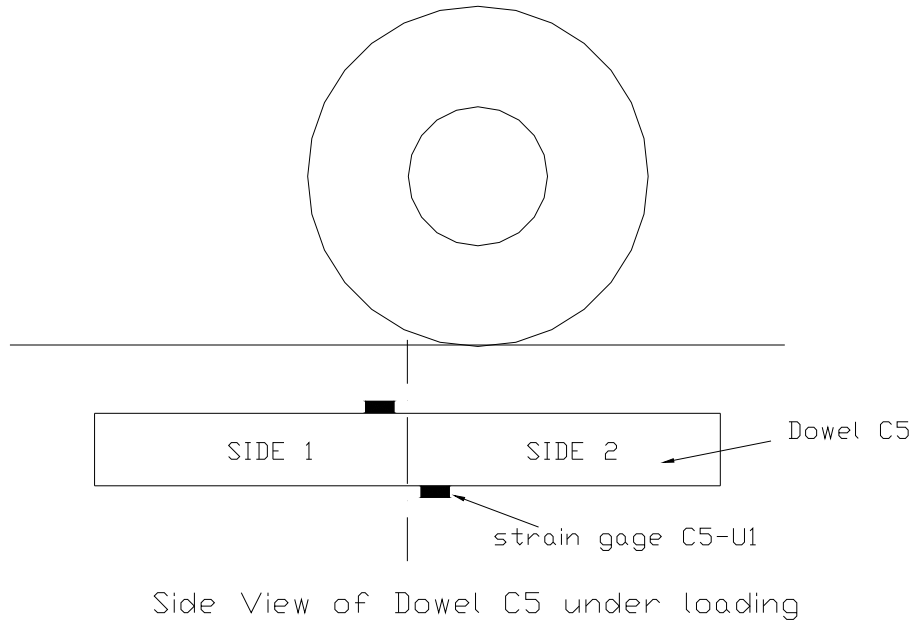


Figure 70. Diagram. Dowel C5 (2.54-cm (1.0-inch) diameter, 15.24-cm (6-inch) spacing); refer to figure 58.

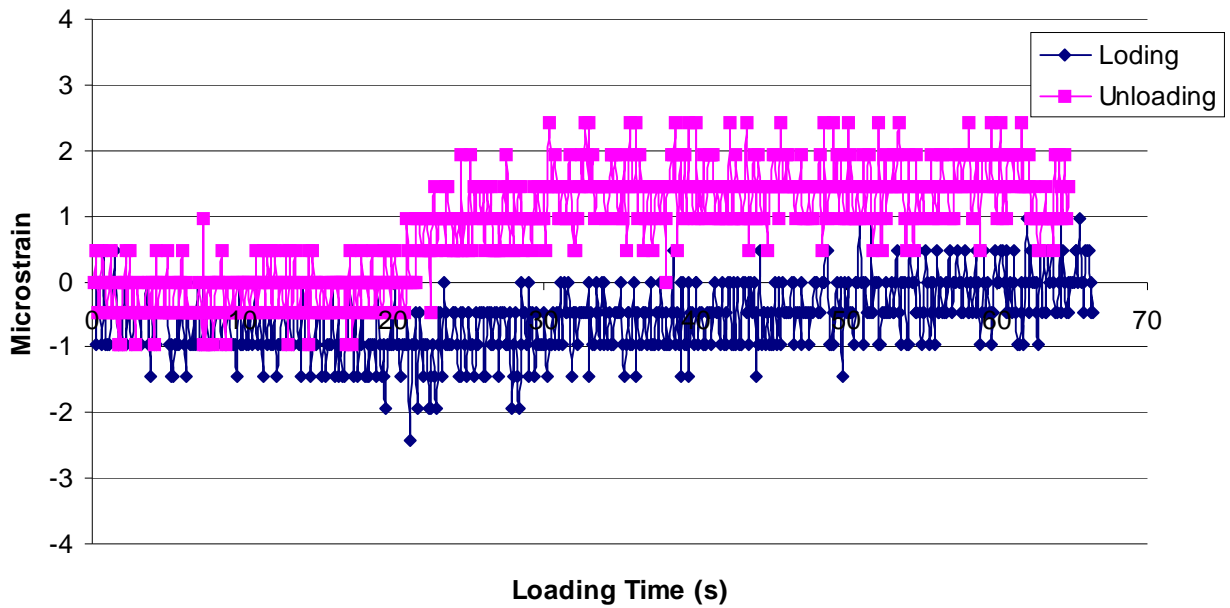
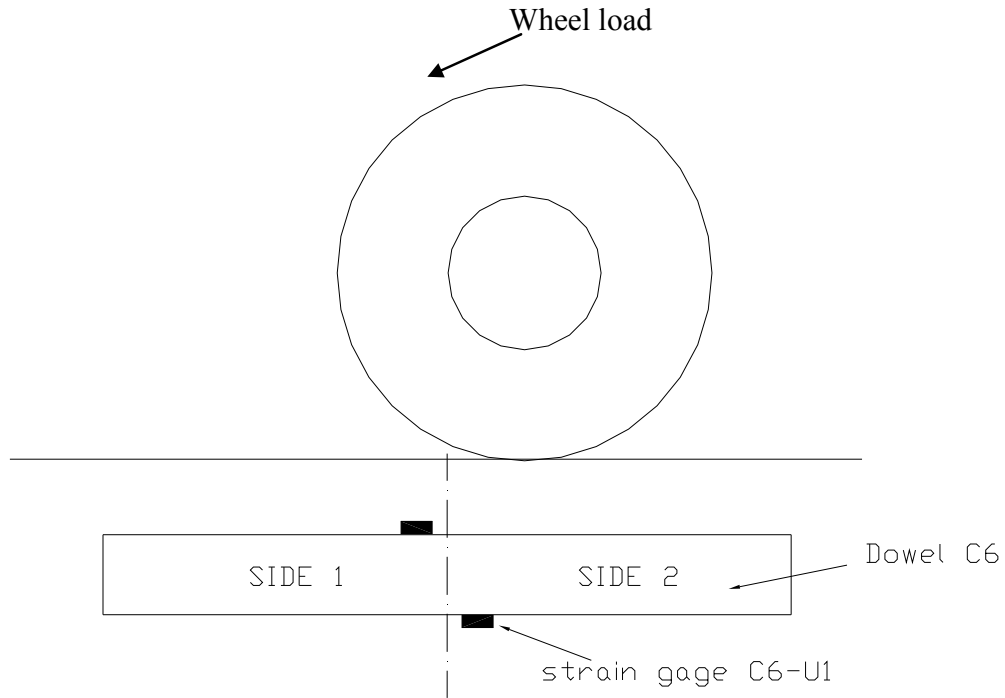


Figure 71. Chart. Strains in dowel during loading case for gauge C5-U1 (2.54-cm (1.0-inch) diameter, 15.24-cm (6-inch) spacing); refer to figure 58.



Side View of Dowel C6 under loading

Figure 72. Diagram. Dowel C6 (2.54-cm (1.0-inch) diameter, 20.32-cm (8-inch) spacing); refer to figure 58.

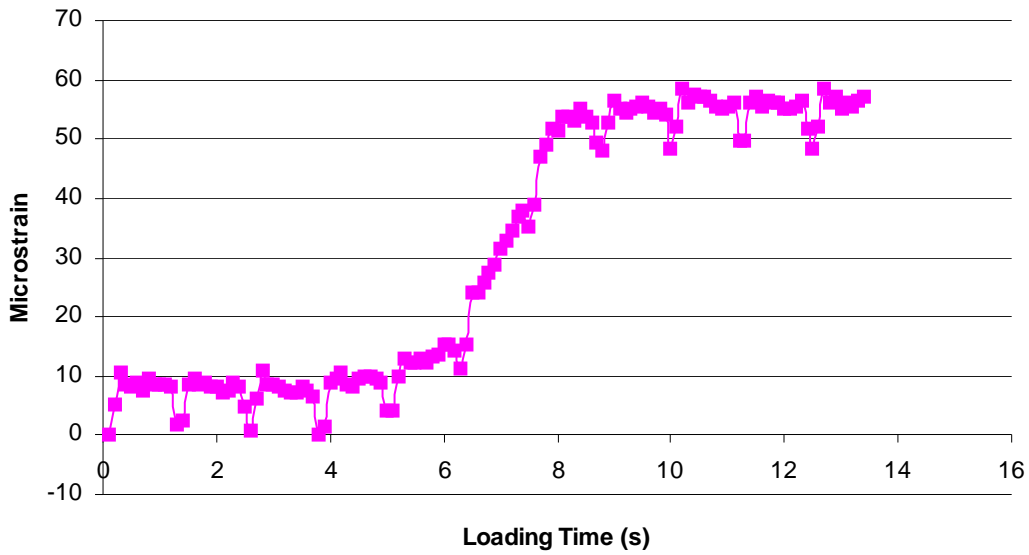
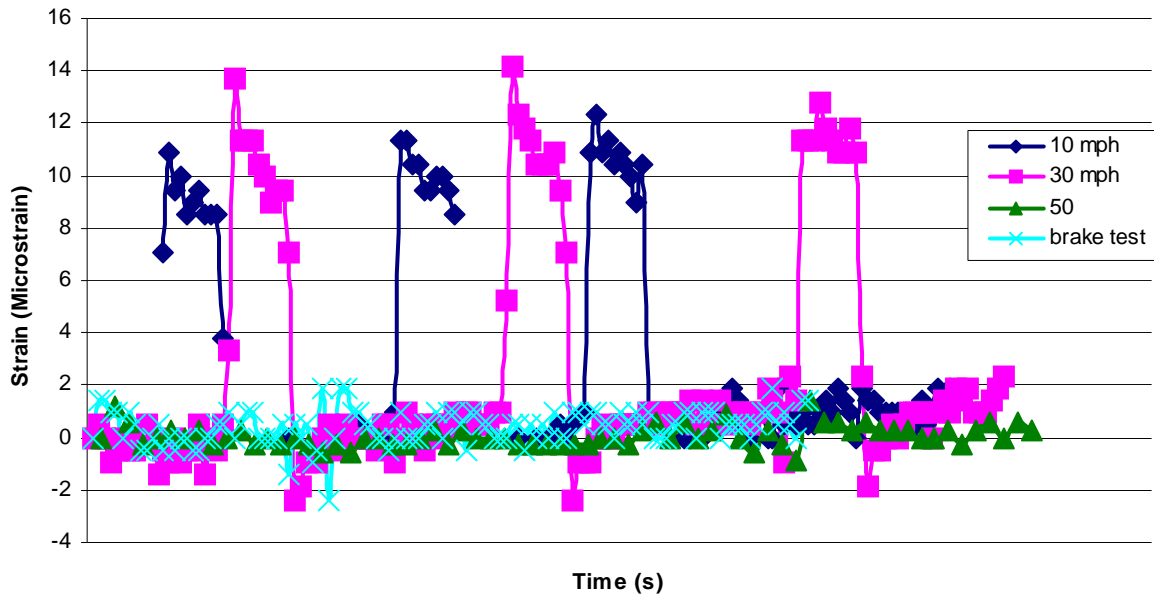


Figure 73. Chart. Strains on dowel during loading case for gauge C6-U1 (2.54-cm (1.0-inch) diameter, 20.32-cm (8-inch) spacing); refer to figure 58.

Strain Data from Dynamic Tests:

Dynamic tests were conducted in this field evaluation. The loaded WVDOT truck with speeds of 16.09, 32.19, 48.28, and 80.47 km/h (10, 20, 30, and 50 mi/h) crossed the selected joint containing instrumented FRP dowels. Data were collected through the automatic data acquisition system during truck speeding and braking of the speeding truck at 48.28 km/h (30 mi/h) close to the joint. Test results are shown in figure 74 and figure 75.



1 mi/h = 1.61 km/h

Figure 74. Chart. Strain from gauge A1-LT (3.81-cm (1.5-inch)-diameter FRP dowel at 22.86-cm (9-inch) spacing) from dynamic tests.

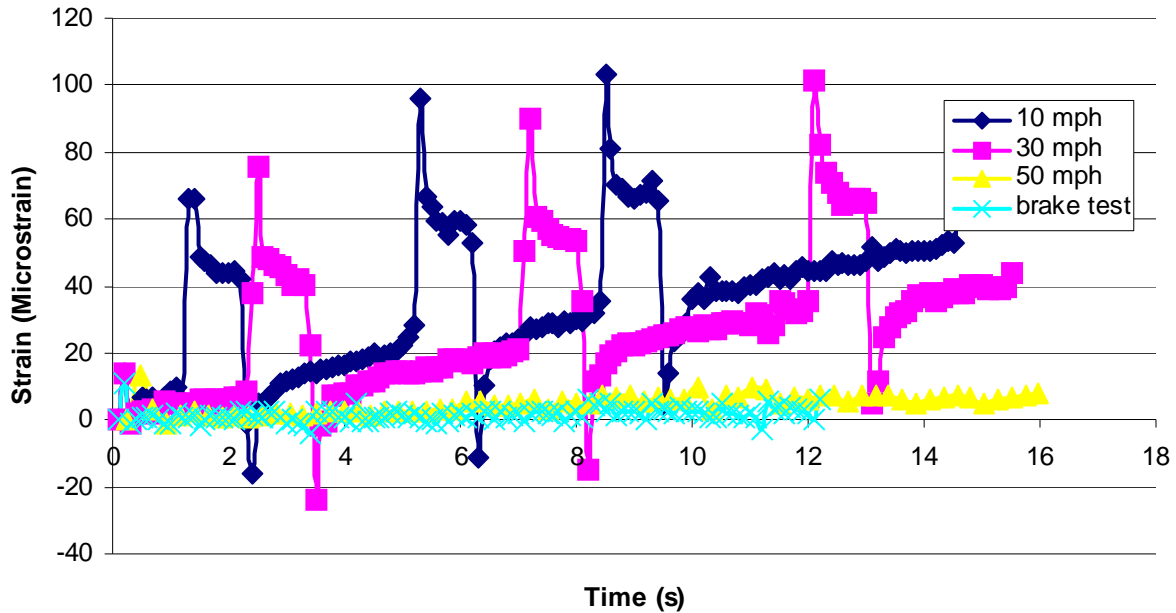


Figure 75. Chart. Strain from gauge A2-LT (3.81-cm (1.5-inch)-diameter FRP dowel at 30.48-cm (12-inch) spacing) from dynamic tests.

Dynamic test results recorded contained significant noise, and hence, data are not further discussed.

Analysis of test result:

Figure 66 through figure 73 show changes in dowel strain near pavement joints during truck loading and unloading. Stresses at points on individual dowels can also be obtained according to the stress-strain relationship under bending. Table 26 contains a summary of the above strain values.

Table 26. Summary of FRP dowel strain during loading and unloading.

Dowel No.	Dowel Diameter (inches)	Dowel Spacing (inches)	Maximum Strain (microstrain)	
			Loading	Unloading
A1	1.5	9	9	12
A2	1.5	12	31	29
C5	1.0	6	3	3
C6	1.0	8	60	N/A

1 inch = 2.54 cm

The following can be found from table 26:

- Change in strain value for the same dowel during loading and unloading cases was almost the same.
- Effect of dowel spacing:
 - For FRP dowels (A1 and A2) with 3.81-cm (1.5-inch) diameters, dowel A2 with larger spacing (30.48 cm (12 inches)) had a greater strain change (31 microstrain) than dowel A1 with 22.86-cm (9-inch) spacing (change of 9 microstrain). Similarly, for FRP dowels C5 and C6 with the same 2.54-cm (1.0-inch) diameter, the dowel C5 with smaller spacing (15.24 cm (6 inches)) showed a small strain change (3 microstrain) when compared with C6 with 20.32-cm (8-inch) dowel spacing (60 microstrain).
 - Decreasing the spacing by 25 percent (from 30.48 to 22.86 cm (12 to 9 inches) and from 20.32 to 15.24 cm (8 to 6 inches) resulted in more dowels sharing the load within the radius of relative stiffness (l_r , chapter 6), leading to 30 percent or higher strain reductions in dowels.
 - For FRP dowels with 2.54-cm (1.0-inch) diameter (C5 and C6), a spacing increase from 15.24 to 20.32 cm (6 to 8 inches) had a greater influence on strain value change (3 versus 60 microstrain) than the increase of spacing from 22.86 to 30.48 cm (9 to 12 inches) in dowels (A1 and A2) with 3.81-cm (1.5-inch) diameters (9 versus 31 microstrain).
 - Dowels with different diameters and spacings could be compared with each other with strain value only. Because FRP dowels acted as a group, spacing and diameter were both important factors for the group action. It should also be noted that FRP dowels with smaller diameter typically had better mechanical properties per unit area than larger-diameter dowels due to shear lag effects (refer to chapter 6).

Deflection Data:

The WVDOT truck was guided toward the pavement joint on top of the chosen dowel location so that a heavier wheel load, which was located in the rear axles, could be applied. Pavement deflections increased when the WVDOT truck slowly approached the joint, but most of the deflection changes were less than the detectable range of the dial gauges with a count of 0.0254 cm (0.001 inch). In the second field test, LVDTs were used instead of dial gauges for better precision in deflection detection.

Field Test after Highway Opened to Traffic, June 2003

This field test was conducted about 1 year after opening the pavement to traffic. Test parameters are listed in table 27. They are similar to those for the first field test, except that the deflection measurements were made using LVDTs, and there were no dynamic/brake tests. The main purpose of this field test was to investigate deflection behavior and LTE of concrete pavement joints with different diameters and spacing of FRP dowel bars. Figure 76 through figure 79 show details of the field test setup.

Table 27. Parameters of the field test, June 2003.

Dowel material	FRP
Dowel diameter	3.81 and 2.54 cm (1.5 and 1.0 inches)
f'_c	24.132 MPa (3,500 psi)
Dowel spacing	30.48, 22.86, 20.32, and 15.24 cm (12, 9, 8, and 6 inches)
Type of loading	AASHTO Type 3 (regular two-axle truck) loaded truck, similar to the one described in table 24
Types of tests	Static
Instrumentations	Strain gauges LVDT for measuring pavement deflection Data acquisition system
Measurements	Pavement deflection Strain
Computation	LTE RD

It should be noted that the wheel load due to AASHTO HS25 is 9.071 metric tons (20,000 lbs), which is about twice the WVDOT truck wheel load used for this test. Under the AASHTO wheel load, larger deflections and strains can be expected.



Figure 76. Photo. WVDOT truck used for field tests.



Figure 77. Photo. WVDOT truck positioned near a joint for the test.



Figure 78. Photo. Two LVDTs measuring pavement deflections across a joint.



Figure 79. Photo. Measuring distance from tire to LVDTs (when loading is away from the selected dowel).

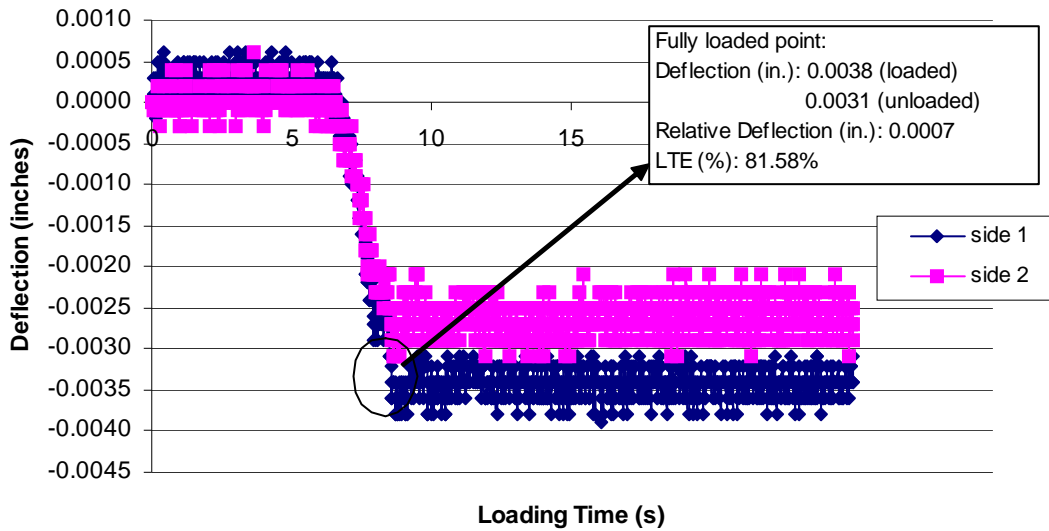
Test Results from Field Test

Four concrete pavement joints with instrumented dowels were tested during the second field test. Details of the joints and FRP dowels are shown in table 28.

Table 28. Pavement joint for deflection analysis.

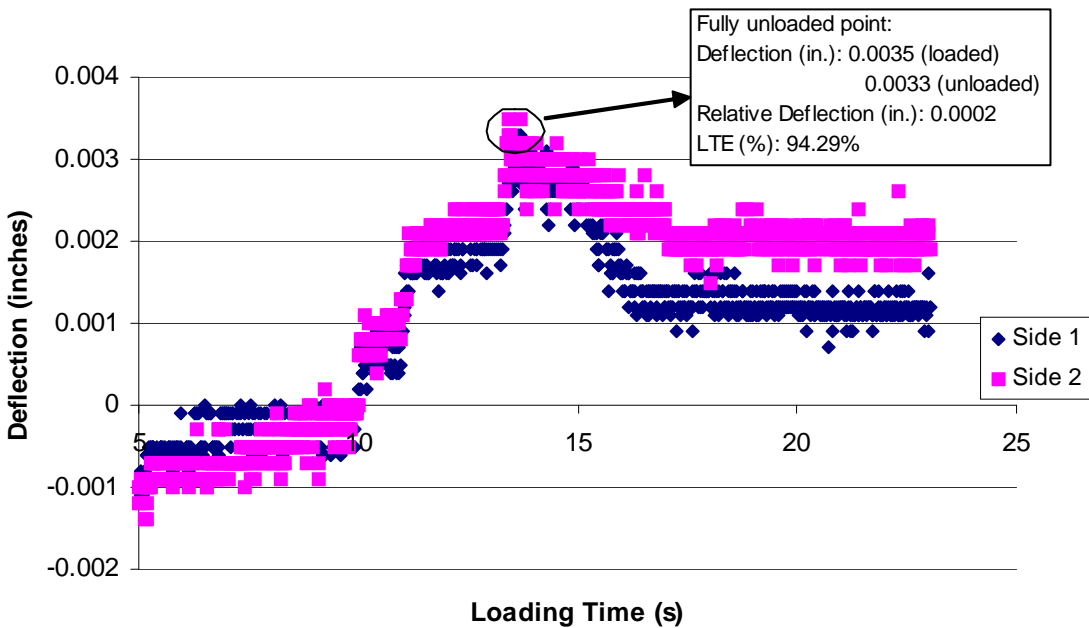
Joint Number	Dowel Bar Diameter, cm (inches)	Dowel Bar Spacing, cm (inches)	Data Sets Analyzed
3	3.81 (1.5)	30.48 (12)	2
2	3.81 (1.5)	22.86 (9)	2
5	2.54 (1.0)	20.32 (8)	1
6	2.54 (1.0)	15.24 (6)	1

Test results are shown in figure 80 through figure 86 and further analyzed in the next section.



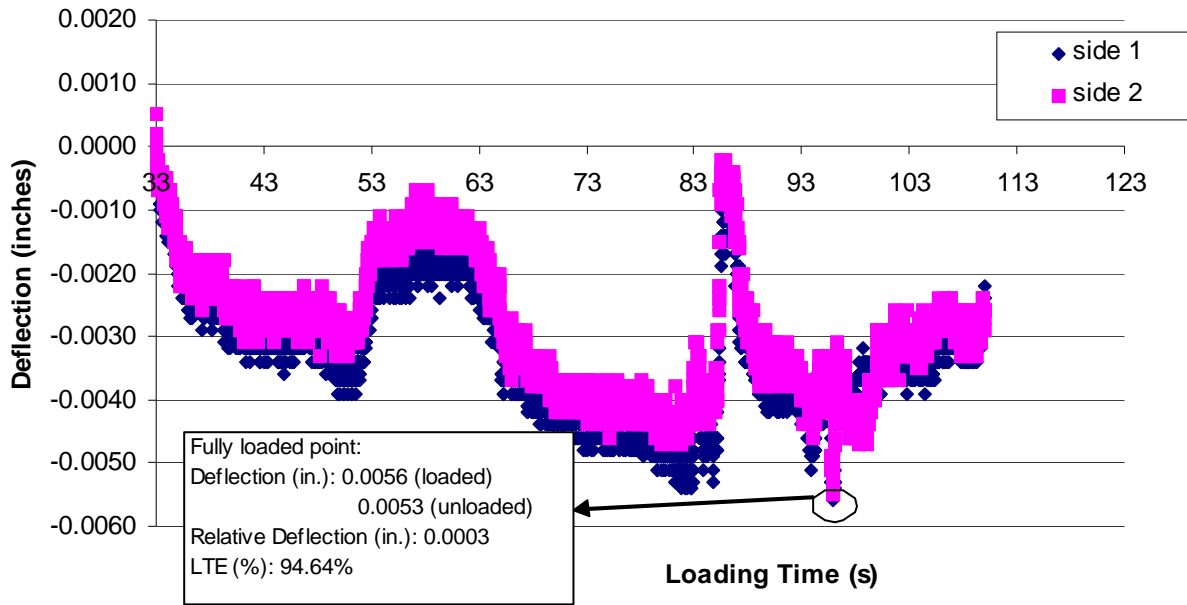
1 inch = 2.54 cm

Figure 80. Chart. Deflection on pavement joint 3 (with 3.81-cm (1.5-inch)-diameter and 30.48-cm (12-inch)-spacing FRP dowels) under loading.



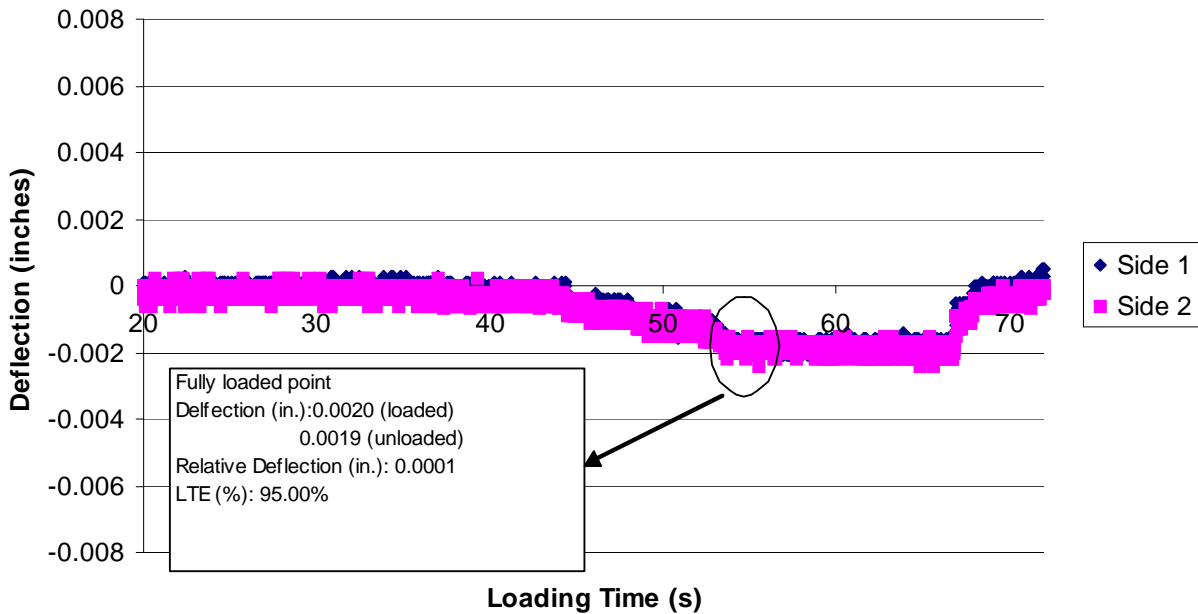
1 inch = 2.54 cm

Figure 81. Chart. Deflection on pavement joint 2 (with 3.81-cm (1.5-inch)-diameter and 22.86-cm (9-inch)-spacing FRP dowels) under unloading.



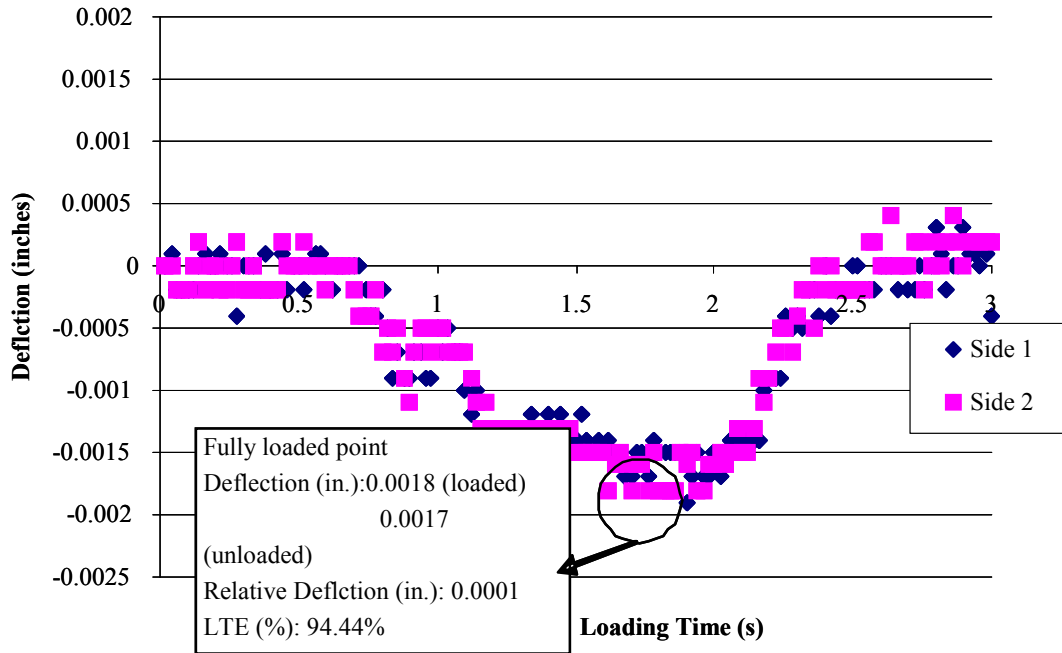
1 inch = 2.54 cm

Figure 82. Chart. Deflection on pavement joint 2 (with 3.81-cm (1.5-inch)-diameter and 22.86-cm (9-inch)-spacing FRP dowels) under loading.



1 inch = 2.54 cm

Figure 83. Chart. Deflection on pavement joint 5 (with 2.54-cm (1.0-inch)-diameter and 20.32-cm (8-inch)-spacing FRP dowels) under loading.



1 inch = 2.54 cm

Figure 84. Chart. Deflection on pavement joint 6 (with 2.54-cm (1.0-inch)-diameter and 15.24-cm (6-inch)-spacing FRP dowels) under loading.

Summary and Analysis of Test Results

A summary of the test results shown in figure 80 through figure 84 is provided in table 29 in terms of pavement deflection, LTE, and RD for pavement joints having 3.81- and 2.54-cm (1.5- and 1.0-inch)-diameter FRP dowels with different spacings of 30.48, 22.86, 20.32, and 15.24 cm (12, 9, 8, and 6 inches).

Table 29. Summary of joint deflection under maximum loading force.

Joint Number (Diameter and Spacing)— Refer to Table 28	Pavement Deflection (10 ⁻⁴ inch)		LTE (percent)	RD (10 ⁻⁴ inch)
	Loaded side	Unloaded side		
Joint 3 (1.5 inch at 12 inches c/c)	38	31	81.58	7
Joint 2 1st and 2nd (1.5 inch at 9 inches c/c)	35	33	94.29	2
	56	53	94.64	3
Joint 5 (1.0 inch at 8 inches c/c)	20	19	95.00	1
Joint 6 (1.0 inch at 6 inches c/c)	18	17	94.44	1

1 inch = 2.54 cm

Values in table 29 cannot be compared to each other directly because, in addition to diameter and spacing, deflections depended on combinations of other parameters such as base/sub-base properties, contact area between concrete and base, and others. It should also be noted that truck wheel load position on dowels embedded in concrete may vary from one dowel to the other.

The pavement surface was serrated to provide friction, and hence, there was the possibility of LVDT shaft tips sliding into those slots and showing slightly higher deflections. However, additional tests will be conducted in the future to compare LTE and RD. For this field test, LTE is shown in figure 85 and table 30, and RD is shown in figure 86 and table 31.

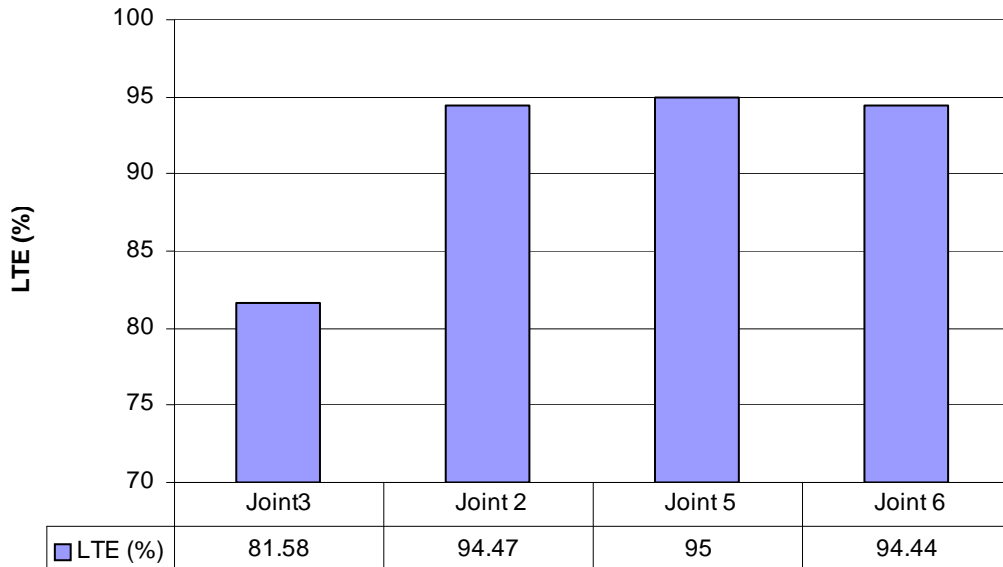


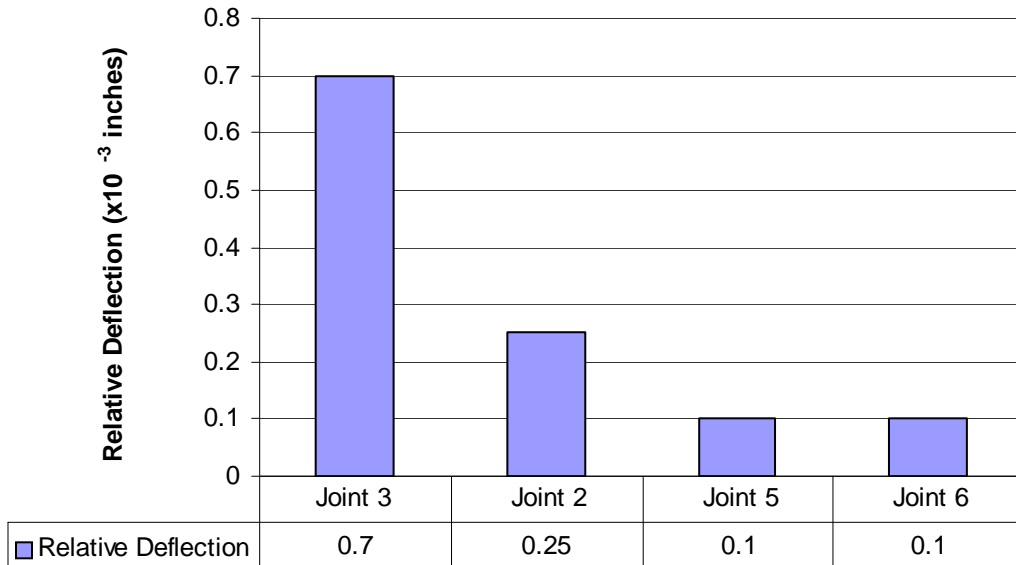
Figure 85. Graph. Comparison of LTE from field test (average value was used for joint 2).

Table 30. Values for LTE comparison from field test.

	Joint 3	Joint 2	Joint 5	Joint 6
LTE (percent)	81.58	94.47	95	94.44
Diameter (inches)	1.5	1.5	1.0	1.0
Spacing (inches)	12	9.0	8.0	6.0

1 inch = 2.54 cm

Joint 3, with the largest dowel spacing of 30.48 cm (12 inches), had the lowest value of LTE among all tested joints (figure 84). It should be noted that small variations in deflection were being measured through LVDTs. Hence, additional field tests will be conducted in the future to ascertain LTE of joints with 30.48 cm (12 inches) of spacing. Table 32 compares LTE and RD from joint 2 and 3 testing.



1 inch = 2.54 cm

Figure 86. Graph. Comparison of RD from field test (average value was used for joint 2).

Table 31. Comparison of RD values from field test.

	Joint 3	Joint 2	Joint 5	Joint 6
Relative deflection (× 10 ⁻³ inch)	0.70	0.25	0.10	0.10
Diameter (inches)	1.5	1.5	1.0	1.0
Spacing (inches)	12	9.0	8.0	6.0

1 inch = 2.54 cm

Table 32. Comparing joint 2 and 3.

	Joint 2, 2.54 cm at 22.86 cm (1.5 inches at 9 inches) c/c	Joint 3, 2.54 cm at 30.48 cm (1.5 inches at 12 inches) c/c	Percentage of Difference (percent)
LTE	94.47	81.58	15.8
Relative deflection (× 10 ⁻³ inch)	0.25	0.70	64.3

1 inch = 2.54 cm

The following can be observed from this table:

- Both 3.81-cm (1.5-inch)-diameter FRP dowel groups and 2.54-cm (1.0-inch)-diameter FRP dowel groups with spacing varying from 30.48 to 15.24 cm (12 to 6 inches) provided very good LTE (greater than LTE of 60 percent, which corresponds to ACPA’s 75 percent joint effectiveness value).

- For dowel groups in pavement joints 2 and 3 that had the same dowel diameter (3.81 cm (1.5 inches)), joint 2, with smaller dowel spacing (22.86 cm (9 inches)), had higher LTE (94 percent) than that provided by joint 3, with 30.48-cm (12-inch) dowel spacing (81.58 percent). Additional tests will be conducted on other joint locations.
- Joint 2, with 22.86-cm (9-inch) dowel spacing, had smaller RD (6.35×10^{-3} mm (0.25×10^{-3} inch)) than joint 3, with 30.48-cm (12-inch) dowel spacing (17.78×10^{-3} mm (0.70×10^{-3} inch)) for a dowel diameter of 3.81 cm (1.5 inches).
- Joint 2, with 22.86 cm (9 inches) of spacing), provided a 15.4-percent increase in LTE in addition to a 64.3-percent reduction in RD compared with joint 3, with 30.48-cm (12-inch) spacing for a dowel diameter of 3.81 cm (1.5 inches) (refer to table 28).
- For pavement joints 5 and 6 (with 2.54-cm (1.0-inch) dowel diameters, 20.32- and 15.24-cm (8.0- and 6.0-inch) dowel spacing, respectively), the LTEs were very close (95 percent and 94.44 percent). Relative joint deflections were also similar (2.54×10^{-3} cm (1×10^{-3} inch)).
- Currently, there is no requirement or limitation for the RD from AASHTO's *Guide for Pavement Structures*.⁽¹⁾

FRP DOWELS USED FOR HIGHWAY PAVEMENT REHABILITATION

FRP dowels were used for pavement rehabilitation at the junction of Routes 119 and 857, University Avenue, Morgantown, WV. Two joints were selected; one with 3.81-cm (1.5-inch)-diameter FRP dowels and 30.48-cm (12-inch)-c/c spacing, the other with 3.81-cm (1.5-inch)-diameter steel dowels at 30.48-cm (12-inch)-c/c spacing. Dowel installation and field test setup are discussed in this section. Test results from both FRP and steel dowels are analyzed and discussed under the results and analysis subsection.

Field Location

Two joints were selected for rehabilitation of an existing pavement near the junction of Routes 119 and 857, University Avenue, Morgantown, WV, as shown in figure 87. Rehabilitation was carried out in October 2002.

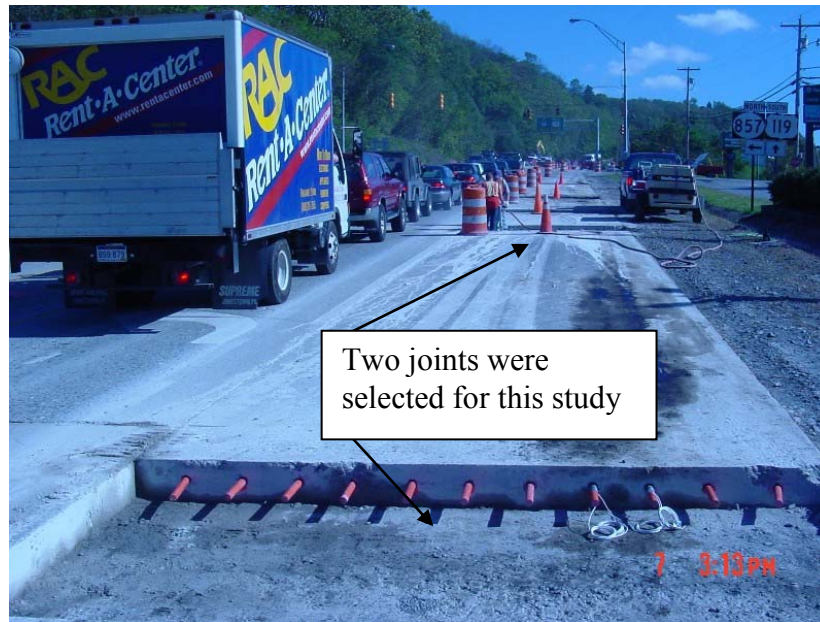


Figure 87. Photo. Locations of FRP and steel-doweled pavement joints.

Field Installation

Deteriorated concrete slabs were cut by a special concrete sawcutting machine and then lifted out. Next, 3.81-cm (1.5-inch)-diameter holes were drilled through the concrete slabs up to 22.86 cm (9 inches) deep (half of dowel length). Each pavement joint consisted of 11 dowels with 3.81-cm (1.5-inch) diameters spaced at 30.48 cm (12 inches) c/c. Each joint was provided with two instrumented dowels. Strain gauges were bonded onto both top and bottom surfaces of those dowels prior to installation. Strain gauges were about 1.27 cm (0.5 inch) away from the centerline of the joint.

After positioning dowels in the drilled holes, epoxy resin was filled into the circumferential gap between concrete and dowel. Rehabilitation carried out using FRP and steel dowels is shown in figure 88 through figure 91.



Figure 88. Photo. Drilling holes for inserting dowels.

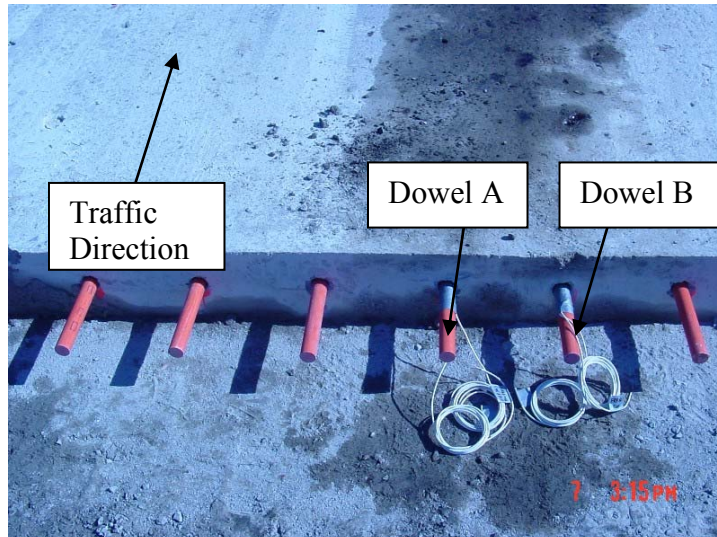


Figure 89. Photo. FRP dowels in position.

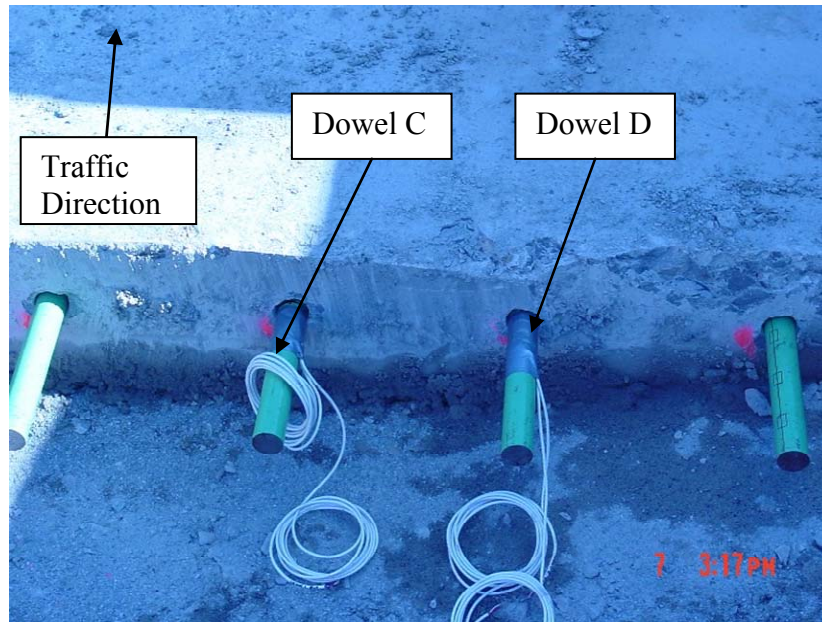


Figure 90. Photo. Steel dowels in position.



Figure 91. Photo. Concrete placement and vibration.

FIELD TESTS

Test Setup

A standard truck load was not used for field loading purposes. Strain readings due to regular traffic (figure 87), including some loaded trucks driving at 32.2–64.4 km/h (25–40 mi/h), were recorded using an automatic data acquisition system (figure 92). Due to the heavy traffic volume existing at this road section, pavement deflection measurements were not recorded.



Figure 92. Photo. Data acquisition recording strain readings.

Results and Analysis

Both strain gauges were installed in the vehicle-approaching side (figure 89 through figure 91) of the pavement joint. Hence, before a vehicle wheel crossed the joint, the strain gauge side of the joint remained the loaded side, and, right after the wheel crossed a joint, the strain gauge side became the unloaded side.

Strain readings due to a truck load from regular traffic are shown in figure 93 and figure 94.

FRP Dowel Group

Strain gauge readings from two instrumented FRP dowels (dowel A and dowel B in figure 89) are discussed in this section. Data from strain gauges mounted on top of these dowels are shown in figure 93. Note that not all data due to continuous traffic are plotted in figure 93; only strain values from a truck load with maximum values are shown.

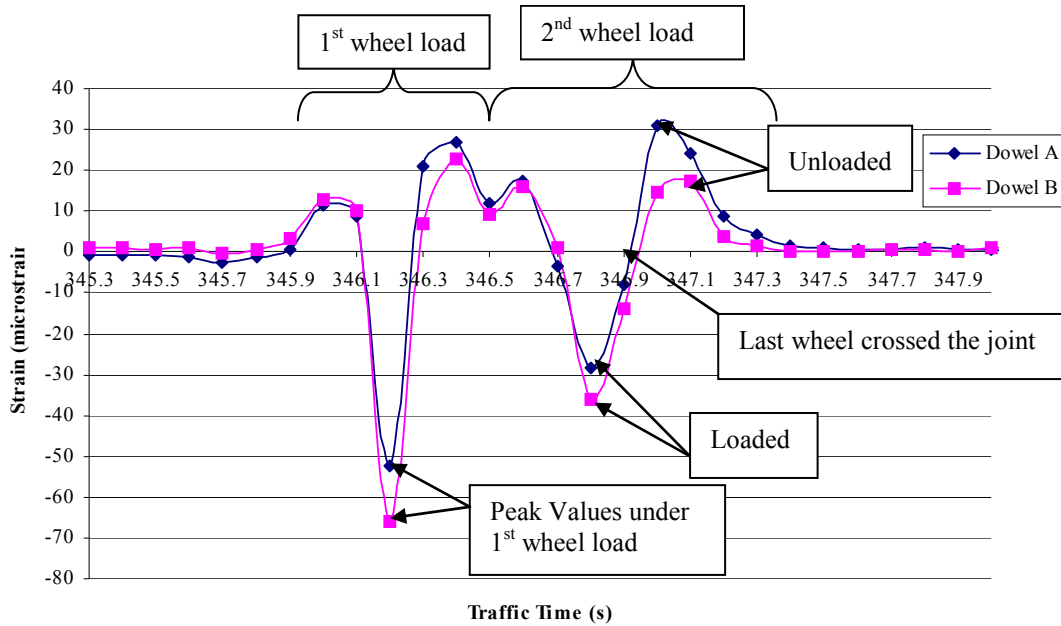


Figure 93. Chart. Strain from FRP dowels in rehabilitated pavement.

Strain gauge data between recorded traffic time of 345.9 and 346.5 s correspond to the movement of the first wheel load. Due to truck load, maximum strains (-52.52 and -65.8 microstrain) occurred when the wheel loads were close to the joint in adjacent dowels. Based on strain values, it appears that the front axle carried more load than the rear axle, and vehicle impact factor could have also played a role.

Strain gauge data between the recorded traffic time of 346.7 and 347.5 s correspond to the movement of the last wheel load crossing the joint. During this time period, gauges from FRP dowels A and B experienced a strain change from loaded status (-28.17 and -36.24 microstrain) to unloaded status (31.04 and 17.16 microstrain), respectively. The total strain change was 59.21 (28.17 + 31.04) microstrain for dowel A and 53.4 (36.24 + 17.16) microstrain for dowel B. The ratio of unloaded value to loaded value was $31.04/28.17 = 1.10$ (dowel A) and $17.16/36.24 = 0.47$ (dowel B). These ratios indicate the possibility of the wheel loads crossing at an angle over the dowel. It should be noted that the pavement was on an upward gradient with respect to traffic direction.

Steel Dowel Group

Strain gauge readings from one instrumented steel dowel (dowel C in figure 90) are discussed here. Data from the strain gauge mounted on top of this dowel are shown in figure 94. Note that not all data due to continuous traffic are plotted in figure 94; only strain values in dowel C from a truck load with maximum values are shown.

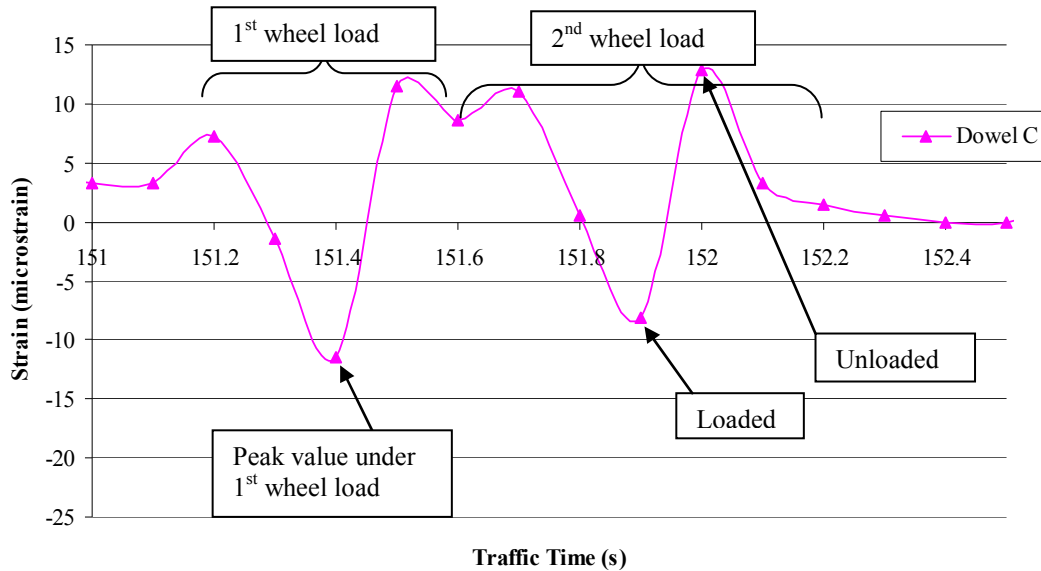


Figure 94. Chart. Strain from steel dowel in rehabilitated pavement.

Strain gauge data between traffic time 151.2 and 151.6 s correspond to the movement of the first wheel load crossing the joint. Maximum compressive strains occurred at the beginning of the load, which was -11.49 microstrain, which may partly include vehicle impact effect.

Strain gauge data between traffic time 151.8 and 152.2 s correspond to the movement of the last wheel load crossing the joint. During this time period, gauges from steel dowel C experienced a strain change from loaded status (-8.14 microstrain) to unloaded status (12.93 microstrain), respectively. The total strain change was 21.07 (8.14 + 12.93) microstrain for dowel C. The ratio of unloaded value to loaded value was $12.93/8.14 = 1.59$ (dowel C). The following factors contributed to this ratio of unloaded/loaded strain > 1 , where readings appeared to be from those vehicles just beginning to accelerate from their stopped position near traffic lights at junction:

- Pavement rehabilitated with dowels was situated on an upward gradient.
- Dowels on the upward portion of the joint were bonded to the concrete with epoxy.

CONCLUSION

From both the first and second field tests conducted on the newly constructed highway in Elkins, WV (see chapter 5), it is concluded that change in strain value for the same dowel during loading and unloading cases was almost the same.

Effect of Dowel Spacing

- For dowel groups in pavement joints 2 and 3 that had the same dowel diameter (3.81 cm (1.5 inches)), joint 2, with smaller dowel spacing (22.86 cm (9 inches)), had higher LTE (94 percent) than that provided by joint 3, with 30.48-cm (12-inch) dowel spacing (81.58 percent). This was attributed to the smaller dowel spacing used in joint 2, which resulted in more dowels sharing the load within the radius of relative stiffness. In addition,

the larger-than-expected difference in LTE for 22.86-cm (9-inch) and 30.48-cm (12-inch) spacing will be investigated in future tests.

- Joint 2, with 3.81-cm (1.5-inch)-diameter dowels and 22.86-cm (9-inch) spacing, had smaller RD (6.35×10^{-3} mm (0.25×10^{-3} inch)) than joint 3, with the same diameter bar and 30.48-cm (12-inch) spacing (17.78×10^{-3} mm (0.70×10^{-3} inch)).
- Joint 2, with 3.81-cm (1.5-inch)-diameter dowels and 22.86-cm (9-inch) spacing, provided a 15.4-percent increase in LTE in addition to a 64.3-percent reduction in RD compared with joint 3, with 3.81-cm (1.5-inch)-diameter dowels and 30.48-cm (12-inch) spacing; refer to table 28.
- For pavement joints 5 and 6 with 2.54-cm (1.0-inch)-dowel diameter, 20.32-cm (8.0-inch) and 15.24-cm (6.0-inch) dowel spacing, respectively, the LTEs were very close (95 and 94.44 percent). Relative joint deflections were also similar (2.54×10^{-3} cm (1×10^{-3} inch)).
- For FRP dowels (A1 and A2) with 2.54-cm (1.5-inch) diameters, dowel A2 with larger spacing (30.48 cm (12 inches)) had a greater strain change (31 microstrain) than dowel A1 with 22.86-cm (9-inch) spacing (9 microstrain). Similarly, for FRP dowels C5 and C6 with the same 2.54-cm (1.0-inch) diameter, the dowel C5 with smaller spacing (15.24 cm (6 inches)) showed small strain change compared to C6 with 20.32-cm (8-inch) dowel spacing (3 versus 60 microstrain).
- Thus, decreasing the spacing by 25 percent (30.48 to 22.86 cm (12 to 9 inches) and 20.32 cm to 15.24 cm (8 to 6 inches)) resulted in more dowels sharing the load within the radius of relative stiffness (l_r , chapter 6), leading to 30 percent or higher strain reductions in dowels.
- For FRP dowels with 2.54-cm (1.0-inch) diameters (C5 and C6), the spacing increase from 15.24 to 20.32 cm (6 to 8 inches) had a greater influence on strain value change (3 versus 60 microstrain) than the increase of spacing from 22.86 to 30.48 cm (9 to 12 inches) in dowels (A1 and A2) with 3.81-cm (1.5-inch) diameters (9 versus 31 microstrain).
- Dowels with different diameters and spacing could not be compared directly by strain value only. Because FRP dowels act as a group, spacing and diameter are both important factors for the group action. It should be also noted that FRP dowels with smaller diameters typically had better mechanical properties per unit area than larger-diameter dowels due to shear lag effects (refer to chapter 6).
- Dynamic test results recorded contained significant noise, and hence, data are not further discussed.

Effect of Dowel Diameter

Both 3.81-cm (1.5-inch)-diameter FRP dowel groups and 2.54-cm (1.0-inch)-diameter FRP dowel groups with spacing varying from 30.48 to 15.24 cm (12 to 6 inches) provided very good LTE (greater than LTE of 60 percent, which corresponds to ACPA's 75 percent joint

effectiveness value). Currently, there is no requirement or limitation for the RD from AASHTO's *Guide for Pavement Structures*.⁽¹⁾ From field tests, the maximum RD was 17.78×10^{-3} mm (0.70×10^{-3} inch), but, from lab testing, it was a maximum of 10.922×10^{-3} mm (43×10^{-3} inch) (table 16). It should be noted that joint width was due to different joint models and thermal variables.

From field tests conducted on the rehabilitated pavement in Morgantown, WV (see chapter 5), the following is concluded:

- Strains at loaded and unloaded status from FRP dowels (A and B) (28.17 and 36.24 micro-strain) were greater than that from steel dowels (C) (11.49 microstrains), which conforms to the analytical finding that shorter lengths are required for FRP dowels than for steel dowels (refer to figure 108).
- The strain value ratio from the same gauge at unloaded status to loaded status did not represent real LTE.
- It was suggested that LTE should be discovered from measuring pavement deflection.

CHAPTER 6. ANALYTICAL EVALUATION

INTRODUCTION

Pavement performance (RD and LTE) in JPCP with the FRP dowel as the load transfer device depends on many design parameters such as dowel diameter, dowel spacing, joint width between adjacent slabs, pavement thickness, concrete strength, base and sub-base properties, and environmental conditions including temperature variation. In this chapter, analytical evaluation is carried out for pavement slabs with FRP dowels.

Several examples provided in this chapter illustrate computations for group action of dowels, maximum bending and shear deflection of dowels, pavement RD, and bearing stresses. Both steel and FRP dowels are used for comparison.

The expansion joint model is used as the analytical model; the contraction joint model is also discussed and compared.

ANALYTICAL MODEL

Computations for a JPCP are carried out by assuming the dowel to be a beam and the concrete to be a Winkler foundation. Based on the original solution by Timoshenko and Lessels for the analysis of beams on an elastic foundation, the differential equation of the deflection of a beam on an elastic foundation is given as follows:⁽¹¹⁾

$$EI \frac{d^4 y}{dx^4} = -ky \quad (4)$$

In equation 4, k is the *modulus of foundation*, a constant, and y is the deflection. The modulus of foundation denotes the reaction due to load per unit length when the deflection is equal to unity. Timoshenko and Lessels gave a solution to the differential equation as follows (equation 5):⁽¹³⁾

$$y = e^{\beta x}(A \cos \beta x + B \sin \beta x) + e^{-\beta x}(C \cos \beta x + D \sin \beta x) \quad (5)$$

Where beta is defined as the following (equation 6):

$$\beta = \sqrt[4]{\frac{k}{4EI}} \quad (6)$$

With relative stiffness of a dowel embedded in concrete, where:

k = Modulus of foundation (MPa (psi)).

E = Modulus of elasticity of the beam (MPa (psi)).

I = Moment of inertia of the beam (cm^4 (inches⁴)).

A , B , C , and D are constants determined from the boundary conditions for a particular beam on an elastic foundation. For a semi-infinite beam on an elastic foundation subject to a point load

and moment applied at its end, as shown in figure 95, constants A and B are equal to zero and C and D are equal to the following (equation 7):

$$C = D = \frac{P}{8\beta^3 EI} \quad (7)$$

After substituting A , B , C , and D (equation 8), equation 5 becomes the following:

$$y = \frac{e^{-\beta x}}{2\beta^3 EI} [P \cos \beta x - \beta M_0 (\cos \beta x - \sin \beta x)] \quad (8)$$

Loads P and M_0 are positive in figure 95. By considering downward deflection as positive and the differentiating equation in equation 8 with respect to x gives slope, dy/dx , of the beam along its axis, as follows (equation 9):

$$\frac{dy}{dx} = \frac{e^{-\beta x}}{2\beta^2 EI} [(2\beta M_0 - P) \cos \beta x - P \sin \beta x] \quad (9)$$

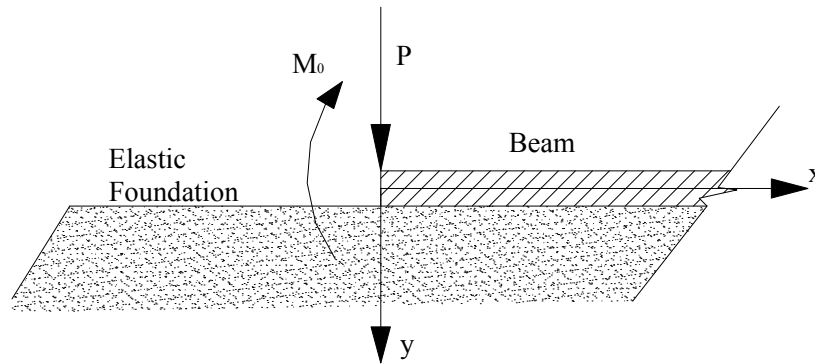


Figure 95. Diagram. Semi-infinite beam on an elastic foundation.

Applying the solution for a semi-infinite beam on an elastic foundation to dowel bars, Friberg developed equations for determining the slope and deflection of a dowel at the face of a joint as shown in figure 96.⁽¹⁴⁾

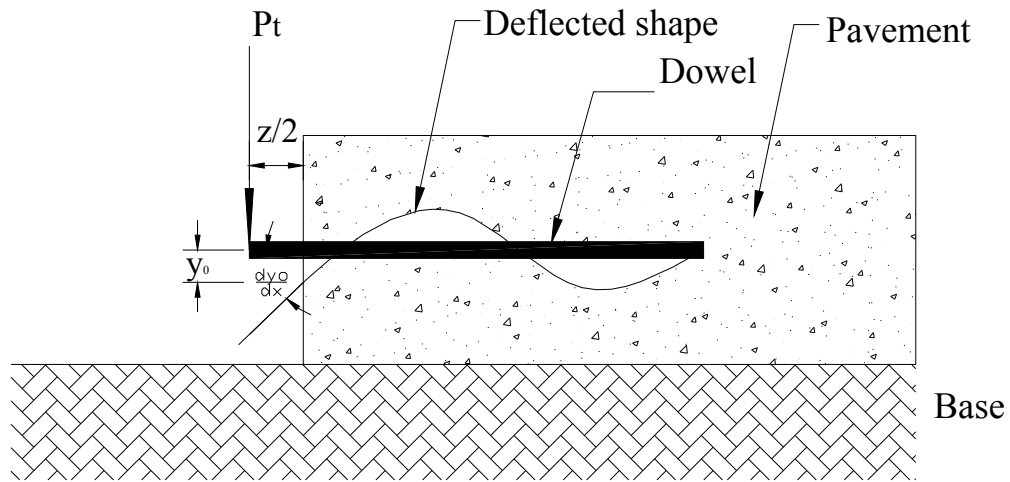


Figure 96. Diagram. Slope and deflection of dowel at joint face.

Substituting $-P_t z/2$ for M_0 (equation 10) and setting x equal to zero in equation 8, slope dy_0/dx and the maximum deflection, y_0 , of the dowel at the face of the joint are given by equation 11 and equation 12, respectively.⁽¹⁴⁾

$$M_0 = \frac{-P_t z}{2} \quad (10)$$

$$\frac{dy_0}{dx} = \frac{-P_t}{2\beta^2 E_d I_d} (1 + \beta z) \quad (11)$$

$$y_0 = \frac{P_t (2 + \beta z)}{4\beta^3 E_d I_d} \quad (12)$$

Where:

β = Relative stiffness of the dowel bar encased in concrete (cm^{-1} (inch^{-1})).

K_0 = Modulus of dowel support (kg/cm^3 (pci)).

E_d = Modulus of elasticity of the dowel bar (MPa (psi)).

I_d = Moment of inertia of the dowel bar (cm^4 (inch^4)).

P_t = Load transferred through the dowel (metric ton (lb)).

d = Diameter of dowel bar (cm (inch)).

z = Joint width (cm (inch)).

Friberg replaced the modulus of foundation k with the expression K_0d . The modulus of dowel support, K_0 , denotes the reaction per unit area due to applied load when the deflection is equal to unity. Thus, relative stiffness of a dowel embedded in concrete, β , is given by (equation 13):⁽¹⁴⁾

$$\beta = \sqrt[4]{\frac{K_0d}{4E_dI_d}} \quad (13)$$

K_0 is an important parameter in Friberg's design equation. K_0 is determined empirically because of the difficulty in establishing it theoretically.⁽¹⁴⁾ Literature reviews indicate a wide range of values for the modulus of dowel support. Modulus of dowel support K_0 increases with increased concrete strength (f_c'), decreases with increased concrete depth below the dowel, and decreases with increased dowel bar diameter. Yoder and Witzczak found that K_0 ranges between 300,000 and 1.5 million pci (8,303.972 and 41,519.858 kg/cm³). For analytical calculations in this chapter, a value of 1.5 million pci (41,519.858 kg/cm³) is used as suggested by Yoder and Witzczak to simulate the worst scenario.⁽¹⁵⁾

Friberg's equations were derived assuming a dowel bar of semi-infinite length.⁽¹⁴⁾ Dowel bars used in practice are of finite length (typically a total length of 45.72 cm (18 inches)); therefore, this equation would not apply. However, Albertson and others have shown that this equation can still be applied to dowel bars with a βL value greater than or equal to 2 with little or no error, where the length of the dowel bar embedded in one side of the slab is denoted as L .⁽¹⁶⁾

Load Transfer Across a Joint

If 100 percent LTE is achieved by the dowel bars, about 50 percent of the wheel load would be transferred to the subgrade while the other 50 percent would be transferred through the dowels to the adjacent slab. However, repetitive loading of the joint results in the creation of a void directly above or beneath the dowel at the face of the joint. According to Yoder and Witzczak, a 5–10 percent reduction in load transfer occurs upon formation of this void; therefore, a design load transfer of 45 percent of the applied wheel load is recommended (equation 14).⁽¹⁵⁾

$$P_t = 0.45P_w \quad (14)$$

Where:

P_t = Load transferred across the joint (metric ton (lb))

P_w = Applied wheel load (metric ton (lb)).

Based on Westergaard's solutions, Friberg found that only the dowels contained within a distance of $1.8 l_r$ from the load carried the applied load, where l_r is the *radius of relative stiffness*, defined as the stiffness of the slab relative to the stiffness of the foundation.⁽¹⁷⁾ Radius of relative stiffness (l_r) is determined by the following formula (equation 15):

$$l_r = \sqrt[4]{\frac{E_c h^3}{12(1-\nu^2)k}} \quad (15)$$

Where:

E_c = Modulus of elasticity of the pavement concrete (MPa (psi)).

$E_c = 57,000(f'_c)^{0.5}$.

h = Pavement thickness (cm (inch)).

ν = Poisson's ratio for the pavement concrete.

k = Modulus of subgrade reaction (g/cm^3 (pci)).

The modulus of subgrade reaction k is a measure of the strength of the supporting soil (equation 16), which may be the sub-base or the subgrade. Its value is given in kilograms per cubic centimeter (kg/cm^3) (pounds per square inch per inch (pci)) deflection as shown in $1 \text{ pci} = 0.02768 \text{ kg/cm}^3$.

$$k = \frac{\text{soil pressure}}{\text{soil deflection}} (\text{pci})$$

$$1 \text{ pci} = 0.02768 \text{ kg/cm}^3 \quad (16)$$

A linear distribution of the load transferred across the joint is typically used, as shown in figure 97:

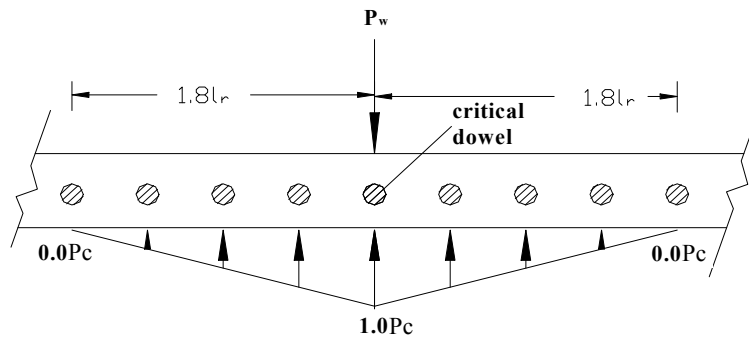


Figure 97. Diagram. Load transfer distribution proposed by Friberg.⁽¹⁴⁾

However, Tabatabaie et al. found that an effective length of $1.0 l_r$ from the applied wheel load is more appropriate for dowels used in practice today (figure 98). A linear approximation was also shown to exist with the maximum dowel shear occurring directly beneath the load and decreasing to a value of zero at a distance $1.0 l_r$ from the load.⁽¹⁸⁾

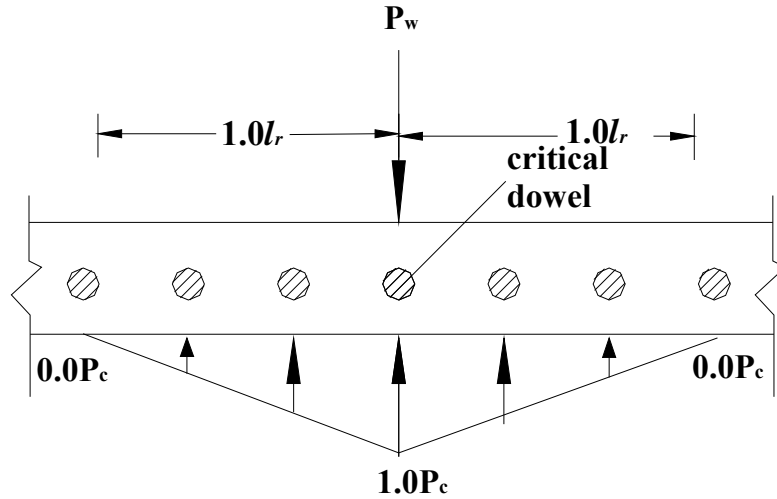


Figure 98. Diagram. Load transfer distribution proposed by Tabatabaie et al.⁽¹⁸⁾

From figure 99, the most critical case is that of the critical dowel being located at the edge of a slab.

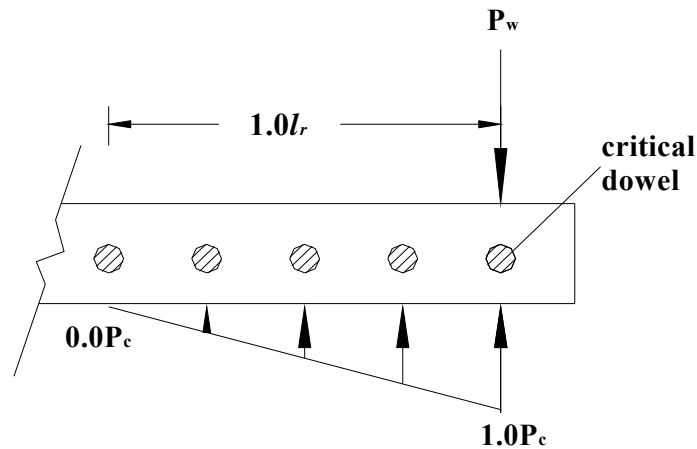


Figure 99. Diagram. Most critical dowel at the edge of a slab.

If the force transferred by a critical dowel, which is located directly beneath the wheel load, is designated as P_c , then the shear force in any other dowel within l_r is determined by multiplying the height of the triangle below that particular dowel by P_c . A value of 1.0 is assumed for the height of the triangle directly below the load, as shown in figure 98. The shear force in the dowel directly under the load is obtained by dividing the transferred load, P_t , by the number of effective dowels, as shown in equation 17. The sum of the heights of the triangle under each dowel within l_r gives the number of effective dowels.

$$P_c = \frac{P_t}{\text{number of effective dowels}} \quad (17)$$

Dowel Bending Moment and Shear

The bending moment (equation 18) and shear force (equation 19) along the dowel from the face of the joint can be expressed as follows:

$$M(x) = -E_d I_d \frac{d^2 y}{dx^2} = \frac{-e^{-\beta x}}{\beta} [P_t \sin \beta x - \beta M_0 (\sin \beta x + \cos \beta x)] \quad (18)$$

$$V(x) = \frac{dM}{dx} = -e^{-\beta x} [(2\beta M_0 - P_t) \sin \beta x + P_t \cos \beta x] \quad (19)$$

Where:

x = Distance along dowel from face of concrete (cm (inch)).

M_0 = Bending moment on dowel at face of concrete (see equation 10).

P_t = Transferred load.

$E_d I_d$ = Flexural rigidity of dowel.

Dowel Bar Deflection and Bearing Stress

The RD between slabs is shown in figure 100, and the expression of Δ is shown in equation 20.

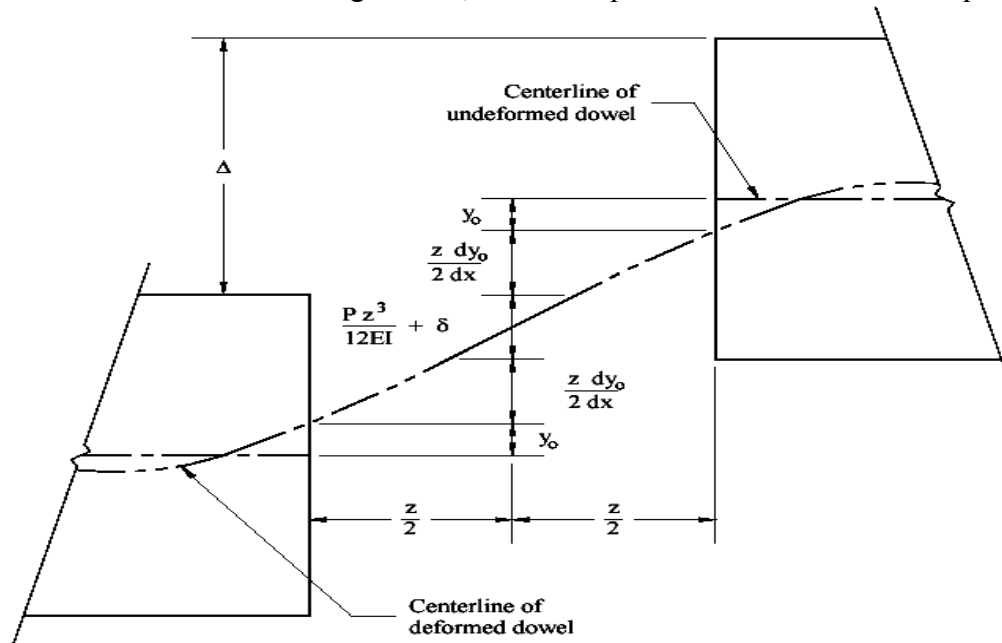


Figure 100. Diagram. RD between concrete slabs (Porter and Guinn).⁽¹⁹⁾

$$\Delta = 2y_0 + z\left(\frac{dy_0}{dx}\right) + \delta + \frac{Pz^3}{12EI} \quad (20)$$

Where:

y_0 = Dowel deflection (from equation 12).

$z\left(\frac{dy_0}{dx}\right)$ = Deflection due to the slope of dowel

$$\delta = \frac{\lambda P_t z}{AG} \quad (21)$$

Where:

λ = Form factor, equal to 10/9 for solid circular section.

A = Cross-sectional area of the dowel bar.

G = Shear modulus.

P_t = Load transferred by critical dowel.

z = Joint width.

$\frac{Pz^3}{12EI}$ = Flexural deflection.

For small joint width, deflections due to slope and flexure are very small, thus neglecting those terms in equation 20 and obtaining equation 22, as follows:

$$\Delta = 2y_0 + \delta \quad (22)$$

Bearing Stress Between Dowel/Concrete Interfaces

The load acting on a dowel is transferred to the supporting/embedding concrete through bearing. Assuming the dowel behaves as a beam on an elastic foundation, the bearing stress at the face of the joint σ_b is proportional to the deformation as shown in equation 23, as follows:

$$\sigma_b = Ky_0 = KP_c \frac{2 + \beta z}{4\beta^3 E_d I_d} \quad (23)$$

The bearing stress defined by equation 23 should not exceed the allowable value. The following equation 24 was given by American Concrete Institute's (ACI) Committee 325.⁽²⁰⁾

$$f_b = \frac{(4-d)f_c'}{3} \quad (24)$$

Where:

f_b = Allowable bearing stress (MPa (psi)).

d = Dowel diameter (cm (inch)).

f_c' = Ultimate compressive strength of concrete slab (MPa (psi)).

Pavement Joint Efficiency

Joint efficiency is determined by the pavement's ability to transfer part of an applied load across the joint to the adjacent slab. AASHTO and ACPA use deflection measurements to determine the efficiency of a joint. Equation 25 is given by ACPA as a means of rating joint effectiveness.⁽¹¹⁾

$$E = \frac{2d_U}{d_L + d_U} \times 100\% \quad (25)$$

Where:

E = Joint effectiveness (percent).

d_U = Deflection of the unloaded side of a joint (cm (inch)).

d_L = Deflection of the loaded side of a joint (cm (inch)).

A joint effectiveness of 75 percent or more is considered adequate for medium to heavy truck loadings. AASHTO adopts the 75 percent criteria and gives equation 26 for determining joint effectiveness associated with a 4.082-metric ton (9,000-lb) wheel load, as follows:⁽¹⁾

$$LTE = \frac{d_U}{d_L} \times 100\% \quad (26)$$

Where:

LTE = Load transfer efficiency (percent).

AASHTO also suggests that a LTE value between 70 and 100 percent is very good load transfer; the joint provides sufficient load transfer.⁽¹⁾ Deflection measurements for use in equations 25 and 26 should be taken at the location of the outside wheel path.

However, LTE and E are related by equation 27:

$$LTE = \left(\frac{2}{2 - E} - 1 \right) \times 100\% \quad (27)$$

According to equation 3, an LTE of 60 percent corresponds to an E of 75 percent. When the value of LTE is between 60 and 100 percent, the joint still provides sufficient load transfer for heavy load.

In this research, the joint LTE defined by AASHTO will be used to evaluate the performance of jointed pavements containing dowels.

THEORETICAL CALCULATION SAMPLES FOR FRP AND STEEL DOWEL GROUP

Calculations have been carried out for two dowel diameters (3.81 cm (1.5 inches) and 2.54 cm (1.0 inch) for both FRP and steel dowels. Other parameters considered for calculation are listed in examples 1 through 4.

Theoretical Calculation for Dowel Group with 3.81-cm (1.5-inch)-Diameter Dowels

Theoretical calculations for concrete pavement joints having FRP and steel dowels with 3.81-cm (1.5-inch) diameter (figure 101) are provided in examples 1 through 4.

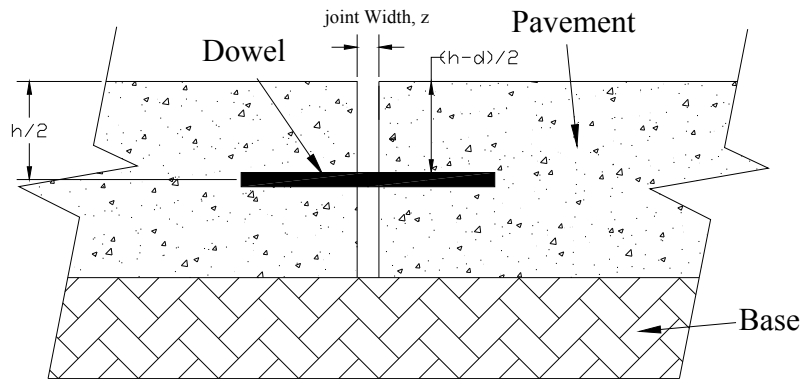


Figure 101. Diagram. Expansion joint model used for theoretical calculation.

Example 1

Example 1 calculates the following items for concrete pavement having 3.81-cm (1.5-inch)-diameter FRP dowels:

1. Radius of relative stiffness.
2. Number of effective dowels.
3. Load carried by the critical dowel.
4. RD Δ between joints.
5. Bearing stress on dowel-concrete interface.

Note that parameters listed below correspond to actual laboratory setup and/or field values that provide with useful comparisons.

- FRP dowel.
 - Diameter, $d = 3.81$ cm (1.5 inches).

- Length, $L = 45.92$ cm (18 inches).
- Spacing between each dowel, $b = 30.48$ cm (12.0 inches).
- Modulus of elasticity, $E_d = 37.921$ MPa (5.5×10^6 psi).
- Shear modulus of dowel, $G = 2.8 \times 10^4$ MPa (0.4×10^6 psi).
- Moment of inertia of the dowel (equation 28),

$$I_d = \frac{\pi \times d^4}{64} = 10.3436 \quad (\text{cm}^4) \quad (0.248505 \text{ in}^4) \quad (28)$$

- Cross-sectional area of dowel, $A = 4.496$ cm² (1.77 inches²).
- Concrete pavement.
 - Compressive strength, $f'_c = 31.026$ MPa (4,500 psi).
 - Modulus of elasticity (equation 29),

$$\begin{aligned} E_c &= 57,000 \times (f'_c)^{0.5} \\ &= 26,363.319 \text{ MPa} (3,823,676.2 \text{ psi}) \\ &= 2.64 \times 10^4 \text{ MPa} (3.82 \times 10^6 \text{ psi}) \end{aligned} \quad (29)$$

- Pavement thickness, $h = 27.94$ cm (11 inches).
- Joint width, $z = 0.635$ mm (0.25 inch).
- Poisson's ratio of concrete, $\nu = 0.2$.
- Modulus of dowel support, $K_0 = 41,519.858$ kg/cm³ (1.5 million) pci.
- Base.
 - Modulus of subgrade reaction, $k = 11.072$ kg/cm³ (400 pci).
- Load.
 - Design traffic load HS25, applied wheel load $P_w = 9.071$ metric tons (20,000 lbs).
 - Design load transfer by joint = 45 percent.
 - $P_t =$ load transferred across the joint = $P_w \times 0.45 = 4.082$ metric tons (9,000 lbs).

Calculation steps are shown in the following flow chart with equations (figure 102).

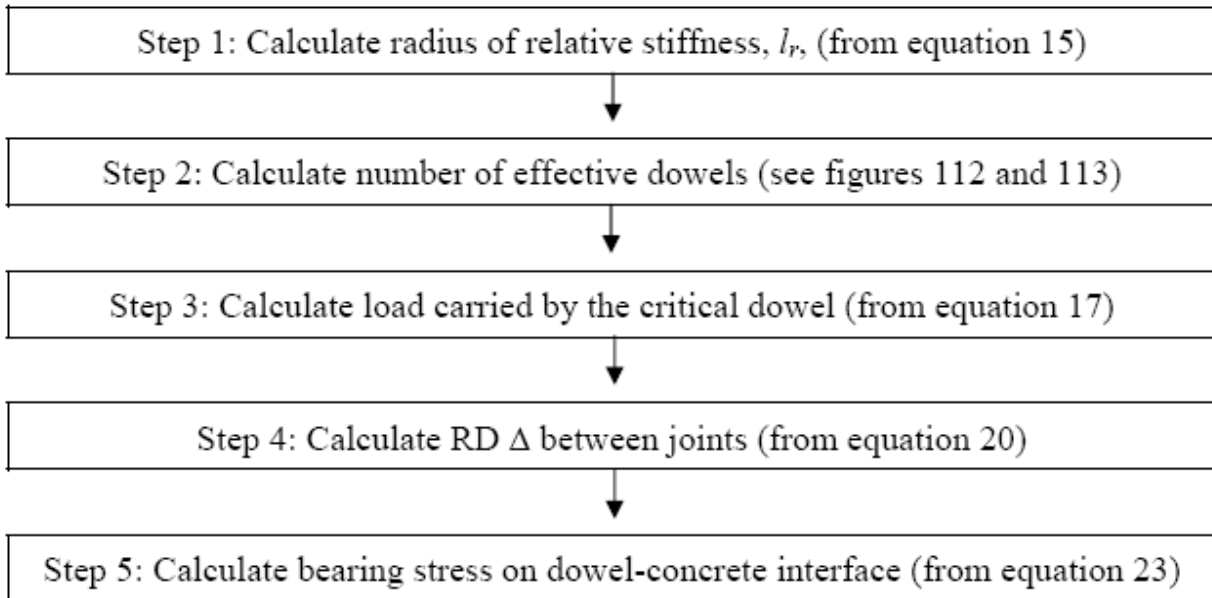


Figure 102. Diagram. Steps for calculating critical dowel load, joint RD, and bearing stress in JPCP.

Details of the calculations are given below from step 1 to step 5.

Step 1. Calculation for radius of relative stiffness (equation 30):

$$\begin{aligned}
 l_r &= \sqrt[4]{\frac{E_c h^3}{12(1-\nu^2)k}} = \sqrt[4]{\frac{3823676 \times 11^3}{12 \times (1-0.2^2) \times 400}} \quad (\text{from equation 15}) \\
 &= 82.34172 \text{ cm (32.4180 inches)}.
 \end{aligned} \tag{30}$$

Step 2. Calculation for number of effective dowels:

The dowels within $1.0 l_r$ distance are effective in load distribution (see figure 98). Number of dowels in $1.0 l_r$ distance (equation 31):

$$\begin{aligned}
 &= 2 \times \text{INT}(l_r/b = 32.4180/12.0 = 2.7) + 1 \\
 &= 2 \times 2 + 1 = 5
 \end{aligned} \tag{31}$$

Where:

l_r = Radius of relative stiffness.

b = Dowel spacing.

The critical dowel in this dowel group, which is the dowel directly under the load, has an effect of 1.0 (figure 98 and figure 99), and other dowel contributions were calculated according to the triangular ratio. Load was distributed on five dowels (one critical dowel plus two effective

dowels on each side) by a triangular variation with due consideration to the available pavement width (see figure 103).

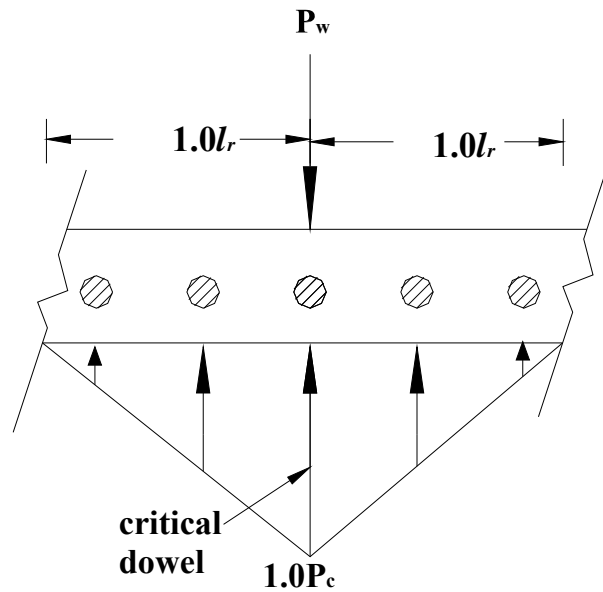


Figure 103. Diagram. Generalized effective dowels for load distribution.

In order to obtain the most critical load condition, it is assumed that the critical dowel is located on the edge of the pavement. Thus, the effective dowel number is reduced to three (one critical dowel and two effective dowels on one side) (see figure 104).

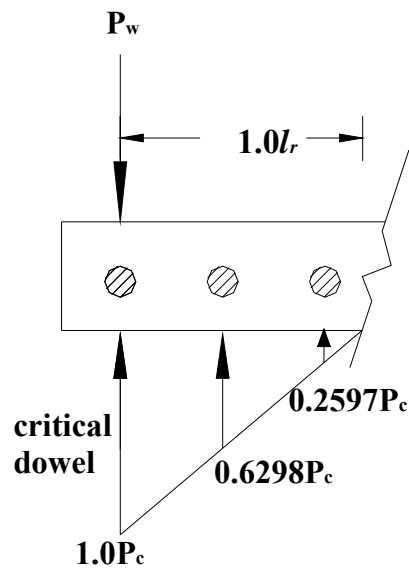


Figure 104. Diagram. Most critical load distribution on effective dowels.

From calculations, the number of effective dowels = $1.0 + 0.6298 + 0.2597 = 1.8895$.

Step 3. Calculation for load carried by the critical dowel:

When wheel load is applied at the edge of the pavement, the critical dowel has to carry most of the transferred load as shown in equation 32 (from equation 17 and figure 97):

$$P_c = \frac{P_t}{\text{number of effective dowels}} \\ = 4.082 \text{ metric tons (9,000 lb)} / 1.8895 = 2.1604 \text{ metric tons (4,763 lb)} \quad (32)$$

Note, that to obtain the same critical load for lab experiments, the following is necessary at the loaded side of the pavement:

$$\frac{P_c}{45\%} = 4.802 \text{ metric tons (10,584.7716 lb)}$$

Step 4. Calculation for RD Δ between joints (from equation 12):

Maximum dowel deflection, as follows:

$$y_0 = \frac{P_c (2 + \beta z)}{4 \beta^3 E_d I_d} \\ = \frac{4763 \cdot 1472 \times (2 + 0.800952 \times 0.25)}{40 \cdot 800952^3 \times 5 \times 10^6 \times 0.2485} \\ (= 0.0037307 \text{ inches}) \\ = 0.009475978 \text{ cm} \quad (33)$$

Where (from equation 13):

$$\beta = \sqrt[4]{\frac{K_0 d}{4 E_d I_d}} \\ = \sqrt[4]{\frac{1,500,000 \times 1.5}{4 \times 5.5 \times 10^6 \times 0.2485}} \\ (= 0.80095168 \text{ inch}^{-1}) \\ = 0.315335 \text{ cm}^{-1} \quad (34)$$

Dowel shear deflection (from equation 21), as follows:

$$\delta = \frac{\lambda P_c z}{AG} = \frac{(10 \div 9) \times 4763 \cdot 1472 \times 0.25}{1.77 \times 4 \times 10^5} \\ (= 0.00187 \text{ inch}) \\ = 0.004750 \text{ cm} \quad (35)$$

Where:

λ = Form factor, equal to 10/9 for solid circular section.

So, total RD between pavement joints is (from equation 22) is shown in equation 36:

$$\begin{aligned}
 \Delta &= 2 y_0 + \delta \\
 &= 2 \times 0.0037307 + 0.00187 \\
 &= 0.00933 \text{ inch} \\
 &= 0.0236982 \text{ cm}
 \end{aligned} \tag{36}$$

Step 5. Calculation for bearing stress on dowel-concrete interface:

Maximum bearing stress occurs at the place where deflection is maximum (from equation 23) as calculated in equation 37.

$$\begin{aligned}
 \sigma_b &= K y_0 \\
 &= 1,500,000 \times 0.0037307 \\
 &= 5596.05 \text{ psi} \\
 &= 38.583 \text{ MPa}
 \end{aligned} \tag{37}$$

The allowable bearing stress is (from equation 24) as calculated in equation 38:

$$\begin{aligned}
 f_b &= \frac{(4 - d) f_c'}{3} \\
 &= \frac{(4 - 1.5) \times 4,500}{3} \\
 &= 3750 \text{ psi} \\
 &= 25.855 \text{ MPa}
 \end{aligned} \tag{38}$$

Thus, $\sigma_b > f_b$ ($5,596.05 > 3,750$); the bearing stress limit is not satisfied.

Discussion for Contraction Joint Model

Theoretical equations derived for dowels from the expansion joint model include the shear deflection term (equation 39) due to the presence of joints with a width of 0.635 cm (0.25 inch).

$$\delta = \frac{\lambda P_c z}{AG} \tag{39}$$

However, depth of contraction and construction joint model (figure 105) (typically $\frac{1}{4}$ to $\frac{1}{3}$ of the pavement thickness) will not reach the dowel surface because the dowel is always surrounded by concrete. To calculate these types of concrete pavement joints, the effective joint width z used for theoretical calculation will be much smaller than 0.635 cm (0.25 inch), say 0.0793 cm (0.0313 inch). This will result in less maximum bending deflection (y_0) and much smaller shear deflection (equation 21) (see table 32 for detailed calculations).

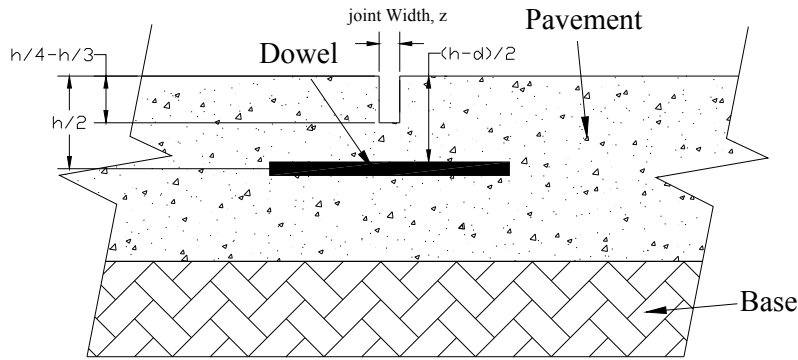


Figure 105. Diagram. Pavement contraction joint model.

Example 2

Example 2 calculates the following items for concrete pavement having 3.81-cm (1.5-inch) steel dowels:

1. Radius of relative stiffness.
2. Number of effective dowels.
3. Load carried by the critical dowel.
4. RD Δ between joints.
5. Bearing stress on dowel-concrete interface.

Parameters used for calculation in example 2 are similar to those in example 1, except that the dowel parameters have been changed to steel dowel properties.

Note that parameters listed below correspond to actual laboratory setup and/or field values that provide useful comparisons.

- Steel dowel.
 - Diameter, $d = 3.81$ cm (1.5 inches).
 - Length, $L = 45.72$ cm (18 inches).
 - Spacing between each dowel, $b = 30.48$ cm (12.0 inches).
 - Modulus of elasticity, $E_d = 20.0 \times 10^4$ MPa (29×10^6 psi).
 - Shear modulus of dowel, $G = 7.58 \times 10^4$ MPa (11×10^6 psi).

- Moment of inertia of the dowel bar,

$$I_d = \frac{\pi \times d^4}{64} = 10.3436 \text{ (cm}^4\text{)} (0.248505 \text{ in}^4) \quad (40)$$

- Cross-sectional area of dowel, $A = 4.496 \text{ cm}^2$ (1.77 inches²).

Calculation steps are the same as those for FRP dowel and are shown in figure 102.

Step 1. Calculation for radius of relative stiffness (from example 1):

$$l_r = 82.342 \text{ cm (32.418 inches)}.$$

Step 2. Calculation for number of effective dowels (from example 1):

$$\begin{aligned} \text{Number of dowels} &= 2 \times \text{INT} (l_r/b = 32.418/12.0 = 2.7) + 1 \\ &= 2 \times 2 + 1 = 5. \\ \text{Number of effective dowels} &= 1.0 + 0.6298 + 0.2597 = 1.8895. \end{aligned} \quad (41)$$

Step 3. Calculation for load carried by the critical dowel (from example 1) as shown in equation 42:

$$\begin{aligned} P_c &= \frac{P_t}{\text{number of effective dowels}} \\ &= 9,000/1.8895 \\ &= 4,763.1472 \text{ lb} \\ &= 2.161 \text{ metric tons.} \end{aligned} \quad (42)$$

Note, that to obtain the same critical load for lab experiments, the calculation shown in equation 43 is necessary (from example 1) at the loaded side of the pavements.

$$\begin{aligned} &\frac{P_c}{45\%} \\ &= 10,584.7716 \text{ lb} \\ &= 4.801 \text{ metric tons} \end{aligned} \quad (43)$$

Step 4. Calculation for RD Δ between joints is done by using equations 44 through equation 46, as follows:

Maximum dowel deflection,

$$\begin{aligned}
 y_0 &= \frac{P_c (2 + \beta z)}{4 \beta^3 E_d I_d} \\
 &= \frac{4763.1472 \times (2 + 0.52856389 \times 0.25)}{4 \times 0.52856389^3 \times 29 \times 10^6 \times 0.2485} \\
 & (= 0.002386 \text{ inch}) \\
 & = 0.006060 \text{ cm}
 \end{aligned} \tag{44}$$

Where:

$$\begin{aligned}
 \beta &= \sqrt[4]{\frac{K_0 d}{4 E_d I_d}} \\
 &= \sqrt[4]{\frac{1,500,000 \times 1.5}{4 \times 29 \times 10^6 \times 0.2485}} \\
 & (= 0.52856389 \text{ inch}^{-1}) \\
 & = 1.404 \text{ cm}^{-1}.
 \end{aligned} \tag{45}$$

Dowel shear deflection,

$$\begin{aligned}
 \delta &= \frac{\lambda P_c z}{AG} \\
 &= \frac{(10 \div 9) \times 4,763.1472 \times 0.25}{1.77 \times 11 \times 10^7} \\
 & (= 0.000007 \text{ inch}) \\
 & = 0.00001778 \text{ cm.} \\
 \text{Total RD ?} &= 2 \times 0.002386 + 0.000007 = 0.012136 \text{ cm (0.004778 inch)}
 \end{aligned} \tag{46}$$

Step 5. Calculation for the bearing stress on dowel-concrete interface (from equation 23) is given by equation 47, as follows:

$$\begin{aligned}
 \sigma_b &= K y_0 \\
 &= 1,500,000 \times 0.002386 \\
 & (= 3578.6247 \text{ psi}) \\
 & = 24.674 \text{ MPa.}
 \end{aligned} \tag{47}$$

The allowable bearing stress is (from equation 24) calculated from equation 48, as follows:

$$\begin{aligned}
 f_b &= \frac{(4 - d) f_c'}{3} \\
 &= \frac{(4 - 1.5) 4500}{3} \\
 &= 3750 \text{ psi} \\
 &= 25.855 \text{ MPa.}
 \end{aligned}
 \tag{48}$$

Thus, $\sigma_b < f_b$, $24.674 < 25.855 \text{ MPa}$ ($3,578.62 < 3,750 \text{ psi}$); the bearing stress limit is satisfied.

Theoretical Calculation for Dowel Group with 2.54-cm (1.0-inch)-Diameter Dowels

Theoretical calculations for concrete pavement joints having FRP and steel dowels with 2.54-cm (1.5-inch) diameter (figure 101) are provided in examples 3 and 4. The expansion joint model (figure 101) is used for calculations. For convenience, figure 101 is shown here again, as figure 106.

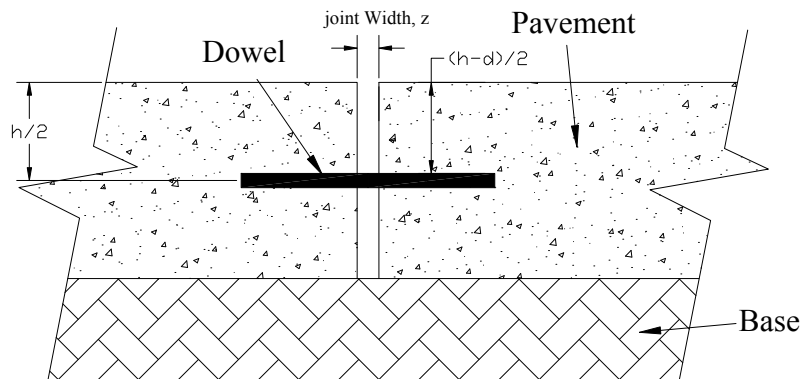


Figure 106. Diagram. Expansion joint model used for theoretical calculation.

Example 3

Example 3 calculates the following items for concrete pavement having 2.54-cm (1.0-inch) FRP dowels:

1. Radius of relative stiffness.
2. Number of effective dowels.
3. Load carried by the critical dowel.
4. RD Δ between joints.
5. Bearing stress on dowel-concrete interface.

Note that parameters listed below correspond to actual laboratory setup and/or field values that provide useful comparisons:

- FRP dowel.
 - Diameter, $d = 2.54$ cm (1.0 inch).
 - Length, $L = 45.72$ cm (18 inches).
 - Dowel spacing, $b = 15.24$ cm (6.0 inches).
 - Modulus of elasticity, $E_d = 4.14 \times 10^4$ MPa (6.0×10^6 psi).
 - Shear modulus of dowel, $G = 0.28 \times 10^4$ (0.4×10^6 psi).
 - Moment of inertia (equation 49),

$$I_d = \frac{\pi \times d^4}{64} = 2.043171 \text{ (cm}^4\text{)} (0.049087 \text{ in}^4) \quad (49)$$

- Cross-sectional area, $A = 1.995$ cm² (0.7854 inch²).
- Concrete pavement.
 - Compressive strength, $f_c' = 31.026$ MPa (4,500 psi).
 - Modulus of elasticity (equation 50),

$$\begin{aligned} E_c &= 57,000 \times (f_c')^{0.5} \\ &= 3,823,676.2 \text{ psi} = 3.82 \times 10^6 \text{ psi} \\ &= 263,633,319 \text{ MPa} = 2.64 \times 10^4 \text{ MPa} \end{aligned} \quad (50)$$

- Pavement thickness, $h = 27.74$ cm (11 inches).
- Joint width, $z = 0.635$ cm (0.25 inch).
- Poisson's ratio of concrete, $\nu = 0.2$.
- Modulus of dowel support, $K_0 = 41,519.858$ kg/cm³ (1.5 million pci).
- Base.
 - Modulus of subgrade reaction, $k = 11.072$ kg/cm³ (400 pci).
- Load.
 - Design traffic load HS25, applied wheel load, $P_w = 9.071$ metric tons (20,000 lbs).

- Design load transfer of 45 percent.
- $P_t =$ load transferred across the joint = $P_w \times 0.45 = 4.082$ metric tons (9,000 lb).

Calculation steps are the same as examples 1 and 2 and are shown in figure 102. Details of the calculations are given below from step 1 to step 5.

Step 1. Calculation for radius of relative stiffness (from equation 15):

$$l_r = \sqrt[4]{\frac{E_c h^3}{12(1-\nu^2)k}} = \sqrt[4]{\frac{3823676 \times 11^3}{12 \times (1-0.2^2) \times 400}}$$

(= 32.4180 inches)
= 82.342 cm

(51)

Step 2. Calculation for number of effective dowels:

The dowels within $1.0 l_r$ distance are effective in load distribution. For the case-critical dowel at slab edge (figure 107), the dowels number in $1.0 l_r$ distance:

$$= \text{INT} (l_r/b = 32.4180/6.0 = 5.40) + 1$$

$$= 5 + 1 = 6,$$

(52)

Where:

l_r = Radius of relative stiffness.

b = Dowel spacing.

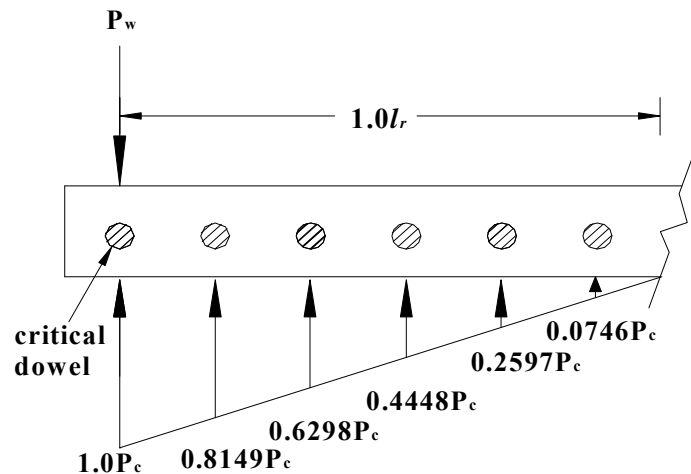


Figure 107. Diagram. Most critical load distribution on effective dowels.

From calculations, the number of effective dowels follows:

$$= 1 + 0.8149 + 0.6298 + 0.4448 + 0.2597 + 0.0746$$

$$= 3.2237$$

Step 3. Calculation for the load carried by the critical dowel:

When wheel load is applied at the edge of the pavement, the critical dowel has to carry most of the transferred load (from equation 17):

$$\begin{aligned}
 P_c &= \frac{P_t}{\text{number of effective dowels}} \\
 &= 9,000/3.2237 \\
 &= 2791.7646 \text{ lbs} \\
 &= 1.266 \text{ metric tons}
 \end{aligned}
 \tag{53}$$

Note that for slabs only containing two 2.54-cm (1.0-inch) FRP dowels, in order to obtain the same critical load for lab experiments, it is necessary to apply the following:

$$\begin{aligned}
 \frac{(1.0+0.8149) \times P_c}{45\%} &= \frac{(1.0+0.8149) \times 2791.76}{45\%} \\
 (= 12,666.93 \text{ lbs}) & \\
 = 5.746 \text{ metric tons} &
 \end{aligned}$$

At loaded side of pavements in lab tests, two dowels are considered.

Step 4. Calculation for the RD Δ between joints (from equation 12) is carried out in equation 54 through equation 56, as follows:

Maximum dowel deflection,

$$\begin{aligned}
 y_0 &= \frac{P_c (2 + \beta z)}{4 \beta^3 E_d I_d} \\
 &= \frac{2791.76 \times (2 + 1.06225 \times 0.25)}{4 \times 1.06225^3 \times 6 \times 10^6 \times 0.049087} \\
 (= 0.00448 \text{ inch}) & \\
 = 0.011379 \text{ cm} &
 \end{aligned}
 \tag{54}$$

Where (from equation 13):

$$\begin{aligned}
 \beta &= \sqrt[4]{\frac{K_0 d}{4 E_d I_d}} \\
 &= \sqrt[4]{\frac{1500000 \times 1.5}{4 \times 6 \times 10^6 \times 0.049087}} \\
 (= 1.0623 \text{ inch}^{-1}) & \\
 = 2.698 \text{ cm}^{-1} &
 \end{aligned}
 \tag{55}$$

Dowel shear deflection (from equation 21):

$$\begin{aligned}\delta &= \frac{\lambda P_c z}{AG} = \frac{(10 \div 9) \times 279176 \times 0.25}{0.7854 \times 0.4 \times 10^6} \\ & (= 0.002468 \text{ inch}) \\ & = 0.006269 \text{ cm}\end{aligned}\tag{56}$$

Where:

λ = Form factor, equal to 10/9 for solid circular section.

So, total RD (equation 57) between pavement joints is as follows (from equation 22):

$$\begin{aligned}\Delta &= 2 y_0 + \delta \\ &= 2 \times 0.0048 + 0.002468 \\ & (= 0.01143 \text{ inch}) \\ & = 0.029032 \text{ cm}\end{aligned}\tag{57}$$

Step 5. Calculation for the bearing stress on dowel-concrete interface:

The maximum bearing stress (equation 58) happens at the place where the deflection is the maximum (from equation 23),

$$\begin{aligned}\sigma_b &= K y_0 \\ &= 1,500,000 \times 0.0048 \\ &= 6718.66 \text{ psi} \\ &= 46.324 \text{ MPa}\end{aligned}\tag{58}$$

The allowable bearing stress (equation 59) is as follows (from equation 24):

$$\begin{aligned}f_b &= \frac{(4 - d) f_c'}{3} \\ &= \frac{(4 - 1.0) 4500}{3} \\ & (= 4500 \text{ psi}) \\ & = 31.026 \text{ MPa}\end{aligned}\tag{59}$$

Thus, $\sigma_b > f_b$, (46.324 > 31.026 MPa (6,718.66 > 4,500 psi)); the bearing stress limit is not satisfied.

Discussion for Contraction Joint Model

In order to meet the bearing stress limit by adjusting dowel spacing only, FRP dowel spacing should not exceed 9.144 cm (3.6 inches). See the detailed data in table 34.

Detailed data of calculations for the contraction joint model (figure 105) are shown in table 34, where joint width z is used as 0.079 cm (0.03125 inches).

Example 4

Example 4 calculates the following items for concrete pavement having 2.54 cm (1.0 inch) steel dowels:

1. Radius of relative stiffness.
2. Number of effective dowels.
3. Load carried by the critical dowel.
4. RD Δ between joints.
5. Bearing stress on dowel-concrete interface.

Parameters used for calculation in example 4 are similar to those in example 3, except dowel parameters have been changed to steel dowel properties.

Parameters listed below correspond to actual laboratory setup and/or field values that provide useful comparisons.

- Steel dowel.
 - Diameter, $d = 2.54$ cm (1.0 inch).
 - Length, $L = 45.72$ cm (18 inches).
 - Spacing between each dowel, $b = 30.48$ cm (12.0 inches).
 - Modulus of elasticity, $E_d = 20 \times 10^4$ MPa (29×10^6 psi).
 - Shear modulus of dowel, $G = 7.58 \times 10^4$ MPa (11×10^6 psi).
 - Moment of inertia of the dowel bar (equation 60):

$$I_d = \frac{\pi \times d^4}{64} = 2.043171(\text{cm}^4) (0.049087 \text{ inches}^4) \tag{60}$$

- Cross-sectional area of dowel, $A = 1.995 \text{ cm}^2 (0.7854 \text{ in}^2)$.

Calculation steps are same as those in example 3, which are for FRP dowels.

Step 1. Calculation for the radius of relative stiffness:

$$l_r = 82.342 \text{ cm (32.4180 inches).}$$

Step 2. Calculation for the number of effective dowels:

The number of dowels = 6

Number of effective dowels = 3.2237.

Step 3. Calculation for the load carried by the critical dowel (equation 61):

$$\begin{aligned} P_c &= \frac{P_t}{\text{number of effective dowels}} \\ &= 9000/3.2237 \\ &= 2791.7646 \text{ lb} \\ &= 1.266 \text{ metric tons.} \end{aligned} \tag{61}$$

Step 4. Calculation for the RDA between joints (equation 62 through equation 65):

Maximum dowel deflection,

$$\begin{aligned} y_0 &= \frac{P_c (2 + \beta z)}{4 \beta^3 E_d I_d} \\ &= \frac{2791.7676 \times (2 + 0.7164 \times 0.25)}{4 \times 0.7164^3 \times 29 \times 10^6 \times 0.04909} \\ &= 0.002906 \text{ inch} \\ &= 0.00738124 \text{ cm} \end{aligned} \tag{62}$$

Where:

$$\begin{aligned} \beta &= \sqrt[4]{\frac{K_0 d}{4 E_d I_d}} \\ &= \sqrt[4]{\frac{1500000 \times 1.0}{4 \times 29 \times 10^6 \times 0.04909}} \\ &= 0.716417 \text{ inch}^{-1} \\ &= 1.819699 \text{ cm} \end{aligned} \tag{63}$$

Dowel shear deflection,

$$\begin{aligned} \delta &= \frac{\lambda P_c z}{AG} \\ &= 0.000009 \text{ inch} \\ &= 0.00002286 \text{ cm} \end{aligned} \tag{64}$$

So, total RD between pavement joints follows:

$$\begin{aligned}\Delta &= 2 y_0 + \delta = 2 \times 0.002906 + 0.000009 (= 0.00582 \text{ inch}) \\ &= 0.01478 \text{ cm}\end{aligned}\tag{65}$$

Step 5. Calculation for the bearing stress (equation 66) on dowel-concrete interface (from equation 23):

$$\begin{aligned}\sigma_b &= K y_0 \\ &= 1,500,000 \times 0.002906 \\ &= 4358.3564 \text{ psi} \\ &= 30.04981 \text{ MPa}\end{aligned}\tag{66}$$

The allowable bearing stress (equation 67) in this case according to ACI is (from equation 24):

$$\begin{aligned}f_b &= \frac{(4 - d) f_c'}{3} \\ & (= 4,500 \text{ psi}) \\ & = 31.026 \text{ MPa}\end{aligned}\tag{67}$$

Thus, $\sigma_b < f_b$, (30.04981 MPa < 31.026 MPa (4,358.3564 psi < 4,500 psi)); the bearing stress limit is satisfied.

DISCUSSIONS ON 3.81-CM (1.5-INCH) AND 2.54-CM (1.0-INCH)-DIAMETER DOWELS

Comparisons for 2.54-cm (1.5-inch)-Diameter Dowel Bars

Additional calculations were conducted, and it was found that in order to meet the bearing stress criteria by adjusting dowel spacing only, FRP dowel spacing should not exceed 17.78 cm (7.0 inches). Detailed data are shown in table 32. Other calculation results are also summarized in table 33.

Table 33. Calculation summaries for 3.81-cm (1.5-inch)-diameter dowel ($k = 11.072 \text{ kg/cm}^3$ (400 pci), $f_c' = 31.026 \text{ MPa}$ (4,500 psi)).

Dowel Material	Spacing (inches)	Radius of Relative Stiffness l_r (inches)	Load Carried by Critical Dowel (lbs)	Effective Dowel Number	Maximum Deflection y_0 (10^{-3} inch)	Shear Deflection δ (10^{-3} inch)	Relative Deflection Δ (10^{-3} inch)	Bearing Stress σ_b (psi)
FRP	12	32.4180	4,763.15	1.8895	3.731	1.872	9.33	5,596.05
Steel	12	32.4180	4,763.15	1.8895	2.386	0.007	4.78	3,578.62
FRP	6	32.4180	2,791.76	3.2238	2.187	1.097	5.47	3,279.92
FRP	7	32.4180	3,168.22	2.8407	2.481	1.245	6.21	3,722.21
FRP*	12	32.4180	4,763.15	1.8895	3.434	0.234	7.10	5,150.39
FRP**	7.5	32.4180	3,350.12	2.6865	2.415	0.165	4.99	3,622.48

Note: Cases FRP* and FRP** are dowel groups in the contraction joint model with joint width $z = 0.079375 \text{ cm}$ (0.03125 inch). Shaded data indicate that bearing stress limit of 28.85 MPa (3,750 psi) in this case is satisfied.

1 inch = 2.54 cm

1 lb = 0.0004536 metric ton

1 psi = 0.006895 MPa

Peak bearing stress at one location does not take into account the stiffness match between FRP dowel and concrete, which allows better distribution of bearing stress leading to reduced bearing stress concentration. Table 34 and table 35 describe the detailed data.

Table 34. Peak bearing stress and average bearing stress in dowel (3.81-cm (1.5-inch) diameter at 30.48 cm (12 inches) c/c) downward area.

	Maximum Deflection y_0 (10^{-3} inch)	Modulus of Dowel Support (pci)	Peak Bearing Stress (psi)	Average Deflection in Dowel Downward Bending Area (10^{-3} inch)	Modulus of Dowel Support (pci)	Average Bearing Stress (psi)	Average/Peak Bearing Stress (percent)
FRP	3.731	300,000	1,119.3	1.321	300,000	396.3	35.40
		1,500,000	5,596.5		1,500,000	1,981.5	
Steel	2.386	300,000	715.8	0.871	300,000	261.3	36.50
		1,500,000	3,578.6		1,500,000	1,307.1	

Note: In table 34, the downward dowel length of FRP and steel dowels ranges from 0 to 5.08 cm (0 to 2 inches) and 0 to 7.62 cm (0 to 3 inches) (figure 108), respectively. The value of the modulus of dowel support ranges from 8303.972 kg/cm^3 to 4,159,858 kg/cm^3 (300,000 to 1.5 million pci).⁽¹⁵⁾

1 inch = 2.54 cm

1 pci = 0.02768 kg/cm^3

1 psi = 0.006895 MPa

Table 35. Peak bearing stress and average bearing stress within 2.54-cm (1-inch) dowel (3.81-cm (1.5-inch) diameter at 30.48 cm (12 inches) c/c length from joint face.

	Maximum Deflection y_0 (10^{-3} inch)	Modulus of Dowel Support (pci)	Peak Bearing Stress (psi)	Average Deflection Within 1.0-inch Distance (10^{-3} inch)	Modulus of Dowel Support (pci)	Average Bearing Stress (psi)	Average/Peak Bearing Stress (percent)
FRP	3.731	300,000	1,119.3	2.275	300,000	682.5	60.98
		1,500,000	5,596.5		1,500,000	3,412.5	
Steel	2.386	300,000	715.8	1.752	300,000	525.6	73.43
		1,500,000	3,578.6		1,500,000	2,628.0	

Note: In table 35, average bearing stresses were calculated for dowel with 2.54-cm (1.0-inch) distance from the face of joint.

1 inch = 2.54 cm
 1 pci = 0.02768 kg/cm³
 1 psi = 0.006895 MPa

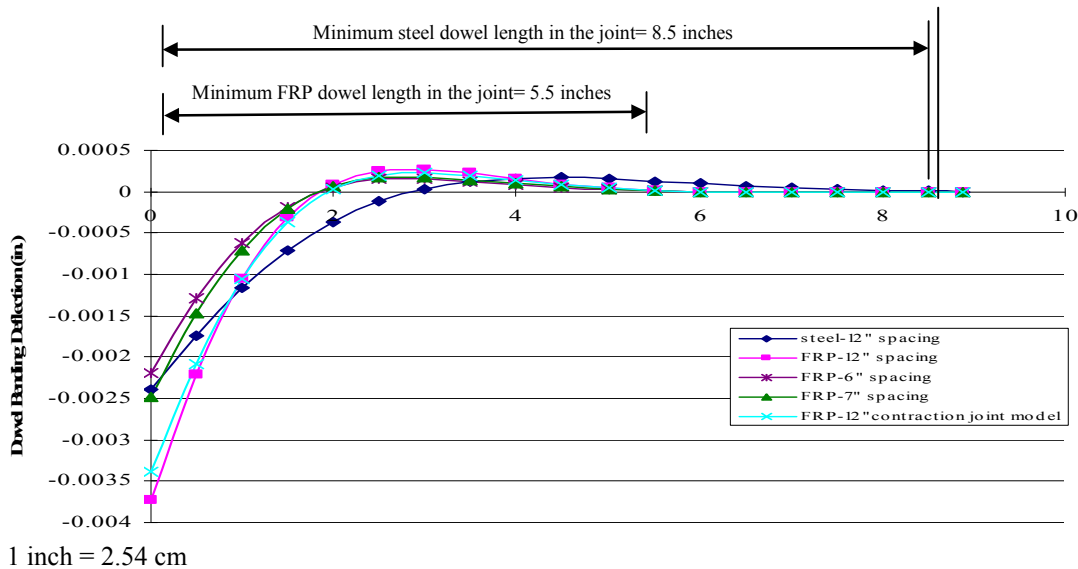


Figure 108. Chart. Dowel deflected shape (2.54-cm (1.5-inch) diameter).

The following can be found for a dowel with 2.54-cm (1.5-inch) diameter:

Effect of Dowel Material

- Equation 4 through equation 24 are developed primarily for concrete pavement with steel dowels. These equations do not take into account better stress distribution and stiffness match between FRP and concrete. For dowels with the same spacing, currently used equations provide a lower value of maximum dowel deflection (y_0), dowel shear deflection (δ), and RD (Δ) for slabs with steel dowels as compared to those with FRP dowels. The bearing stress (σ_b) obtained from analytical evaluation needs to be modified to apply it to FRP dowels because of the lower stiffness of FRP over steel, thus leading to better stress distribution.

- For same-design spacing (30.48 cm (12 inches)), the maximum bending deflection (y_0) of FRP dowels is 56 percent more than that from steel dowels (0.00948 cm versus 0.00606 cm (0.003731 versus 0.002386 inches)). Due to larger shear deflection, the total RD of FRP dowels is 1.95 times the value from steel dowels (0.0236982 versus 0.012141 cm (0.00933 versus 0.00478 milli-inches)). However, the total effective dowel number and load carried by corresponding dowels are the same (refer to table 33).

Effect of Dowel Spacing

- As per currently used equations to evaluate JPCP response to wheel load, FRP and steel dowels have identical values for radius of relative stiffness, number of effective dowels, and critical dowel load for a particular spacing. For example, pavement with 30.48-cm (12-inch)-c/c FRP and steel dowels having $f_c' = 31.026$ MPa (4,500 psi) and joint width of 0.635 cm (0.25 inches) will have identical l_r (82.342 cm (32.4180 inches)), number of effective dowels (1.89), and critical dowel load (2.161 metric tons (4763.15 lbs)).
- To evaluate the wheel load response of JPCP, smaller dowel spacing design will result in the same values for radius of relative stiffness, larger value for number of effective dowels, and lower value for critical dowel load as compared to larger dowel spacing. For example, pavement with 15.24-cm (6-inch)-c/c FRP and steel dowels having $f_c' = 31.026$ MPa (4,500 psi) and joint width of 0.635 cm (0.25 inches) will have identical l_r (82.342 versus 82.342 cm (32.42 versus 32.42 inches)), a larger number of effective dowels (3.22 versus 1.89), and a lower critical dowel load (1.266 versus 2.161 metric tons (2791.76 versus 4763.15 lb)) as compared to dowels with 30.48-cm (12-inch)-c/c spacing.
- Only when spacings between FRP dowels (2.54-cm (1.5-inch) diameter) are reduced to less than 17.78 cm (7 inches) (refer to table 33) would dowel maximum bending deflection (y_0) (6.269×10^{-3} cm (2.481×10^{-3} inch)) be close to the value (6.060×10^{-3} cm (2.386×10^{-3} inch)) of steel dowels (3.81-cm (1.5-inch) diameter) with 30.48 cm (12-inch) spacing.

Effect of Joint Width

- Shear deflection depends on joint width and is significant for FRP dowels. For example, when joint width $z = 0.635$ cm (0.25 inches) with 30.48-cm (12-inch) dowel spacing, shear deflection of FRP dowel (δ) is $1.872/9.33 = 20.06$ percent of the total RD. Shear deflection of steel dowel with 0.635-cm (0.25-inch) joint width is only 0.15 percent (0.007/4.78) of its total RD. When joint width is reduced to 0.079375 cm (0.03125 inch) (FRP* case in table 33), the shear deflection of FRP dowels is only 3.30 percent (0.234/7.10) as compared to 20.06 percent (refer to table 33).
- For same-diameter (3.81-cm (1.5-inch)) FRP dowels, use of the contraction joint model will greatly reduce the shear effect of dowels. For example, RD for joints with FRP dowel bars is greatly reduced (0.0389636 versus 0.019812 cm (0.01534 versus 0.00780 inch)) with the joint width of 0.635 cm (0.25 inches) reduced to 0.079375 cm (0.03125 inches).

Effect of Dowel Length

- Based on inflection points (from figure 108 and figure 109), the minimum total length needed for steel dowels is 43.18 cm (17 inches) (2×21.59 cm (8.5 inches)), whereas FRP dowel bars need a minimum length of 27.94 cm (11 inches) (2×13.97 cm (5.5 inches)). The required FRP dowel length is only 64.7 percent (11/17) of that of the steel dowel.

Effect on Bearing Stress

- For a given set of pavement properties in terms of fc' , thickness, joint width, dowel diameter, and spacing, pavement with FRP and steel dowels shows significant differences in deflection and bearing stress value.
- Bearing stress around the dowel-concrete interface (3.81-cm (1.5-inch) diameter) is only associated with maximum bending deflection. In order to meet the bearing stress limit (25.856 MPa (3,750 psi) in this case), spacings for steel dowels (3.81-cm (1.5-inch) diameter) cannot exceed 30.48 cm (12 inches), whereas spacing for FRP dowels (3.81-cm (1.5-inch) diameter) should not be more than 17.78 cm (7 inches) (expansion joint) or 19.05 cm (7.5 inches) (contraction joint).
- Peak bearing stress at the joint location does not take into account the stiffness match between FRP dowels and concrete, which allows better distribution of bearing stress leading to reduced bearing stress concentration (table 34 and table 35). Theoretical calculations indicate allowable stress is exceeded. However, for 3.81-cm (1.5-inch)-diameter FRP dowel bars with 30.48-cm (12-inch)-c/c spacing, the average bearing stress is only 35.4 percent (the distance from the joint face to the first reflection point) and 0.98 percent (within 2.54 cm (1 inch) distance from the joint face) of the peak bearing stress.

Comparisons for 2.54-cm (1.0-inch)-Diameter Dowel Bars

After additional calculations, it is found that in order to meet the bearing stress criteria by adjusting dowel spacing only, FRP dowel spacing should not exceed 9.398 cm (3.7 inches). For practical purposes, it will be adopted as 8.89 cm (3.5 inches). Detailed data are shown in table 34. Other calculation results are summarized in table 36.

**Table 36. Calculation summaries for 2.54-cm (1.0-inch)-diameter dowel
($k = 11.0719 \text{ kg/cm}^3$ (400 pci), $f_c' = 31.026 \text{ MPa}$ (4,500 psi)).**

Dowel Material	Spacing (inches)	Radius of Relative Stiffness l_r (inches)	Load Carried by Critical Dowel (lbs)	Effective Dowel Number	Maximum Deflection y_0 (10^{-3} inch)	Shear Deflection δ (10^{-3} inch)	Relative Deflection Δ (10^{-3} inch)	Bearing Stress σ_b (psi)
FRP	6	32.4180	2,791.76	3.2237	4.479	2.468	11.43	6,718.66
Steel	6	32.4180	2,791.76	3.2237	2.906	0.009	5.82	4,358.36
FRP	3.5	32.4180	1,750.43	5.1416	2.808	1.548	7.16	4,212.58
FRP*	6	32.4180	2,791.76	3.2237	4.020	0.309	8.35	6,029.56
FRP**	4	32.4180	1,974.54	4.5580	2.843	0.218	5.90	4,264.54

Note: Cases FRP* and FRP** are the calculations for dowel groups in the contraction joint model with joint width $z = 0.079375 \text{ cm}$ (0.03125 inch). Shaded data indicate that bearing stress limit (31.026 MPa (4,500 psi) in this case) is satisfied.

1 inch = 2.54 cm

1 lb = 0.0004536 metric ton

1 psi = 0.006895 MPa

Peak bearing stress at one location does not take into account the stiffness match between FRP dowel and concrete, which allows better distribution of bearing stress, leading to reduced bearing stress concentration. Table 37 and table 38 describe the detailed data.

Table 37. Peak bearing stress and average bearing stress in dowel ((2.54-cm (1.0-inch) diameter at 15.24 cm (6 inches) c/c) downward area.

Material	Maximum Deflection y_0 (10^{-3} inch)	Modulus of Dowel Support (pci)	Peak Bearing Stress (psi)	Average Deflection in Dowel Downward Bending Area (10^{-3} inch)	Modulus of Dowel Support (pci)	Average Bearing Stress (psi)	Average/Peak Bearing Stress (percent)
FRP	4.479	300,000	1,343.7	1.565	300,000	469.5	34.94
		1,500,000	6,718.5		1,500,000	2,347.5	
Steel	2.906	300,000	871.8	1.159	300,000	347.7	39.88
		1,500,000	4,358.4		1,500,000	1,739.1	

NOTE: In table 37, the downward dowel length of FRP and steel dowels ranges from 0 to 3.81 cm (0 to 1.5 inches) and 0 to 7.62 cm (0 to 2 inches)(figure 134), respectively. Values of modulus of dowel support range from 8,303.972 to 4,159.858 kg/cm^3 (300,000 to 1.5 million pci).⁽¹⁵⁾

1 inch = 2.54 cm

1 pci = 0.02768 kg/cm^3

1 psi = 0.006895 MPa

Table 38. Peak bearing stress and average bearing stress within 2.54-cm (1-inch) dowel (2.54-cm (1.0-inch) diameter at 15.24 cm (6 inches) c/c) length from joint face.

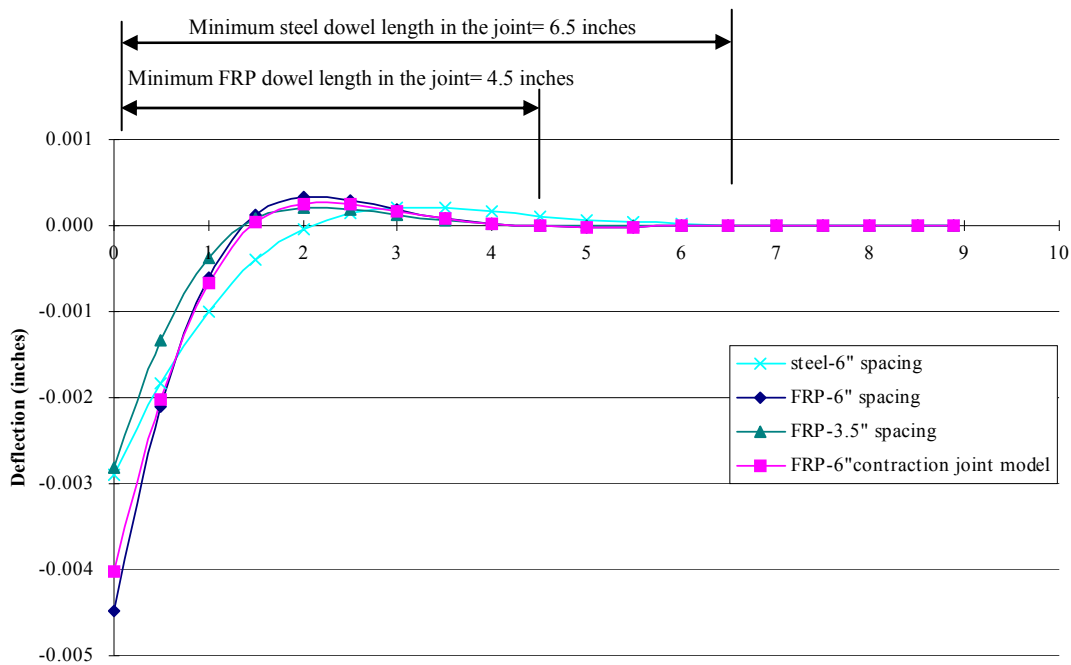
Material	Maximum Deflection y_0 (10^{-3} inch)	Modulus of Dowel Support (pci)	Peak Bearing Stress (psi)	Average Deflection Within 1.0-inch Distance (10^{-3} inch)	Modulus of Dowel Support (pci)	Average Bearing Stress (psi)	Average/ Peak Bearing Stress (percent)
FRP	4.479	300,000	1,343.7	2.259	300,000	677.7	50.44
		1,500,000	6,718.5		1,500,000	3,388.5	
Steel	2.906	300,000	871.8	1.879	300,000	563.7	64.66
		1,500,000	4,358.4		1,500,000	2,818.5	

Note: In table 37, average bearing stresses were calculated for dowels with 2.54 cm (1-inch) distance from the face of joint.

1 inch = 2.54 cm

1 pci = 0.02768 kg/cm³

1 psi = 0.006895 MPa



1 inch = 2.54 cm

Figure 109. Chart. Dowel deflected shape.

The following can be found for dowel with 2.54-cm (1.0-inch) diameter:

Effect of Dowel Material

- Based on equation 4 through equation 24, for dowels with the same spacing, steel dowels provide a lower value of maximum dowel deflection (y_0), dowel shear deflection (δ), RD (Δ) and bearing stress (σ_b).
- For the same-design spacing (15.24 cm (6 inches)), the maximum bending deflection (y_0) of FRP dowels is 54.03 percent more than those from steel dowels (0.01137666 versus 0.00738124 cm (4.479 versus 2.906 milli-inches)). Due to larger shear deflection, the total RD of FRP dowels is 1.96 times the value from steel dowels (0.0290322 versus 0.0147828 cm (11.43 versus 5.82 milli-inches)).

Effect of Dowel Spacing

- As per currently used equations (equation 4 through equation 24) to evaluate JPCP response to wheel load, FRP and steel dowels have identical values for radius of relative stiffness, number of effective dowels, and critical dowel load for a particular spacing. For example, pavement with 15.24-cm (6-inch)-c/c FRP and steel dowels having $fc' = 31.026$ MPa (4,500 psi) and joint width of 0.635 cm (0.25 inches) will have an identical l_r (82.342 cm (32.4180 inches)), number of effective dowels (3.2237), and critical dowel load (1.266 metric tons (2,791.76 lb)).
- To evaluate wheel load response of JPCP, a smaller dowel spacing design will result in the same value for radius of relative stiffness, a larger value for number of effective dowels, and a lower value for critical dowel load as compared to larger dowel spacing. For example, pavement with 8.89-cm (3.5-inch)-c/c FRP and steel dowels having $fc' = 31.026$ MPa (4,500 psi) and joint width of 0.635 cm (0.25 inch) will have identical l_r (82.342 cm (32.4180 inches) versus 82.342 cm (32.4180 inches)), a larger number of effective dowels (5.1416 versus 3.2237) and a lower critical dowel load (0.7940 versus 1.266 metric tons (1,750.43 lb versus 2,791.76 lb)) as compared to dowels with 15.24-cm (6-inch)-c/c spacing.
- Only when spacings between FRP dowels (2.54-cm (1.0-inch) diameter) are reduced to less than 8.89 cm (3.5 inches) (refer to table 36), dowel maximum bending deflection (y_0) (7.132×10^{-3} cm (2.808×10^{-3} inch)) is close to the value (7.381×10^{-3} cm (2.906×10^{-3} inch)) of steel dowels (3.81-cm (1.5-inch) diameter) with 15.24-cm (6-inch) spacing.

Effect of Joint Width

- Shear deflection depends on joint width and is significant for FRP dowels. For example, when joint width $z = 0.0635$ cm (0.25 inches) with 15.24-cm (6-inch) dowel spacing, shear deflection of FRP dowel (δ) was $2.468/11.43 = 21.59$ percent of the total RD. Shear deflection of steel dowel with 0.635-cm (0.25-inch) joint width was only 0.15 percent (0.009/5.82) of its total RD. When joint width was reduced to 0.079 375 cm (0.03125 inch)

(FRP* case in table 33), the shear deflection of FRP dowels is only 3.70 percent (0.309/8.35) as compared to 21.59 percent (refer to table 34).

- For same diameter (2.54-cm (1.0-inch)) FRP dowels, the contraction joint model will greatly reduce the shear effect of dowels. For example, RD for joints with FRP dowel bars are greatly reduced (0.029032 versus 0.021209 cm (11.43 versus 8.35 milli-inches)) with joint width of 0.0635 cm (0.25 inches) reduced to 0.079375 cm (0.03125 inch).

Effect of Dowel Length

- Based on inflection points (from figure 109), the minimum total length for steel dowels is 33.02 cm (13 inches) (2×16.51 cm (2×6.5 inches)), but, for FRP dowel bars, the minimum length is 22.86 cm (9 inches) (2×11.43 cm (2×4.5 inches)). The required FRP dowel length is only 69.23 percent (9/13) of the required length of the steel dowel.

Effect on Bearing Stress

- For a given set of pavement properties in terms of fc' , thickness, joint width, dowel diameter, and spacing, pavement with FRP and steel dowels shows significant differences in deflection and bearing stress value.
- Bearing stress around the dowel-concrete interface (2.54-cm (1.0-inch) diameter) is only associated with the maximum bending deflection. In order to meet the bearing stress limit (31.026 MPa (4,500 psi) in this case), spacings for steel dowels (2.54-cm (1.0-inch) diameter) cannot exceed 30.48 cm (12 inches), whereas spacing for FRP dowels (2.54-cm (1.0-inch) diameter) should not be more than 8.89 cm (3.5 inches) (expansion joint) or 10.16 cm (4.0 inches) (contraction joint).
- For 2.54-cm (1.0-inch)-diameter FRP dowel bars with 15.24-cm (6-inch)-c/c spacing, the average bearing stress is only 34.94 percent (distance from the joint face to the first reflection point) and 50.44 percent (within 2.54 cm (1 inch) of the distance from the joint face) of the peak bearing stress (table 37 and table 38).

COMPARISON OF EXPERIMENTAL VERSUS THEORETICAL DATA

Experimental test results from slabs having normal crack formation were compared with theoretical calculations in table 39. As per the equations (equation 4 through equation 24) used in this chapter, only RDs from static testing were compared.

Table 39. Comparison of experiments versus theory for slab RD in static testing under HS25 loading.

Slab	Experimental Data (10^{-3} inch)		Theoretical Data (10^{-3} inch)	
	Static	Fatigue at 2 million cycles	$K = 1.5$ million pci	$K = 300,000$ pci
Number 1 (FRP dowel, 1.0 inch at 6 inches c/c)	2.27	12.8	11.43	31.26
Number 4 (FRP dowel, 1.5 inch at 12 inches c/c)	29	25	9.33	26.07
Number 5 (steel dowel, 1.5 inch at 12 inches c/c)	11	11	4.78	15.7

1 inch = 2.54 cm

1 pci = 0.027679905 kg/cm³

The following was found:

- For static testing, RDs obtained in concrete slabs (number 4) with large FRP dowel spacing (30.48 cm (12 inches)) in laboratory tests were larger than those from theoretical calculations. Slab number 1 with two FRP dowel bars and small spacing (15.24 cm (6 inches)) had a smaller RD than that from the theory (refer to table 39).
- After 2 million fatigue load cycles, RD of all three slabs were within the theoretical RD range calculated by using modulus of dowel support K from 8,303.972 to 41,519.857 kg/m³ (300,000 to 1.5 million pci).
- The assumption of analytical models does not consider the boundary condition of elastic foundation; in laboratory tests, both ends of concrete slabs were not constrained. Thus, during the testing, both ends were slightly lifted up. Also, the assumed “s” shape (figure 100) for deformation of dowel bars under loading may be more like the “v” shape for unrestrained slabs. Additional tests are necessary to correlate laboratory deflection to analytical evaluations.

ANALYTICAL INVESTIGATION WITH RESPECT TO FRP DOWEL-CONCRETE BEARING STRESS

More extensive analytical investigation for FRP dowel-concrete bearing stress was conducted. More parameters were considered for analysis by using constant values of FRP dowel material properties, as follows:

- Concrete strength f'_c : 20.684, 24.132, 27.579, and 31.026 MPa (3,000, 3,500, 4,000, and 4,500 psi).
- Concrete pavement thickness h : 25.4, 27.94, and 30.48 cm (10, 11, and 12 inches).

- Concrete joint width z : 0.635 and 0.3175 (0.25 and 0.125 inches).
- Dowel length: 30.48, 45.72, and 60.96 cm (12, 18, and 24 inches).
- Dowel diameter d : 2.54, 4.45, 3.81, 4.45, and 5.08 cm (1, 1.25, 1.5, 1.75, and 2 inches).
- Elasticity modulus of Dowel E_d : 3.79×10^4 and 4.14×10^4 MPa (5.5×10^6 and 6×10^6 psi).
- Shear Modulus of Dowel G : 2.8×10^4 MPa (0.4×10^6 psi).
- Dowel spacing b : 15.24, 20.32, 25.4, and 30.48 cm (6, 8, 10, and 12 inches).
- Modulus of subgrade reaction k : 2.768, 11.072, and 22.144 kg/cm³ (100, 400, and 800 pci).
- Modulus of subgrade reaction is a measure of the strength of the supporting soil, which may be the sub-base or the subgrade. Its value is given in kg/cm³ (lb/inch³) of deflection.
- Modulus of dowel supports K : 41,519.878 kg/cm³ (1.5 million pci).

Following are some of the simplified conclusions drawn based on the theoretical analysis using the above parameters:

Bearing stress (σ_b) can be reduced as follows:

- By increasing the following:
 - Dowel diameter (d).
 - Pavement slab thickness (h).
 - Concrete strength (f_c').
- By decreasing the following:
 - Dowel spacing (b).
 - Joint width (z).
 - Modulus of subgrade reaction (k).
 - Modulus of dowel support (K).

Bearing stress (σ_b) cannot be significantly affected by the dowel length beyond a certain length; for FRP dowels, this length is 64.7 percent and 69.23 percent of steel dowels for 3.81- and 2.54-cm (1.5- and 1.0-inch)-diameter dowels, respectively.

Allowable bearing stress (f_b) can be increased by the following:

- Decreasing the dowel diameter (d).
- Increasing the concrete strength (f_c).

CHAPTER 7. CONCLUSIONS AND RECOMMENDATIONS

INTRODUCTION

In this research, FRP dowel bars with 3.81- and 2.54-cm (1.5- and 1.0-inch) diameters spaced at different intervals as load transferring devices in JPCP were evaluated under static and fatigue loads corresponding to HS25 trucks. Their responses were compared with JPCP consisting of steel dowels under laboratory and field conditions. Performance of JPCP rehabilitated with FRP and steel dowels was also evaluated.

Analysis and discussions corresponding to experimental results and theoretical calculations are summarized in this chapter.

CONCLUSIONS FOR LABORATORY TESTS

Laboratory evaluations were carried out on contraction joints (figure 105) with FRP and steel dowels similar to field implementation. During laboratory tests, crack formations were noted under the joint (referred to as proper crack formation, figure 18) or away from the joint near dowel edges (figure 19 and figure 20). Proper crack formation at joint location was noted in slab number 1 (15.24-cm (6-inch)-c/c spacing for 2.54-cm (1.0-inch)-diameter FRP dowels), slab number 4 (30.48-cm (12-inch)-c/c spacing for 3.81-cm (1.5-inch)-diameter FRP dowels), and slab number 5 (30.48-cm (12-inch)-c/c spacing for 3.81-cm (1.5-inch)-diameter steel dowels).

Crack formation at locations away from the joint and close to the edge of the dowel end was observed in slab number 2 (15.24-cm (6-inch)-c/c spacing for 2.54-cm (1.0-inch) diameter for steel dowels) and slab number 3 (15.24-cm (6-inch)-c/c spacing for 2.54-cm (1.5-inch) diameter for steel dowels).

Results mainly focused on slabs with proper crack formation at the mid-joint. Conclusions on laboratory tests are provided with respect to the following:

- RD.
- LTE.
- Pavement pumping.
- Strains on dowels.

Joint RD

For Specimens (Numbers 1, 4, and 5) Having Proper Crack Formation at Joint Locations (Table 6)

- For static testing, RD decreased by decreasing the dowel bar diameter and spacing (0.0577 cm (0.00227 inch), i.e., 2.54-cm (1.0-inch) diameter at 15.24 cm (6 inches) c/c versus 0.00738 cm (0.029 inch) for 3.81-cm (1.5-inch)-diameter FRP dowel at 30.48-cm (12-inch)-c/c spacing).
- RD for slab number 4 reduced (0.00738 to 0.0635 cm (0.029 to 0.025 inch)) with the progression of the fatigue load from 0 to 2 million cycles. RD for slab number 5 remained the same (0.0278 cm (0.011 inch)). This is attributed partly to compaction/settlement of aggregate base underneath the pavement slabs with increasing fatigue cycles, resulting in smaller RD. It can also be attributed to similarities in stiffness between FRP ($\approx 3.79 \times 10^4$ MPa (5.5×10^6 psi)) and concrete ($\approx 2.64 \times 10^4$ MPa (3.8×10^6 psi)). Benefits of these reductions may be more evident with freeze-thaw variations.
- In static tests (table 14), RD in slab number 1 with two 2.54-cm (1.0-inch)-diameter FRP dowels had low RD (0.0577 cm (0.00227 inch)) corresponding to HS25 loading. Analytical values for RD were found to be larger than the experimental value (0.0212 cm (0.0084 inch) for the contraction joint and 0.2903 cm (0.01143 inch) for expansion joint).
- In static tests (table 16), slab number 4 with 3.81-cm (1.5-inch)-diameter FRP dowel had a larger RD (0.0738 cm (0.029 inch)) than slab number 5 with 3.81-cm (1.5-inch)-diameter steel dowel (0.029 cm (0.011 inch)) where the ratio of RDs was 2.64 (0.029/0.011) corresponding to HS25 loading.

For Specimens Having Crack Formation away from Joint Location (Table 7)

Slightly larger RD were noted under static tests (table 15) for slab number 2 (2.54-cm (1.0-inch) steel dowels) and slab number 3 (1.5-inch) FRP dowels) due to crack formation at dowel edges. In addition to higher RD, the load transferred by dowels was less due to that crack formation.

For Base Material Properties (Table 6)

Experimental results on RD were sensitive to supporting base stiffness (k). During tests, the base property (modulus of subgrade reaction, k) value changed from 11.072 to 22.144 kg/cm³ (400 to 800 pci) after 5 million fatigue cycles were applied on slab number 4. RD was expected to increase due to the increase in value of subgrade reaction k .

Joint LTE

AASHTO characterizes LTE value greater than 70 percent as “very good.”⁽¹⁾ APCA suggests that 75 percent of joint effectiveness (E) is sufficient for heavy traffic load, which corresponds to 60 percent of LTE as defined by AASHTO.⁽¹¹⁾

For Specimens (Numbers 1, 4, and 5) Having Proper Crack Formation at Joint Location

- In static tests, all slabs provided good LTE, which was greater than AASHTO and APCA requirements. Slab number 1 (2.54-cm (1.0-inch)-diameter FRP dowels with 15.24-cm (6-inch)-c/c spacing) had a greater than 90 percent LTE. Both slab number 4 (3.81-cm (1.5-inch)-diameter FRP dowel with 30.48-cm (12-inch)-c/c spacing) and slab number 5 (3.81-cm (1.5-inch)-diameter steel dowels with 30.48-cm (12-inch)-c/c spacing) had an LTE of more than 88 percent.
- The LTE was found to be 93.79 percent when 1.5 times design load (HS25 loading) was applied for slab number 1 (2.54-cm (1.0-inch)-diameter FRP dowel at 15.24-cm (6-inch)-c/c spacing) after finishing 1 million fatigue cycles. Later, an increased joint width (increased from 0.635 to 1.02 cm (0.25 to 0.4 inch)) after 2 million cycles was considered; the observed LTE in slab number 1 reduced from 93.79 percent to 71.57 percent, but it was still higher than 60 percent of LTE (corresponding to 75 percent of joint effectiveness, E) (ACPA).
- In fatigue tests, slab number 4 provided good LTE, greater than 80.5 percent after 5 million fatigue load cycles when the base surface and base material under the slab remained in good condition. When the base aggregates were crushed and some of the aggregates were pushed outside of the slab-base contact area (poor base condition), LTEs were found to decrease to about 55 percent, but they were still around 92.1 percent of the 60 percent LTE, which corresponds to the ACPA recommended value on joint effectiveness, E , 75 percent. Detailed data are shown in figure 43.
- At 2 million cycles, slab number 4 containing FRP dowels provided slightly lower LTE (85.1 percent versus 90.21 percent) than slab number 5 containing steel dowels (table 21). With poor base condition (as defined in the previous finding), LTE of the slab with FRP dowels over the slab with steel dowels was 50.71 percent versus 90.21 percent. The most plausible reason causing the low LTE was poor base condition. It should be noted that the modulus of subgrade reaction k changed from 11.072 to 22.144 kg/cm³ (400 to 800 pci) after 5 million cycles.
- Compaction of the base was noted especially under the loaded side of slabs during the tests, which could have created slight concave surfaces under the slabs, possibly leading to reduction in LTE. It is suggested to check the base property (such as k , modulus of subgrade reaction) before and after each fatigue test.

For Specimens Having Crack Formation away from Joint Location (Table 7)

Due to the crack formation, LTEs from slab number 2 (2.54-cm (1-inch)-diameter steel dowels with 15.24-cm (6-inch) spacing) and slab number 3 (3.81-cm (1.5-inch)-diameter FRP dowels with 15.24-cm (6-inch) spacing) were slightly lower than that from slab number 1 in static tests (table 18).

Investigation of Pavement Pumping Problem

- LTEs were observed in cases investigated for simulated pavement pumping problems with supporting base removal up to a certain length near the joint (figure 47 and figure 50). LTEs were not less than the LTEs obtained from intact base condition (table 20). However, under fatigue load cycles, LTE was expected to reduce significantly for specimens without support near the joint.
- The LTE obtained in test case two (30.48 cm (12 inches) base material removal under both sides of slabs) was greater than 90 percent at 13.345 kN (3 kips) loading, and, after loading exceeded 13.345 kN (3 kips), two joint faces would bear against each other. Thus, case two (30.48 cm (12 inches) base removal under both slabs) with unsupported slab areas on both sides of the slab was more detrimental than case one (60.96 cm (24 inches) base removal under loaded slab).

Strains on Dowels

Strain values at the unloaded side of dowels during static tests from slab number 1 and slab number 5 were 513.04 and 376.43 microstrains, respectively. Both values were less than those from analytical evaluation (ranges from 1,000 to 1,200 microstrains) (appendix C). However, strain values are typically not used for LTE calculation.

CONCLUSIONS FOR FIELD APPLICATIONS AND TEST RESULTS

Conclusions for FRP Dowels Used for New Highway Pavement Construction

Effect of Dowel Spacing

- For dowel groups in pavement joints 2 and 3 that had the same dowel diameter (3.81 cm (1.5 inches)), joint 2, with smaller dowel spacing (22.86-cm (9-inches)), had a higher LTE (94 percent) than that provided by joint 3, with 30.48-cm (12-inch) dowel spacing (81.58 percent).
- Joint 2, with 3.81-cm (1.5-inch) diameter and 22.86-cm (9-inch) spacing, had smaller RD (6.35×10^{-3} cm (0.25×10^{-3} inch)) than joint 3, with same diameter bar and 30.48-cm (12-inch) spacing (17.78×10^{-3} cm (0.70×10^{-3} inch)).
- Joint 2, with 3.81-cm (1.5-inch)-diameter dowels and 22.86-cm (9-inch) spacing, provided a 15.4-percent increase in LTE in addition to a 64.3-percent reduction in RD over joint 3, with 3.81-cm (1.5-inch)-diameter dowels and 30.48-cm (12-inch) spacing; refer to table 28.
- For pavement joints 5 and 6 with 2.54-cm (1.0-inch) dowel diameters, 20.32- and 15.24-cm (8.0- and 6.0-inch) dowel spacing, respectively, the LTEs were very close (95 percent and 94.44 percent). Relative joint deflections were also identical (2.54×10^{-3} cm (1×10^{-3} inch)).
- For JPCP with 2.54- or 3.81-cm (1.0- or 1.5-inch) FRP dowels, larger dowel spacings of 30.48 cm (12 inches) (for 2.54-cm (1.0-inch)-diameter dowels) or 20.32 cm (8 inches) (for

2.54-cm (1.0-inch)-diameter dowels) resulted in higher dowel strains compared to those with 22.86- or 15.24-cm (9- or 6-inch) spacing (for 3.81-cm (1.5-inch) diameter dowels and 2.54-cm (1.0-inch)-diameter dowels, respectively) under AASHTO Type 3 truck loading.

- For example, for 2.54-cm (1.5-inch)-diameter FRP dowels (A1 and A2), dowels A2 with larger spacing (30.48 cm (12 inches)) had greater strain change (31 microstrain) than dowels A1 with 22.86-cm (9-inch) spacing (strain change of 9 microstrain). Similarly, for FRP dowels C5 and C6 with the same 2.54-cm (1.0-inch) diameter, the dowel C5 with smaller spacing (15.24 cm (6 inches)) showed a small strain change (3 versus 60 microstrain) compared to dowels C6 with 20.32-cm (8-inch) spacing.
- Decreasing the spacing by 25 percent (30.48 to 22.86 cm (12 to 9 inches) and 20.32 to 15.24 cm (8 to 6 inches)) resulted in more dowels sharing the load within the radius of relative stiffness (lr , see equation 15), leading to 30 percent or higher strain reductions in dowels.
- For FRP dowels with 2.54-cm (1.0-inch) diameters (C5 and C6), the increase of spacing from 15.24 to 20.32 cm (6 to 8 inches) had a higher influence on strain value change (3 versus 60 microstrain) than the increase of spacing from 22.86 to 30.48 cm (9 to 12 inches) for dowels (A1 and A2) with 3.81-cm (1.5-inch) diameters (9 versus 31 microstrain).
- Dowels with different diameters and spacing could be compared with one another based only on strain value. Because FRP dowels act as a group, spacing and diameter are both important factors for the group action. It should be noted that FRP dowels with smaller diameters typically had better mechanical properties per unit area than larger diameter dowels due to shear lag effects (refer to chapter 6).

Effect of Dowel Diameter

- Both 3.81-cm (1.5-inch)-diameter and 2.54-cm (1.0-inch)-diameter FRP dowel groups with spacing varying from 30.48 to 15.24 cm (12 to 6 inches) provided very good LTE (81 percent and higher)—they had LTE greater than 60 percent, which corresponds to ACPA’s 75 percent joint effectiveness (E) value.

Relative Deflection

- Currently, there is no requirement or limitation for the RD from AASHTO’s *Guide for Pavement Structures*.⁽¹⁾ From field tests the maximum RD was 17.78×10^{-3} cm (0.70×10^{-3} inch), corresponding to AASHTO Type 3 truck loading, but, for the laboratory test, the maximum value was 0.109 cm (43×10^{-3} inch) (table 15) corresponding to HS25 loading. It should be noted that joint width due to different joint models (contraction versus expansion joint models) and thermal variables also affected field LTE values.

Conclusions for FRP Dowels Used for Highway Pavement Rehabilitation

Pavement rehabilitation was successfully carried out using FRP dowels near the junction of Routes 119 and 857, University Avenue, Morgantown, WV. After nearly 7 years of rehabilitation, this pavement is performing well without any pavement distress. Strains were monitored on this pavement, which is one of the busiest traffic routes in Morgantown, WV.

- Strains at loaded and unloaded status from FRP dowels (A and B) (28.17 and 36.24 microstrain) were greater than those from steel dowels (C) (11.49 microstrain), which conforms to analytical findings of shorter FRP dowel length required than the length required for steel dowels and higher deflection in FRP dowels (refer to figure 108).
- The strain value ratio from the same gauge at unloaded to loaded status does not represent a proper measure of LTE. It is suggested that LTE should be calculated from the pavement deflection measurement.

CONCLUSIONS FOR ANALYTICAL EVALUATION

Calculations have been carried out for dowel diameters (3.81 and 2.54 cm) (1.5 and 1.0 inches) for both FRP and steel dowels. The base modulus of subgrade reaction $k = 11.072 \text{ kg/cm}^3$ (400 pci), $f_c' = 31.026 \text{ MPa}$ (4,500 psi), and other parameters considered for calculation are listed in examples 1 through 4.

Conclusions for 3.81-cm (1.5-inch)-Diameter Dowels with 30.48-cm (12-inch)-c/c Spacing

Effect of Dowel Material

- Based on current equations, for dowels with the same spacing, steel dowels provided lower values of maximum dowel deflection (y_0), dowel shear deflection (δ), RD (Δ), and bearing stress (σ_b) as compared to FRP dowels.
- For the same-design spacing (30.48 cm (12 inches)), the maximum bending deflection (y_0) of FRP dowels was 56 percent more than those from steel dowels (0.00948 versus 0.00606 cm (3.731 versus 2.386 milli-inches)). Due to a larger shear deflection, the total RD of FRP dowels was 1.95 times the value of RD from steel dowels (0.0237 versus 0.0121 cm (9.33 versus 4.78 milli-inches)).

Effect of Dowel Spacing

- Current equations to evaluate JPCP response to wheel load do not include dowel material properties. The radius of relative stiffness, number of effective dowels, and critical dowel load remained identical for FRP and steel dowels for a given spacing.
 - For example, for pavement with 30.48-cm (12-inch)-c/c spacing, FRP and steel dowels with $f_c' = 31.026 \text{ MPa}$ (4,500 psi) and a joint width of 0.635 cm (0.25 inch) had identical l_r (82.342 cm (32.4180 inches)), number of effective dowels (1.89), and critical dowel load (2.161 metric tons (4,763.15 lb)).

- Current equations for evaluating JPCP response to wheel load have smaller dowel spacing design results in the same values for the radius of relative stiffness, larger values for the number of effective dowels, and lower values for critical dowel load as compared to a larger dowel spacing.
 - For example, for pavement with 15.24-cm (6-inch)-c/c spacing, FRP and steel dowels with $f_c' = 31.026$ MPa (4,500 psi) and joint width of 0.635 cm (0.25 inch) had an identical l_r (82.342 cm (32.4180 inches)), a larger number of effective dowels (3.2238 versus 1.8895), and a lower critical dowel load (1.266 versus 2.161 metric tons (2,791.76 versus 4,763.15 lb)) as compared to dowels with 30.48-cm (12-inch)-c/c spacing.
- Spacings between FRP dowels (3.81-cm (1.5-inch) diameter) less than 17.78 cm (7 inches) provided a maximum dowel bending deflection (y_0) (0.006 302 cm (2.481×10^{-3} inch)) that was close to the value (0.00606 cm (2.386×10^{-3} inch)) provided by steel dowels with 3.81-cm (1.5-inch) diameter and 30.48-cm (12-inch) spacing (refer to table 33).

Effect of Joint Width

- Shear deflection depended on joint width and was significant for FRP dowels.
- For example, when joint width $z = 0.635$ cm (0.25 inches) with 30.48-cm (12-inch) dowel spacing, shear deflection of the FRP dowels (δ) was $1.872/9.33 = 20.06$ percent of the total RD. Shear deflection of the steel dowels with 0.635-cm (0.25-inch) joint width was only 0.15 percent (0.007/4.78) of its total RD. When joint width was reduced to 0.07938 cm (0.03125 inch) (FRP* case in table 33), the shear deflection of FRP dowels was only 3.30 percent (0.234/7.10) as compared to 20.06 percent with 0.635-cm (0.25-inch) joint width (refer to table 33).
- For same-diameter (3.81-cm (1.5-inch)) FRP dowels, use of the contraction joint model greatly reduced the shear effect of dowels.
 - For example, RD for joints with FRP dowel bars were greatly reduced (0.03896 versus 0.019812 cm (15.34 versus 7.80 milli-inches) with joint width of 0.635 cm (0.25 inch) reduced to 0.0794 cm (0.03125 inch).

Effect of Dowel Length

- The required FRP length for 3.81-cm (1.5-inch)-diameter dowels was only 64.7 percent (11/17) of that of steel dowels with the same diameter. Based on inflexion points (figure 108), the minimum total length needed for steel dowels was 43.18 cm (17 inches) (2 by 21.59 cm (2 by 8.5 inches)), whereas FRP dowel bars needed 27.94 cm (11 inches) (2 by 13.97 cm (2 by 5.5 inches)).

Effect on Bearing Stress

- For a given set of pavement properties in terms of f_c' , thickness, joint width, dowel diameter, and spacing, pavement with FRP and steel dowels showed significant differences in deflection and bearing stress value.
- For current analytical models, bearing stress around the dowel-concrete (3.81-cm (1.5-inch) diameter) interface is only associated with maximum bending deflection. In order to meet the bearing stress limit (25.856 MPa (3,750 psi) in this case), spacings for steel dowels (3.81-cm (1.5-inch) diameter) cannot exceed 30.48 cm (12 inches), whereas spacing for FRP dowels (3.81-cm (1.5-inch) diameter) should not be more than 17.78 cm (7 inches) (expansion joint) or 19.05 cm (7.5 inches) (contraction joint) (refer to table 33).
- Peak bearing stress at the joint location did not take into account the stiffness match between FRP dowel and concrete, which allowed better distribution of bearing stress, leading to reduced bearing stress concentration. Theoretical calculations indicated that allowable stress was exceeded. However, for 3.81-cm (1.5-inch)-diameter FRP dowel bars with 30.48-cm (12-inch)-c/c spacing, the average bearing stress was only 35.4 percent (distance from the joint face to the first inflexion point) and 60.98 percent (within 2.54-cm (1-inch) distance from the joint face) of the peak bearing stress (table 34 and table 35).
- Bearing stress (σ_b) could be reduced by increasing dowel diameter (d), pavement slab thickness (h), and concrete strength (f_c'), or it could be reduced by decreasing dowel spacing (b), joint width (z), modulus of subgrade reaction (k), and modulus of dowel support (K_0).

Conclusions for 2.54-cm (1.0-inch)-Diameter Dowels with 15.24-cm (6-inch)-c/c Spacing

Effect of Dowel Material

- For same-design spacing (15.24 cm (6 inches)), the maximum bending deflection (y_0) of FRP dowels was 54.03 percent more than those from steel dowels (0.01138 versus 0.007381 cm (4.479 versus 2.906 milli-inches)). Due to larger shear deflection, the total RD of FRP dowels was 1.96 times the value from steel dowels (0.02903 versus 0.01478 cm (11.43 versus 5.82 milli-inches)).

Effect of Dowel Spacing

- Trends of the effect of dowel spacing were found to be similar to those of 3.81-cm (1.5-inch)-diameter FRP dowel bars.
- Spacings between FRP dowels (2.54-cm (1.0-inch) diameter) less than 8.89 cm (3.5 inches) provided a dowel maximum bending deflection (y_0) (7.132×10^{-3} cm (2.808×10^{-3} inch)) that was close to the value (7.381×10^{-3} cm (2.906×10^{-3} inch)) of steel dowels (3.81-cm (1.5-inch) diameter) with 15.24-cm (6-inch) spacing (refer to table 36).

Effect of Joint Width

- Shear deflection depended on joint width and was significant for FRP dowels.
 - For example, when joint width $z = 0.635$ cm (0.25 inch) with 15.24-cm (6-inch) dowel spacing, shear deflection of FRP dowels (δ) was $2.468/11.43 = 21.59$ percent of the total RD. Shear deflection of steel dowels with 0.635-cm (0.25-inch) joint width was only 0.15 percent ($0.009/5.82$) of its total RD. When joint width was reduced to 0.07938 cm (0.03125 inches) (FRP* case in table 32), the shear deflection of FRP dowels was only 3.70 percent ($0.309/8.35$) as compared to 21.59 percent (refer to table 33).
- For same-diameter (2.54-cm (1.0-inch)) FRP dowels, use of the contraction joint model greatly reduced the shear effect of dowels.
 - For example, RD for joints with FRP dowel bars were greatly reduced (0.0290 versus 0.0212 cm (11.43 versus 8.35 milli-inches)) with joint width of 0.635 cm (0.25 inch) reduced to 0.0794 cm (0.03125 inch).

Effect of Dowel Length

- The required length of 2.54-cm (1.0-inch)-diameter FRP dowels was only 69.23 percent (9/13) of the required length of steel dowels with the same diameter. Based on inflexion points (figure 109), the minimum total length for steel dowel was 33.02 cm (13 inches) (2×16.51 cm (2×6.5 inches)), whereas, for FRP dowels, the minimum length was 22.86 cm (9 inches) (2×11.43 cm (2×4.5 inches)).

Effect on Bearing Stress

- In order to meet the bearing stress limit (31.026 MPa (4,500 psi) in this case), spacings for steel dowels (2.54-cm (1.0-inch) diameter) should be limited to 30.48 cm (12 inches), whereas spacing for FRP dowels (2.54-cm (1.0-inch) diameter) should not be more than 8.89 cm (3.5 inches) (expansion joint) or 10.16 cm (4.0 inches) (contraction joint) (table 36).
- For 2.54-cm (1.0-inch)-diameter FRP dowel bars with 15.24-cm (6-inch)-c/c spacing, the average bearing stress was only 34.94 percent (distance from joint face to the first reflection point) and 50.44 percent (within 2.54 cm (1 inch) distance from joint face) of the peak bearing stress (table 37 and table 38). Hence, based on stress redistribution, peak bearing stress did not appear to have damaged the concrete surface.

GENERAL CONCLUSIONS FROM THIS RESEARCH

1. In this research, FRP dowels were found to be good alternatives to traditional steel dowels for transferring joint loads in JPCP pavements. Joints with FRP dowels provided adequate LTE, exceeding the values recommended by AASHTO (75 percent) and ACPA (60 percent) in both laboratory and field tests.

2. FRP dowel-concrete interfaces in slabs number 1 and 4 were found to be in excellent condition after 5 million HS25 load cycles with no visible damage, microcracks, or separation between FRP dowels and surrounding concrete (refer to figure 36 and figure 44).
3. The stiffness match between FRP dowels and concrete led to comparable FRP dowel flexing under joint loads, leading to shorter FRP dowel length. The required length of FRP dowels with 3.81-cm (1.5-inch) diameter was 64.7 percent of that for steel dowels with the same diameter. The required length of FRP dowels with a 2.54-cm (1.0-inch) diameter was 69.23 percent of that for steel dowels with the same diameter.
4. Under the static loading test, slabs with smaller-diameter FRP dowels and smaller spacing provided lower RD than FRP dowels with larger diameter and spacing. During fatigue load cycles up to 5 million, RD from slab number 1 with the smaller diameter and spacing of FRP dowels appeared to increase (0.3256 to 2.0396 cm (0.0128 to 0.0803 inches) from 2 to 5 million cycles with a joint width of 1.016 cm (0.4 inches)), whereas RD from slab number 4 with a larger diameter and spacing of FRP dowels appeared to decrease 32 percent (0.0635 to 0.0432 cm (0.025 to 0.017 inches) from 2 to 5 million cycles with a joint width of 0.0635 cm (0.25 inches)).
5. The LTE from slabs with FRP dowels of smaller diameter and spacing (2.54 cm (1 inch) and 15.24 cm (6 inches)) was found to be sufficient (71.57 percent, when an increased joint width of 1.016 cm (0.4 inch) and higher loading of $1.5 \times$ HS25 were considered) after 5 million load cycles as per AASHTO (70 percent of LTE) and ACPA (75 percent of E or 60 percent of LTE) suggested values. When a good base condition was provided during 5 million loading cycles, slabs with FRP dowels having 3.81-cm (1.5-inch) diameter and 30.48-cm (12-inch) spacing provided good LTE (greater than 80.5 percent). However, with a poor base condition (aggregate movement leading to a concave surface under the slab), the LTE was reduced to 55.26 percent (which is 92.1 percent of 60 percent LTE, corresponding to the ACPA recommended value on joint effectiveness, $E = 75$ percent). Hence, it is very important to have the proper slab casting procedure and compacted aggregate base.
6. LTE affected the slab integrity and slab stresses, whereas RD affected ride comfort and impact on the slab at joints. It was important to consider both RD and LTE when the performance of JPCP was evaluated. For example, at 5 million cycles, slab number 4 with 3.81-cm (1.5-inch)-diameter FRP dowels spaced at 30.48 cm (12 inches) c/c had 55.26 percent LTE, but its RD (0.043 cm (0.017 inch)) was less than that of slab number 1 with 2.54-cm (1.0-inch)-diameter FRP dowels and 71.6 percent LTE spaced at 15.24 cm (6 inches) c/c (2.04 cm (0.0803 inch)).
7. FRP dowels can be used as effective alternatives for construction and rehabilitation of JPCP under highway traffic with advantages of corrosion resistance and decreased maintenance. Long-term performance evaluation of JPCP with FRP dowels is being continued by the Constructed Facilities Center, WVU.

RECOMMENDATIONS

1. Test more laboratory specimens for establishing possible ranges of LTE and RD values for different diameter, spacing, and length of dowel.
2. Further investigate crack formation location by using increased FRP dowel length, including deflection shapes.
3. Evaluate actual dowel bar deflected shapes in the slab under different base removal conditions.
4. Evaluate the effect of peak bearing stress and average bearing stress on dowel/concrete interface.
5. Evaluate the effect of fiber volume fraction on dowel behavior, including shear properties that affect joint LTE and RD.
6. Evaluate the durability of the FRP dowel.
7. Utilize finite element modeling to envision stress field in the concrete pavement.
8. Continue long-term field monitoring.

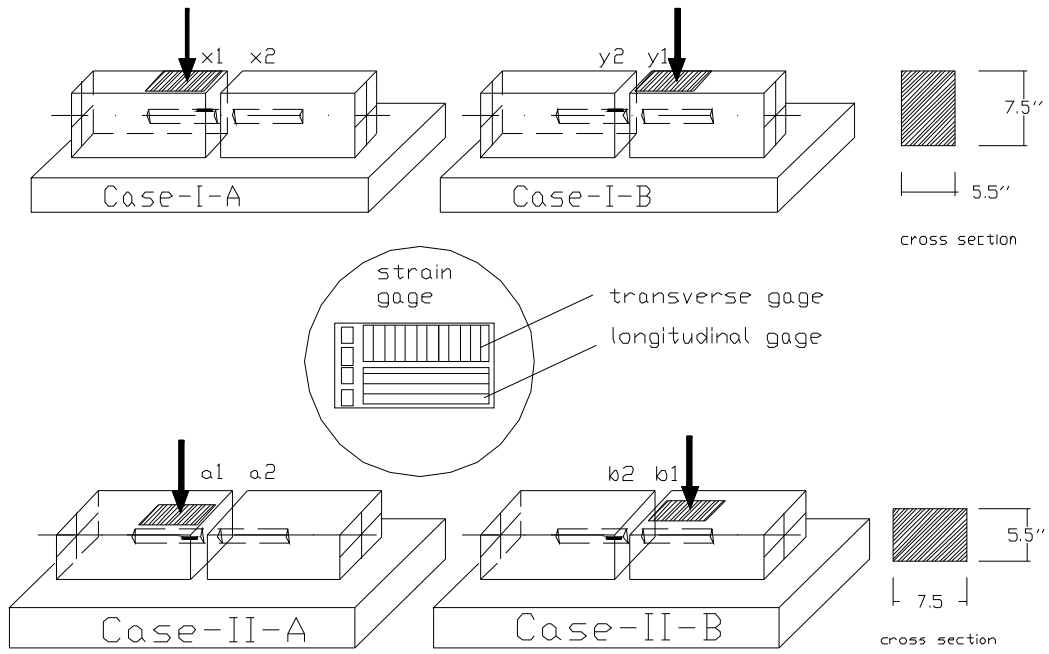
APPENDIX A. TEST OF TIMBER TIE WITH FRP DOWELS

Before evaluating FRP dowels in concrete slabs joints, pilot tests were carried out using rectangular timber beams. A long timber beam was cut into two halves and drilled with 4.45-cm (1.75-inch)-diameter holes to simulate dowel sockets in a slab. Dowel sockets facilitated placement of instrumented dowels inside the timber beams. Load tests were conducted by turning dowels at 45-degree angles to measure dowel strains from longitudinal and transverse gauges (figure 110 to figure 112).

Four cases were evaluated based on loading position and timber depth (corresponding to positioning of the timber beam surface on the base). Test setup of each case is shown in figure 111.



Figure 110. Photo. Lab test of timber tie with FRP dowel bar as the load transfer device.



1 inch = 2.54 cm

Figure 111. Diagram. Four timber test cases.

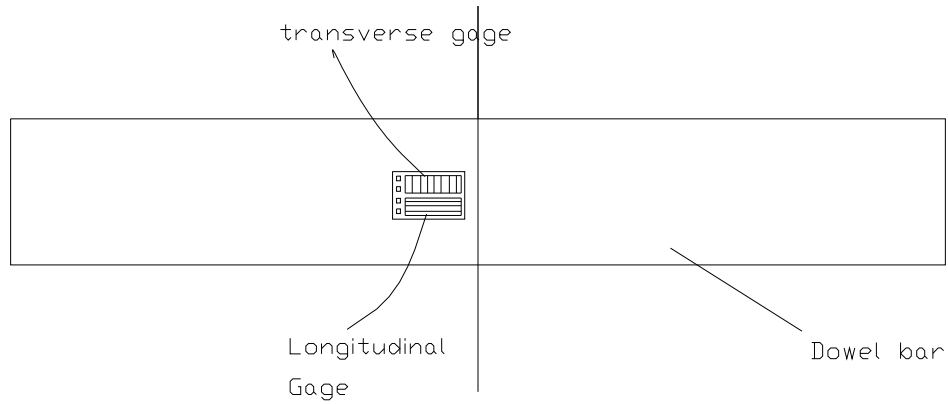


Figure 112. Diagram. Rosette strain gauges.

Table 40. Strains during loading and unloading on case I-A.

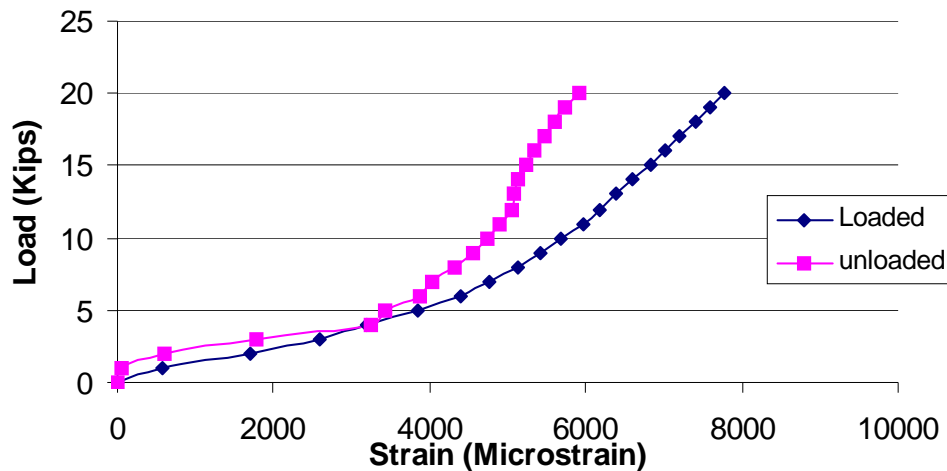
Loading			Unloading		
Load (kips)	Transverse Gauge	Longitudinal Gauge	Load (kips)	Transverse Gauge	Longitudinal Gauge
0	0	0	20	1,627	7,836
1	64	576	19	1,610	7,797
2	229	1,707	18	1,580	7,752
3	377	2,585	17	1,554	7,707
4	493	3,182	16	1,527	7,662
5	624	3,848	15	1,498	7,609
6	725	4,389	14	1,467	7,562
7	804	4,770	13	1,432	7,522
8	871	5,118	12	1,391	7,420
9	933	5,415	11	1,346	7,365
10	1,021	5,668	10	1,292	7,167
11	1,105	5,962	9	1,226	7,032
12	1,166	6,188	8	1,135	6,982
13	1,223	6,384	7	1,032	6,670
14	1,285	6,584	6	940	6,495
15	1,347	6,844	5	790	5,957
16	1,393	7,011	4	674	5,610
17	1,451	7,204	3	560	4,971
18	1,515	7,409	2	605	3,987
19	1,564	7,599	1	171	2,370
20	1,627	7,781	0	0	0

1 kip = 4.448 kN

Table 41. Strains during loading and unloading on case I-B.

Loading			Unloading		
Load (kips)	Transverse Gauge	Longitudinal Gauge	Load (kips)	Transverse Gauge	Longitudinal Gauge
0	0	0	20	1,357	5,920
1	59	49	16	1,332	5,976
2	220	592	12	1,302	5,931
3	511	1,787	8	1,265	5,863
4	734	3,238	4	1,081	5,066
5	799	3,419	0	0	136
6	899	3,872			
7	908	4,040			
8	1,012	4,325			
9	1,040	4,559			
10	1,067	4,740			
11	1,106	4,901			
12	1,137	5,044			
13	1,144	5,091			
14	1,152	5,119			
15	1,186	5,241			
16	1,206	5,339			
17	1,251	5,473			
18	1,277	5,610			
19	1,310	5,746			
20	1,357	5,920			

1 kip = 4.448 kN



1 kip = 4.448 kN

Figure 113. Chart. Plot for longitudinal strain gauges (case I-A and case I-B).

Table 42. Strains during loading and unloading on case II-A.

Loading			Unloading		
Load (kips)	Transverse Gauge	Longitudinal Gauge	Load (kips)	Transverse Gauge	Longitudinal Gauge
0	0	0	20	1	7
2	1	8	16	1	6
4	1	7	12	1	6
6	1	7	8	1	6
8	1	7	4	1	6
10	1	7	0	0	0
12	1	7			
14	1	7			
16	1	6			
18	1	7			
20	1	7			

1 kip = 4.448 kN

Table 43. Deflections of timber tie on case I-A.

Load (kips)	Dial Gauge Reading at Loaded End (inch)	Deflection at x1 (inch)	Dial Gauge Reading at Unloaded End (inch)	Deflection at x2 (inch)
0	0.469	0.000	0.515	0.000
1	0.402	0.067	0.490	0.025
2	0.335	0.134	0.465	0.050
3	0.238	0.231	0.468	0.047
4	0.170	0.299	0.467	0.048
5	0.130	0.339	0.466	0.049
6	0.080	0.389	0.465	0.050
7	0.048	0.421	0.465	0.050
8	0.020	0.449	0.465	0.050
9	-0.190	0.659	0.465	0.050
10	-0.170	0.639	0.465	0.050
11	-0.160	0.629	0.465	0.050
12	-0.150	0.619	0.465	0.050
13	-0.162	0.631	0.465	0.050
14	-0.176	0.645	0.466	0.049
15	-0.197	0.666	0.466	0.049
16	-0.215	0.684	0.467	0.048
17	-0.229	0.698	0.467	0.048
18	-0.247	0.716	0.468	0.047
19	-0.262	0.731	0.468	0.047
20	-0.275	0.744	0.469	0.046

1 kip = 4.448 kN

1 inch = 2.54 cm

Table 44. Deflections of timber tie on case I-B.

Load (kips)	Dial Gauge Reading at Loaded End (inch)	Deflection at $y1$ (inch)	Dial Gauge Reading at Unloaded End (inch)	Deflection at $y2$ (inch)
0	0.915	0.000	0.525	0.000
1	0.870	0.045	0.501	0.024
2	0.825	0.090	—	—
3	0.660	0.255	—	—
4	0.575	0.340	0.406	0.119
5	0.515	0.400	—	—
6	0.462	0.453	—	—
7	0.430	0.485	—	—
8	0.390	0.525	0.397	0.128
9	0.365	0.550	—	—
10	0.331	0.584	—	—
11	0.300	0.615	—	—
12	0.272	0.643	0.388	0.137
13	0.250	0.665	—	—
14	0.228	0.687	—	—
15	0.202	0.713	—	—
16	0.185	0.730	0.383	0.142
17	0.165	0.750	—	—
18	0.140	0.775	—	—
19	0.123	0.792	—	—
20	0.090	0.825	0.382	0.143

— No data at corresponding loads.

1 kip = 4.448 kN

1 inch = 2.54 cm

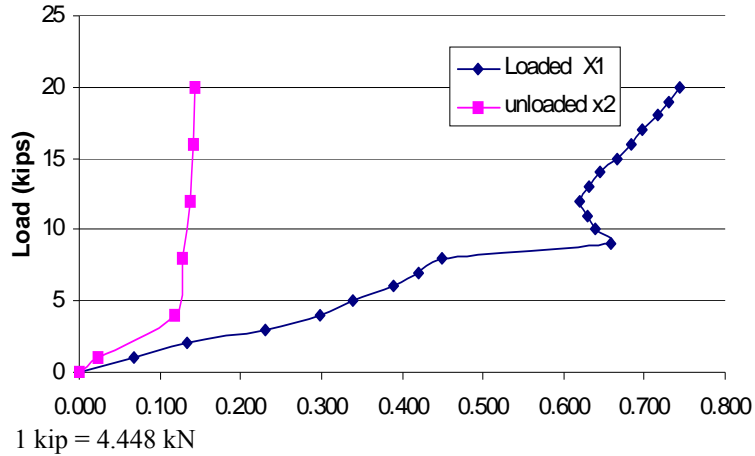


Figure 114. Chart. Load versus deflection (inches) of timber tie for case I-A.

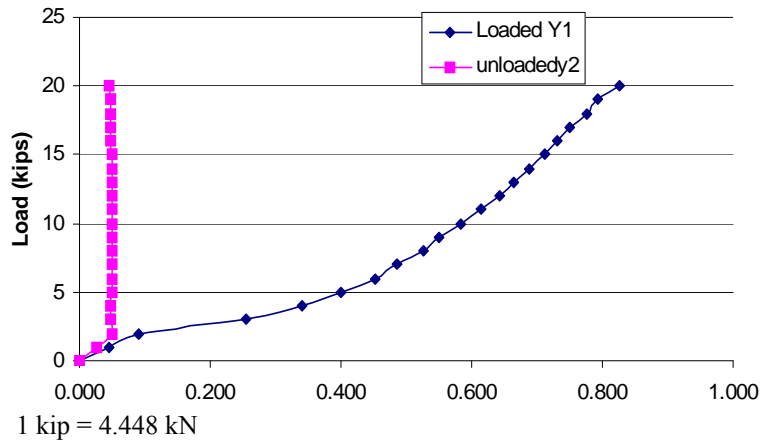


Figure 115. Chart. Load deflection (arm with regular gauge) for case I-B.

Joint Effectiveness from Case I-A and Case I-B Under 20 kips Loading

Case I-A

$$\frac{2 \times \text{Deflection at Unloaded Side}}{\text{Deflection Total of Both Sides}} = \frac{2 \times 0.046}{(0.744 + 0.046)} \times 100\% = 12.15\% \quad (68)$$

Case I-B

$$\frac{2 \times \text{Deflection at Unloaded Side}}{\text{Deflection Total of Both Sides}} = \frac{2 \times 0.143}{(0.825 + 0.143)} \times 100\% = 29.55\% \quad (69)$$

In this preliminary test, joint effectiveness obtained in timber with 3.81-cm (1.5-inch) FRP dowels was low. This was due to several factors, such as the low stiffness of timber material and the larger hole diameter (4.45 cm (1.75 inches)) for accommodating 3.81-cm (1.5-inch)-diameter FRP dowels.

APPENDIX B. ANALYTICAL EVALUATION OF EFFECT OF FRP DOWEL SHEAR MODULUS ON PAVEMENT RD

Analytical evaluation was conducted to find the effect of a dowel shear modulus on pavement RD. Parameters used for calculation are listed below. Detailed data are shown in tables 44 and 45, and figure 16 and figure 17:

- FRP dowel.
 - Diameter, $d = 3.81$ and 2.54 cm (1.5 and 1.0 inches).
 - Length, $L = 45.72$ cm (18 inches).
 - Spacing between each dowel, $b = 15.24, 30.32, 25.4,$ and 30.48 cm (6, 8, 10, and 12 inches).
 - Modulus of elasticity, $E_d = 3.79 \times 10^4$ MPa (5.5×10^6 psi) for 3.81-cm (1.5-inch)-diameter dowel and $E_d = 4.14 \times 10^4$ MPa (6.0×10^6 psi) for 2.54-cm (1.0-inch) diameter.
 - Shear modulus of dowel, low $G_d = 0.28 \times 10^4$ MPa (0.4×10^6 psi), and high $G_d = 5.17 \times 10^4$ MPa (0.75×10^6 psi).
 - Moment of inertia of the dowel,

$$I_d = \frac{\pi \times d^4}{64} = 0.248505 \text{ (in}^4\text{)}. \quad (70)$$

- Cross-sectional area of dowel, $A = 4.496 \text{ cm}^2$ (1.77 inches²).
- Concrete pavement.
 - Compressive strength, $fc' = 31.026$ MPa (4,500 psi).
 - Modulus of elasticity,

$$\begin{aligned} E_c &= 57000 \times (fc')^{0.5} \\ &= 3823676.2 \text{ psi} = 3.82 \times 10^6 \text{ psi} \\ &= 2.64 \times 10^4 \text{ MPa.} \end{aligned} \quad (71)$$
 - Pavement thickness, $h = 27.94$ cm (11 inches).
 - Joint width, $z = 0.635$ cm (0.25 inch).
 - Poisson's ratio of concrete, $\nu = 0.2$.
 - Modulus of dowel support, $K_\theta = 4.15 \times 10^4 \text{ kg/cm}^3$ (1.5 million pci).

- Base.
 - Modulus of subgrade reaction, $k = 11.072 \text{ kg/cm}^3$ (400 pci).
- Load.
 - Design Traffic Load HS25, applied wheel load $P_w = 9.071$ metric tons (20,000 lb).
 - Design load transfer by joint = 45 percent.
 - P_t = load transferred across the joint

$$\begin{aligned}
 &= P_w \times 0.45 \\
 &= 9000 \text{ lb} \\
 &= 4.082 \text{ metric tons.}
 \end{aligned}
 \tag{72}$$

Table 45. RD with low dowel shear modulus ($G_d = 2.758 \times 10^3 \text{ MPa}$ ($0.4 \times 10^6 \text{ psi}$)).

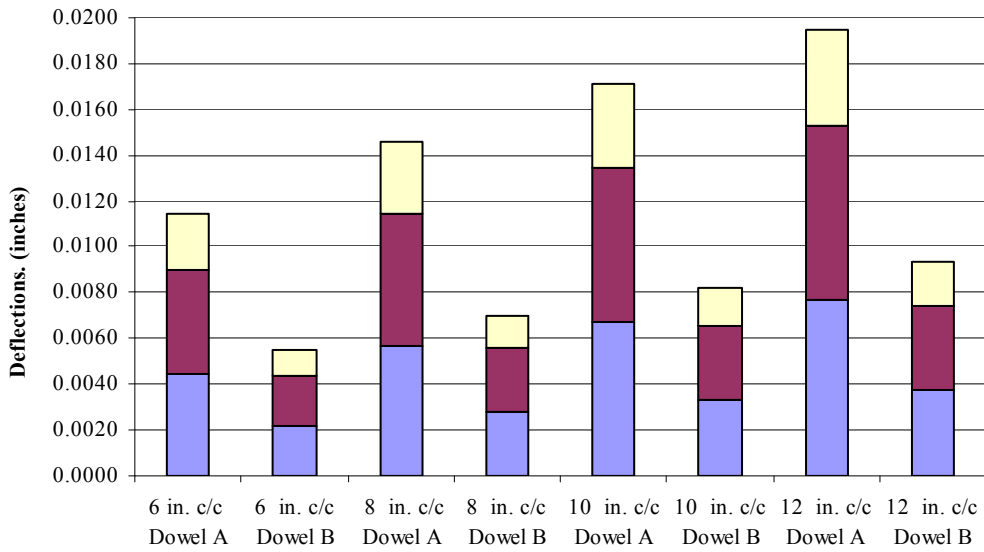
Diameter of Dowel (inches)	Bending Deflection (inch)	Bending Deflection (inch)	Shear Deflection (inch)	Total Relative Deflection (inch)
1.0	0.0045	0.0045	0.0025	0.0114
1.5	0.0022	0.0022	0.0011	0.0055
1.0	0.0057	0.0057	0.0031	0.0145
1.5	0.0028	0.0028	0.0014	0.0070
1.0	0.0067	0.0067	0.0037	0.0171
1.5	0.0033	0.0033	0.0016	0.0082
1.0	0.0076	0.0076	0.0042	0.0195
1.5	0.0037	0.0037	0.0019	0.0093

1 inch = 2.57 cm

Table 46. RD with high dowel shear modulus ($G_d = 5.17 \times 10^3 \text{ MPa}$ ($0.75 \times 10^6 \text{ psi}$)).

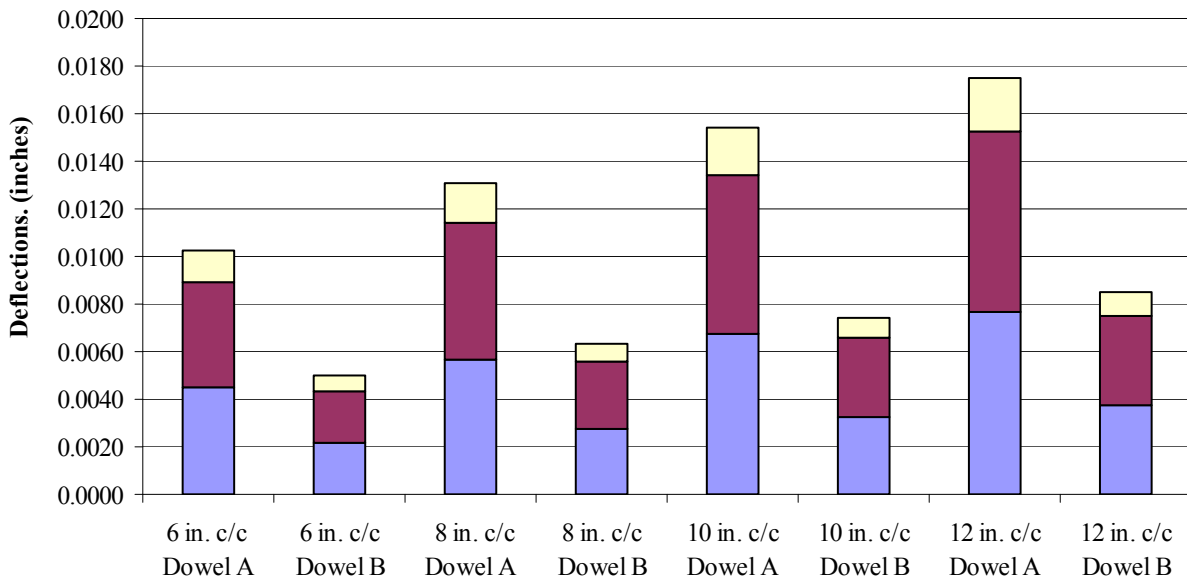
Diameter of Dowel (inches)	Bending Deflection (inch)	Bending Deflection (inch)	Shear Deflection (inch)	Total Relative Deflection (inch)
1.0	0.0045	0.0045	0.0013	0.0103
1.5	0.0022	0.0022	0.0006	0.0050
1.0	0.0057	0.0057	0.0017	0.0131
1.5	0.0028	0.0028	0.0007	0.0063
1.0	0.0067	0.0067	0.0020	0.0154
1.5	0.0033	0.0033	0.0009	0.0074
1.0	0.0076	0.0076	0.0022	0.0175
1.5	0.0037	0.0037	0.0010	0.0085

1 inch = 2.57 cm



1 inch = 2.54 cm

Figure 116. Graph. Components of RD for dowel types A (2.54-cm (1.0-inch) diameter) and B (3.81-cm (1.5-inch) diameter), with $k = 11.072 \text{ kg/cm}^3$ (400 pci), $f'_c = 31.026 \text{ MPa}$ (4,500 psi), joint width = 0.635 cm (0.25 inch), and $G_d = 2.8 \times 10^3 \text{ MPa}$ ($0.4 \times 10^6 \text{ psi}$).



1 inch = 2.54 cm

Figure 117. Graph. Components of RD for dowel types A (2.54-cm (1.0-inch) diameter) and B (3.81-cm (1.5-inch) diameter), with $k = 5.17 \times 10^3 \text{ MPa}$ ($0.75 \times 10^6 \text{ psi}$), joint width = 0.635 cm (0.25 inches), and $G_d = 5.17 \times 10^3 \text{ MPa}$ ($0.75 \times 10^6 \text{ psi}$).

APPENDIX C. FIBER BURNOUT TESTS FOR DETERMINING FIBER WEIGHT FRACTION AND FIBER VOLUME FRACTION FOR FRP DOWELS

Burnout tests were conducted to determine the FWF and FVF for both 2.54-cm (1.0-inch)-diameter FRP dowels and 3.81-cm (1.5-inch)-diameter FRP dowel. Details are listed in table 46 and table 47.

Table 47. FWF and FVF for FRP dowel with 2.54-cm (1.0-inch) diameter.

Sample	FRP Sample Total		Resin Weight (g)	E-glass Fiber		Fiber Weight Fraction (FWF, percent)	Fiber Volume Fraction (FVF, percent)
	Weight (g)	Volume (inches ³)		Weight (g)	Volume (inches ³)		
A1	23.00	0.7399	6.38	16.62	0.3977	72.26	53.75
A2	23.12	0.7383	6.40	16.72	0.4001	72.31	54.20
Average						72.29	53.98

Note: E-glass fiber volume was calculated by using E-glass fiber weight divided by its density (2.55 g/cm³), a converter factor 1 cm³ = 0.06102374 in³ was used for the calculations.
1 inch = 2.54 cm

Table 48. FWF and FVF for FRP dowel with 3.81-cm (1.5-inch) diameter.

Sample	FRP Sample Total		Resin Weight (g)	E-glass Fiber		Fiber Weight Fraction (FWF, percent)	Fiber Volume Fraction (FVF, percent)
	Weight (g)	Volume (in ³)		Weight (g)	Volume (in ³)		
B1	54.81	1.7737	16.736	38.074	0.9111	69.47	51.37
B2	54.19	1.7576	16.546	37.644	0.9009	69.47	51.25
Average						69.47	51.31

Note: E-glass fiber volume was calculated by using E-glass fiber weight divided by its density (2.55 g/cm³ (0.092 lb/in³)); a conversion factor of 1 cm³ = 0.06102374 in³ was used for the calculations.
1 inch = 2.54 cm

REFERENCES

1. American Association of State Highway and Transportation Officials (AASHTO), *AASHTO Guide for Design of Pavement Structures*. AASHTO. Washington, DC, 1993.
2. Friberg, B.F., “Design of Dowels in Transverse Joints of Concrete Pavements,” *Transactions, American Society of Civil Engineers*, Vol. 105, No. 2081, 1940.
3. Vijay, P.V. and GangaRao, H.V.S., *Development of Fiber Reinforced Plastics for Highway Application: Aging Behavior of Concrete Beams Reinforced with GFRP Bars*. CFC-WVU Report No. 99-265 (WVDOH RP #T-699-FRP1), 1999.
4. Washington State Department of Transportation (WSDOT), *Pavement Guide*, May 2005.
5. VanWijk, A.J., Larradale J., Lovell, C.W., and Chen W.F., “Pumping Prediction Model for Highway Concrete Pavements,” *Journal of Transportation Engineering*, Vol. 115, Issue 2, pp. 161–175, 1989.
6. Brown, V. L. and Bartholomew, C.L. “FRP Dowel Bars in Reinforced Concrete Pavements,” *Proceedings of the International Symposium on FRP Reinforcement for Concrete Structures*, ACI, 1993.
7. Ahmed, S., Scott, M., “Using Fiber-Reinforced Polymer Load Transfer Devices in Jointed Concrete Pavements,” *7th International Conference on Concrete Pavements—Orlando, FL, September 9–13, 2001*.
8. Eddie, D., Shalaby, A., and Rizkalla, S., “Glass Fiber-Reinforced Polymer Dowels for Concrete Pavements,” *American Concrete Institute Structural Journal*, Vol. 98, No. 2, 2001.
9. Porter, M.L., Guinn, Jr., R.J., Lundy, A.L., Davis, D.D., and Rhner J.G., “Investigation of Glass Fiber Composite Dowel Bars For Highway Pavement Slabs,” *Project No. TR-408, Iowa State University, 2001*.
10. American Standard for Testing and Materials (ASTM), “Annual Book of ASTM Standards,” *Concrete and Aggregates*, Vol. 0402.
11. American Concrete Pavement Association (ACPA). *Design and Construction of Joints for Concrete Highways*. ACPA, Skokie, Illinois, 1991.
12. American Association of State Highway and Transportation Officials (AASHTO), *Standard Specifications for Highway Bridges*. 15th ed. AASHTO. Washington, DC, 1992.
13. Timoshenko, S. and Lessels, J.M. *Applied Elasticity*. Westinghouse Technical Night School Press, Pittsburgh, PA, 1925.
14. Friberg, B. F. “Load and Deflection Characteristics of Dowels in Transverse Joints of Concrete Pavements.” *Proceedings of Highways Research Board No. 18. National Research Council*. Washington, DC, pp. 140–154, 1938.
15. Yoder, E.J. and Witczak, M.W. *Principles of Pavement Design*, 2nd ed. John Wiley & Sons, Inc., New York, NY, 1975.

16. Albertson, M.D. "Fiber Composite and Steel Pavement Dowels." Master's Thesis. Iowa State University, 1992.
17. Westergaard, H.M. "Computation of Stresses in Concrete Roads." Proceedings, 5th Annual Meeting of the Highway Research Board. Washington, DC, 1925.
18. Tabatabaie, A.M., Barenburg, E.J., and Smith, R.E. "Longitudinal Joint Systems in Slipformed Rigid Pavements." *Vol. II-Analysis of Load Transfer Systems for Concrete Pavements*, Report No. DOT/FAA.RD-79/4, Federal Aviation Administration, 1979.
19. Porter, M.L., Guinn, Jr., R.J. *Assessment of Dowel Bar Research*. Iowa DOT Project HR-1080, Center for Transportation Research and Education, Iowa State University, 2002.
20. ACI Committee 325. "Structural Design Considerations for Pavement Joints." *ACI Journal*, Vol. 53, July, pp. 1-29, 1956.

